Duration-Based Volatility Estimation

Torben G. Andersen, Dobrislav Dobrev, Ernst Schaumburg*

First version: March 10, 2008
This version: July 2, 2008
Preliminary Draft: Comments Welcome

Abstract

We develop a novel approach to estimating the integrated variance of a general jump-diffusion with stochastic volatility. Our approach exploits the relationship between the speed (distance traveled per fixed time unit) and passage time (time taken to travel a fixed distance) of the Brownian motion. The new class of duration-based IV estimators derived in this paper is shown to be robust to both jumps and market microstructure noise. Moreover, their asymptotic and finite sample properties compare favorably to those of commonly used robust IV estimators.

*Torben G. Andersen: Northwestern University, Kellogg School, *t-andersen@northwestern.edu*
Dobrislav Dobrev: Federal Reserve Board of Governors, *Dobrislav.P.Dobrev@frb.gov*
Ernst Schaumburg: Northwestern University, Kellogg School, *e-schaumburg@northwestern.edu*
We are grateful to the participants of the 2008 SITE-CREATES workshop at Stanford University and seminar participants at the Federal Reserve Board of Governors for their comments.
The views in this paper are solely the responsibility of the authors and should not be interpreted as reflecting the views of the Board of Governors of the Federal Reserve System or of any other person associated with the Federal Reserve System.
Andersen gratefully acknowledges financial support from the NSF through a grant to the NBER and by CREATES funded by the Danish National Research Foundation.

1 Introduction

The importance of return volatility for asset pricing theory as well as practical financial management has led to a rich literature on volatility estimation, mostly based on time series observations of asset prices. Information regarding asset values has historically been available to the research community only through selective transaction and settlement prices such as daily opening and closing prices and recorded high and low prices during the trading day. However, within the last decade tick-by-tick data for many liquid financial markets, detailing all transactions and quotes with corresponding time stamps, have become commonplace. The price history is available as a sequence of observations on a two-dimensional vector whose coordinates take values on a price and time grid dictated by the institutional set-up of the market.[1] For example, for stocks traded on the New York Stock Exchange (NYSE) prices are recorded in increments of one cent and time in increments of one second.

The task of volatility estimation is therefore to convert the sequence of recorded high-frequency price-time data into a measure of return variation for a given period of interest such as a trading day. A common trait of the prevailing approaches to measuring the realized return variation is to directly measure the size of the price changes over an exogenously given time grid, either in the form of equidistant sampling (calendar time) or over a certain number of transactions or quotes (event or tick time). Such measures readily map into corresponding volatility measures expressed in terms of the observed price variation per time unit.

In this paper we introduce a natural dual approach to volatility estimation which focuses instead on measuring the time duration per unit of price change and develop a new family of robust volatility estimators based on the theory of passage times for Brownian excursions. While the concept of duration-based volatility estimation is not new to financial econometrics it has, to our knowledge, not been used for measuring the realized return variation in models with stochastic volatility and jumps in a systematic way, nor have its robustness properties been fully explored. The closest precursor to our work is arguably Cho and Frees (1988) who also consider duration based volatility estimation. However, they limit attention to the unduly restrictive case of constant volatility and do not consider the significant biases

[1] Often additional information may be available, such as the depth of the order book and size of transactions, etc. We do not consider procedures which draw on such auxiliary information. The expanded information set can be analyzed using the theory of marked point processes, see, e.g., the surveys by Engle and Russell (2004), Bauwens and Hautsch (2008) and Pacurar (2008).

induced by finite samples and duration censoring.[2,3]

The main complication is that return volatility is stochastically evolving throughout the trading day: it displays a pronounced intraday pattern (diurnal effect), is subject to large short-lived shocks (e.g. news release effect), and features a strong degree of temporal persistence at the inter-daily horizon (volatility clustering effect). This raises a number of questions regarding the underlying concept of volatility. First, should we think of volatility in continuous time or as a discrete-time process updated at equidistant points (in calendar time) or for each new transaction or quote (in tick time)? Second, do we estimate volatility at each point in time within the trading day and then subsequently aggregate to obtain a measure covering the interval of interest, or should we aim more directly for an overall daily measure in one step? Third, how do we formally interpret the volatility measure if it represents return variation over a period where the underlying high-frequency volatility potentially is fluctuating strongly?

We adopt the coherent framework for addressing these issues which has been developed within the recent literature on realized volatility. We posit an underlying continuous-time setting and a frictionless market in which the observed (equilibrium) price dynamics does not allow for risk-free arbitrage opportunities and expected returns are finite. This implies that the asset price process constitutes a special semimartingale for which the relevant asset return variation is given by the associated quadratic variation process, see, e.g., Back (1991) and Andersen, Bollerslev, and Diebold (2008) for discussion. A general representation of a continuous-time semimartingale in financial economics is the stochastic volatility (SV) jump-diffusion. The standard "plain vanilla" realized volatility (RV) estimator is given by the cumulative sum of equidistant high-frequency intraday squared returns and, under the

[2]This early application of the price duration approach to volatility estimation appears to have generated little, if any, subsequent research. We have identified one actual application, namely Park (1993), while less directly related papers, which fail to cite Cho and Frees (1988), include Zumbach (1998) who considers the scaling properties of price durations across different thresholds and Kamstra and Milevsky (2005) who develop a test for the geometric Brownian motion with drift for the S&P 500 index based on the closed-form expression for the first hitting time distribution.

[3]A more fertile literature with applications exploiting price durations is the discrete-time parametric approach to high-frequency trade dynamics using point processes. These are extensions of the Autoregressive Conditional Duration (ACD) models, pioneered by Engle and Russell (1998). Later work develops Stochastic Duration and Stochastic Intensity models, but all rely on discrete time ARCH or SV style specifications, see e.g., Lunde and Timmermann (2004) and the survey by Bauwens and Hautsch (2008)). The conceptual differences between our approach and this literature mirror the distinction between the realized volatility measures and high-frequency intraday ARCH and SV models. The realized volatility approach is nonparametric and model-free, based on a general continuous-time setting and focused on ex-post volatility measurement over a non-trivial interval, while ACD type models are parametric, cast in discrete time and focus on estimation of the spot volatility or price intensity at each transaction or quote, that is, an ex-ante forecast of return variation over the next instant. As such, they represent distinct methodologies, even if they explore similar quantities.

given (ideal) conditions, it is consistent for the underlying quadratic return variation as the intraday return horizon shrinks to zero. The attraction of the standard RV approach is thus that it constitutes a valid volatility measure for a very general class of underlying processes while the implementation is model independent. In practice, however, one must contend with the fact that market imperfections introduce significant microstructure noise in ultra high-frequency data. Consequently, most implementations of RV estimators are limited to exploit the data at relatively low frequencies, such as 1-5 minute returns.

A similar natural limitation applies to the duration-based volatility (DV) estimators developed in this paper. However, the rule of thumb for limiting the impact of noise on the DV estimators is expressed explicitly in the domain of price thresholds rather than implicitly in the time domain. In particular, we show that our DV estimators require price thresholds larger than 2-3 bid-ask log-spreads for the measured price durations to be sufficiently robust to market microstructure features reflected in real data quotes. Moreover, the DV estimators are inherently robust to consecutive price duplicates, frequently encountered in real data due to price discreteness, since such duplicates do not affect the point in time at which the price is observed to exceed a chosen threshold. These features of the dual duration-based approach render the DV estimators viable and interesting alternatives for robust volatility measurement in the presence of microstructure noise without any need for delicate noise filtering techniques. In particular, we show that our duration-based estimators have excellent asymptotic efficiency relative to existing comparable noise-robust IV estimators.

When price jumps are present, the standard RV measures include the squared jump components. A number of extensions of RV have been developed to estimate the jump and continuous components of volatility separately. In this context, an important feature of our duration-based approach is that it explicitly limits the impact of jumps exceeding the chosen price change threshold. Thus, we show that our DV estimators are robust to jumps in the sense that they are consistent for the continuous part of the quadratic variation as the threshold shrinks to zero.[4] We confirm that these properties carry over to practical settings with actual equity price quote data and further illustrate the point through extensive Monte Carlo simulation studies. Specifically, analyzing tick-by-tick data for the full sample of 30 Dow Jones stocks over January 2005 through May 2007, we find that our DV estimators perform well compared with leading sub-sampled RV and bi-power variation estimators of the integrated variance. Moreover, our duration based estimators are not substantially harder to implement and are not sensitive to the choice of threshold in the range of 3 to 6 bid-ask log-spreads. Since the duration approach extracts information from the same un-

[4]This feature is akin to jump truncation in the RV context, see e.g. Mancini (2006), but is a natural feature of the basic estimation technique rather than necessitating the choice of a separate bandwidth parameter.

derlying data as RV estimators, but does so in a very different manner, the two procedures are natural complements, even ignoring the rather compelling efficiency properties of the duration-based measures. Finally, we note that the same duration-based approach delivers jump- and noise-robust estimators for the more general notion of integrated power-variation. Such measures are useful for deriving feasible inference tools for the integrated volatility and for the construction of formal jump tests among other things.

The remainder of the paper is organized as follows. Section 2 briefly reviews the related literature and introduces the basic theory of Brownian excursions in the constant volatility case. Sections 3 and 4 develop the DV estimators following a duration-based dual approach to RV and derive the asymptotic properties based on a localization argument. Section 5 applies the DV estimators to the set of 30 Dow Jones stocks and confirms that the desirable robustness and efficiency properties hold when applied to real data. Section 6 separately investigates the robustness of the DV estimators to noise and jumps in a Monte Carlo setting. Section 7 concludes.

2 Related Realized Volatility Literature

In the literature on continuous-time volatility estimation, the evolution of the log price of a single financial asset is typically given in reduced form by a semi-martingale characterized as the unique (weak) solution to the stochastic differential equation

$$ds_t = \mu_t \, dt + \sigma_t \, dW_t + \Delta X_t, \;\; s_0 \equiv s \tag{1}$$

The solution to (1) is known as a jump-diffusion process with instantaneous drift μ_t, instantaneous volatility σ_t and jumps given by the finite activity jump process X_t. Two key objects of interest in financial applications are the integrated volatility (IV) and quadratic variation (QV) of the log price process, defined as

$$IV_t = \int_0^t \sigma_u^2 \, du \;, \quad QV_t = IV_t + \sum_{0<u\leq t} \Delta X_u^2 \tag{2}$$

The quadratic variation has two separate components, namely, first, the return variation generated by the diffusive volatility term and, second, the cumulative sum of squared jump sizes. The latter component is important for a variety of reasons, including the interpretation of news and practical risk management. However, the former is often of key importance for

volatility forecasting as the continuous or diffusive component of return variation is the main driver of the pronounced persistence in return volatility. As such, methods have been developed to separately identify these two components, as we discuss below.

Although the volatility process of asset returns is itself inherently unobservable, the volatility path $\{\sigma_t\}$ and jumps $\{\Delta X_t\}$ are de facto observable when the econometrician observes the log price process $\{s_t\}$ in continuous time. This is due to the convergence in probability (see e.g. Karatzas and Shreve (1991, Theorem 1.5.8)):

$$\forall t : \mathrm{p}\lim_{m\to\infty}\left(\int_0^t \sigma_u^2\, du \;+\; \sum_{0<u\leq t} \Delta X_u^2 - \;\sum_{k=0}^{m}\left[s_{\frac{kt+1}{m}} - s_{\frac{kt}{m}}\right]^2\right) = 0 \tag{3}$$

In practice, however, the choice of sampling frequency is limited by the liquidity of the given asset as well as the significant market microstructure noise found in the data from most financial markets. The presence of such noise in high-frequency returns implies that the log price process itself is latent and the limit (3) cannot be expected to hold in practice. Nonetheless, (3) motivates the use of *realized volatility* (RV), as an estimator of the quadratic variation:[5]

$$RV_t = \sum_{i=1}^{N}\left[s_{t_i} - s_{t_{i-1}}\right]^2 \tag{4}$$

The sampling frequency of the N observations $\{t_i\}_{i=1,\ldots,N}$ in (4) is often deliberately chosen to be lower than the actual frequency of the data in order to ameliorate the potential bias due to the aforementioned market microstructure effects. Improving the robustness and efficiency of the basic RV estimator (4) to market micro structure noise as well as devising methods for estimating integrated volatility (i.e., filtering out jumps) has been an extremely active area of recent research spurring the development of a new generation of volatility estimators. These include:

- *Subsampled RV* estimators in which (4) is applied to relatively low frequency intraday returns but overlapping subsamples are used to produce a sequence of robust, albeit individually inefficient, estimators of QV which can be averaged to produce the subsampled QV estimate, see, e.g., Zhang, Mykland, and Ait Sahalia (2005). The resulting

[5]The term *'realized volatility'* was coined by Fung and Hsieh (1991) to describe their ad-hoc daily volatility estimate calculated as the sum of squared 15 min returns across a number of markets, including S&P500 futures, Bond futures and Currency futures. Such measures were only later put in a proper probabilistic context as an approximation of the quadratic variation of a semi-martingale, see, e.g. Andersen and Bollerslev (1998) and Barndorff-Nielsen and Shephard (2002)).

estimator gains in robustness to market microstructure noise but it will estimate the full QV and does not involve an attempt to correct for jumps.[6]

- *Kernel based RV* estimators that are closely related to the subsampled RV estimators and can be constructed to have good robustness against micro structure noise as shown by Barndorff-Nielsen, Hansen, Lunde, and Shephard (2007).

- *Bi-power variation* estimators exploiting the finite activity of large jumps to produce a jump-robust estimator of IV. Rather than squaring returns, Bi-power estimators cumulate products of adjacent absolute returns, thereby ensuring that isolated jumps will cease to matter asymptotically (see e.g. Barndorff-Nielsen and Shephard (2004)).[7]

- *Range based RV* estimators that differ from the aforementioned methods which all conceptually rely on the relationship between squared or absolute returns and volatility (4). Instead, as a natural extension to Parkinson (1980), range based RV estimators exploit the distribution of the maximum and minimum of the log-price process. Recent contributions include Christensen and Podolskij (2007b), Christensen and Podolskij (2007a) and Dobrev (2007).

In this paper we take a conceptually different approach to robust IV estimation that relies on the theory of durations for Brownian excursions. While duration based volatility estimation is not new to financial econometrics, it has to our knowledge not been used for IV estimation in models of stochastic volatility in a systematic way nor have its robustness properties been explored. We develop the duration analogues to the sub-sampled RV, bi-power and range based estimators and show that these have better asymptotic properties in the hypothetical no-noise continuous time limit and argue that they conceptually should exhibit similar robustness properties to both market microstructure noise and jumps as the existing estimators. These conjectures are substantiated by our Monte Carlo simulations and further supported by our analysis of the tick-by-tick data of Dow Jones 30 index stocks.

[6]Further refinements along these lines include the *Two-scale* and *Multiscale RV* estimators of Zhang, Mykland, and Ait Sahalia (2005) and Zhang (2006).

[7]Extensions of this approach include alternative transformations of the bipower variation statistic and different lag choices between the nearby absolute returns whose product is cumulated. In addition, bipower variation has been extended to the concept of *multi-power variation*, see, e.g., Barndorff-Nielsen, Graversen, Jacod, and Shephard (2006) and Barndorff-Nielsen, Shephard, and Winkel (2006). In addition, many alternative jump detection procedures have also been proposed. For a recent overview of these developments, see Andersen and Todorov (2007).

3 Constant Volatility Estimators Based on Passage Times

A great number of classic results exist on the properties of Brownian passage times. Although these results are limited to the constant drift and volatility case, they can be extended to a more general class of diffusions by a suitable time-change or localization argument. In this section we, for simplicity, introduce our estimators under the assumption of zero drift and constant volatility, deferring the more general stochastic volatility case to Section 4 below.

3.1 Duality between transition times and the magnitude of Brownian increments

Consider a Brownian motion $\{B_t\}$ with constant instantaneous volatility σ and zero drift

$$B_t = \sigma \int_0^t dW(t),\ t \geq 0,\ B_0 \equiv 0$$

If the object of interest is to obtain an estimate of the instantaneous variance of the process, one can rely on the fact that the increments $h_t = (B_{t_0+t} - B_{t_0})$ over a given time interval t satisfy $h_t \sim N(0, \sigma^2 t)$ leading to the moment condition

$$\mathbb{E}\left[h_t^2\right] = \sigma^2 t \tag{5}$$

from which σ^2 can be estimated e.g. based on a sample of equispaced returns. This is of course the basic logic underlying the RV estimator (4). Rather than measuring the (squared) size of Brownian increments over a fixed time interval, one can instead measure the time it takes the Brownian motion to travel a given distance. Denoting the fixed distance h, we can measure time in several alternative ways, each giving rise to a distinct estimator:

$$\begin{array}{lcl} \textit{first exit time} & : & \tau_h = \inf\{t > 0 \,|\, |B_t| > h\} \\ \textit{first range time} & : & \tau_h = \inf\left\{t > 0 \,\middle|\, \max\limits_{0\leq s\leq t} B_s - \min\limits_{0\leq s\leq t} B_s > h\right\} \\ \textit{first hitting time} & : & \tau_h = \inf\{t > 0 \,|\, B_t = h\} \end{array} \tag{6}$$

In the sequel, we use the term "passage time" to denote either of these three measures of duration. As we shall see below, estimators based on the expected first exit time are the natural analogues to RV estimators based on (5) while the estimators based on the expected

first range time are the natural analogues to the intraday range estimator of Christensen and Podolskij (2007b) and the generalized range proposed by Dobrev (2007).[8]

The moment generating functions for the passage times τ_h are well known but the probability densities (shown in Figure 1) are only known in closed form for the first hitting time (see e.g. Borodin and Salminen (2002)). From the simple form of the moment generating functions given in Table 1, it is immediately clear (see Lemma A.2) that

$$\tau_h \stackrel{\mathcal{D}}{=} \frac{h^2}{\sigma^2}\tilde{\tau}_1 \tag{7}$$

where $\tilde{\tau}_1$ is the passage time of a standard Brownian motion with respect to the threshold $h = 1$. This implies that the case of a general volatility σ^2 and threshold h can always be reduced to the baseline case of a standard Brownian motion and unit threshold through scaling of all passage times by the factor $\frac{\sigma^2}{h^2}$. This fact will be extremely convenient since it allows us to derive all relevant passage time properties from the baseline case.

3.2 Estimation based on passage time moments

The expected passage times can be retrieved from the moment generating functions for the first exit time, the first range time and the first hitting time given in Table 1:

$$\mathbb{E}\left[\tau_h\right] = \begin{cases} \frac{h^2}{\sigma^2} & \text{(first exit time)} \\ \frac{1}{2}\frac{h^2}{\sigma^2} & \text{(first range time)} \\ \infty & \text{(first hitting time)} \end{cases} \tag{8}$$

A method of moments estimator of volatility can then be obtained based on an observed sample of passage times, except in the case of the first hitting time which does not have a first moment. Comparing (5) and (8), the duality between *fixed-threshold* passage times and *fixed-time interval* Brownian increments is clear and gives rise to two separate yet closely related approaches to variance estimation. The moment condition for the first exit time was used by Cho and Frees (1988) who studied the effect of price discretization on volatility estimation and considered (8) as a more robust alternative to the existing return-based estimation procedures. Kamstra and Milevsky (2005) used the moment for the first hitting

[8]Passage times for other Brownian functionals can be defined in a similar way. For example, the maximum drawdown of a Brownian motion can be used to define the first drawdown time, which is identical in distribution to the first exit time and leads to estimators of exactly the same form as the first exit time.

time, but in the case of a Brownian motion with drift so that the expected hitting time is finite. An important, but often overlooked, issue that arises when applying the moment conditions of the form (8) to estimate σ^2 is that they can suffer from quite severe small sample biases induced by Jensen's inequality. This is because the expected passage time is *inversely* proportional to the instantaneous variance. For a given sample of passage times of size N, we show in Proposition A.3, that[9]

$$\mathbb{E}\left[\frac{h^2}{\frac{1}{N}\sum_{i=0}^{N-1}\tau_{i,h}}\right] = \mu_1^{(N)}\,\sigma^2 \quad \text{where} \quad \mu_1^{(N)} = \begin{cases} 1+\frac{2}{3N}+O(\frac{1}{N^2}) & \text{(first exit time)} \\ 1+\frac{1}{3N}+O(\frac{1}{N^2}) & \text{(first range time)} \\ \frac{1}{N} & \text{(first hitting time)} \end{cases} \tag{9}$$

In applications it is often more convenient to work with an unbiased estimator for which no sample size dependent correction is necessary. A particularly convenient small sample unbiased estimator can be based on the first moment of the *reciprocal* passage times derived in Corollary A.4:

$$\mathbb{E}\left[\frac{h^2}{\tau_h}\right] \equiv \mu_1\,\sigma^2 = \begin{cases} 2\mathcal{C}\,\sigma^2 & \text{(first exit time)} \\ (4\log 2)\,\sigma^2 & \text{(first range time)} \\ \sigma^2 & \text{(first hitting time)} \end{cases} \tag{10}$$

where $\mu_1 = \mu_1^{(1)}$ and $\mathcal{C} \approx 0.91597$ is the Catalan constant. The moment conditions (10) have, to our knowledge, not previously been applied to the problem of volatility estimation. Moreover, we see that while the expected hitting time is infinite, the expected reciprocal hitting time is well behaved. The reciprocal passage time moment (10) leads to the local volatility estimator, based on a single observed transition,

$$\hat{\sigma}_h^2 = \frac{1}{\mu_1}\frac{h^2}{\tau_h} \tag{11}$$

where the value of the scaling factor μ_1 is given in equation (10) and Table 1. The estimator (11) will be the basic building block in constructing an estimator of IV in Section 4 below.

[9]The exact value of the Jensen correction factors $\mu_1^{(N)}$ can be calculated explicitly for each N. For the first exit time, we have $\mu_1^{(1)} \equiv \mu_1 = 2\mathcal{C}$, $\mu_1^{(2)} = \log(4)$, $\ldots, \mu_1^{(5)} = \frac{5}{25}(18\mathcal{C}-11), \ldots$ where $\mathcal{C} \approx 0.91597$ is the Catalan constant. Thus the Jensen effect is quite substantial for small N but is well approximated by (9) for $N \geq 20$.

In Corollary A.7 we show that the estimator $\hat{\sigma}_h^2$ satisfies

$$\mathbb{E}[\hat{\sigma}_h^2] = \sigma^2 \quad \text{and} \quad \mathbb{V}[\hat{\sigma}_h^2] \approx \begin{cases} 0.7681\ \sigma^4 & \text{(first exit time)} \\ 0.4073\ \sigma^4 & \text{(first range time)} \\ 2.0000\ \sigma^4 & \text{(first hitting time)} \end{cases} \tag{12}$$

Note that the range time based estimator is the most efficient since it exploits more information about the joint infimum and supremum of the process than the first exit or first hitting time. The variance of the estimator depends on the fourth moment (the so called quarticity) of the log price process but crucially does *not* depend on the choice of threshold h.[10]

When applying (8) or (10) to the estimation of volatility in markets with periodic market closures, one faces the familiar issue of right censoring. This implies that the distribution of the observed passage times τ_h will depend on the amount of time remaining until markets close since it is a draw from a conditional distribution where the conditioning event is that the transition took place prior to end-of-trading. The effect of censoring is illustrated in Figure 2 for the baseline case ($\sigma/h = 1$). The x-axis represents the time remaining until end-of-trading and the horizontal dashed thin lines denote the unconditional expectation of the reciprocal stopping times given in (10). It is clear from the figure that the impact of censoring is quite severe for the first hitting time as we approach the censoring time but much less pronounced for the exit time and especially the first range time. To see the effect for an arbitrary (σ, h), the distributional identity (7) implies that the time axis should be scaled by σ^2/h^2. Thus we see that the conditioning will tend to have a large impact whenever the (unconditional) expected passage time represents a large fraction of the remaining time until the end of a trading day. As a practical matter, we find that the conditioning can safely be ignored for estimation purposes when there is more than 3 (first exit time) or 2 (first range time) expected passage times until end of trading. For the first hitting time on the other hand, the conditional expectation should always be used.

The appropriate censored moment, $\mathbb{E}\left[\frac{1}{\tau_h}|\tau_h \leq T\right]$, is known in closed form for the first hitting time and can be represented as an infinite series for the first exit and first range times. Estimation using the conditional moment is therefore feasible. However, it is important to note the relationship between the expected reciprocal passage times and σ^2 will no longer be linear and, moreover, the appropriate Jensen correction terms will depend on both the time remaining as well as the true σ^2. We therefore advocate a different approach, exploiting

[10]The reciprocal passage times can be used also to define (locally) unbiased estimators of any integer power σ^p based on the moment $\mathbb{E}[\tau_h^{-p/2}]$, as shown in Appendix A.2. In particular, local estimators of volatility, σ, or quarticity, σ^4, can be considered and the corresponding integrated quantities constructed as in Section 4 below. These and related developments are the subject of ongoing research.

the time-reversibility of the Brownian motion. In particular, we define the equivalent (in distribution) backward passage times:

$$\begin{array}{lll} \textit{first exit time} & : & \tau_h^- = \inf\{t > 0 \,|\, |B_{-t}| > h\} \\ \textit{first range time} & : & \tau_h^- = \inf\left\{t > 0 \,\middle|\, \max_{0\le s\le t} B_{-s} - \min_{0\le s\le t} B_{-s} > h\right\} \\ \textit{first hitting time} & : & \tau_h^- = \inf\{t > 0 \,|\, B_{-t} = h\} \end{array} \tag{13}$$

In applications, this allows us to use the regular (forward) passage times (6) during the first half of a trading day and the reverse (backward) passage times (13) during the second half thereby effectively eliminating the need for conditioning for all but the most extreme thresholds.

3.3 Finite Activity Jumps

The occurrence of jumps is a prominent feature of many financial time series and it is clear from (2) that RV will not be a consistent estimator of IV in this case. This fact has lead to the development of jump robust IV estimators, most notably the bi-power variation (BV) estimator of Barndorff-Nielsen, Graversen, Jacod, and Shephard (2006) and subsequent multi-power variation estimators developed in Barndorff-Nielsen, Shephard, and Winkel (2006).[11] While these estimators are consistent for IV, the occurrence of large jumps still pose a significant challenge in finite samples as seen in the Monte Carlo experiments in Section 6 below.

By contrast, the duration based volatility estimators (DV) inherently posses a significant degree of jump robustness due to the implicit jump truncation at the chosen threshold level: if a large jump occurs it may lead to an early threshold crossing (and hence an upward bias in the local volatility estimate), but the amount by which the jump exceeds the threshold will not matter. As the threshold is lowered, jumps will cease to matter in the limit.

The discreteness of actual data will in practice limit the ability to lower thresholds beyond a certain point. It is therefore of interest to study simple modifications of the baseline DV estimator which exhibit additional jump robustness in finite samples. One such, asymptotically equivalent estimator, is the "previous tick" DV estimator. The previous tick estimator is identical to the regular DV, except that it utilizes the threshold, $\tilde{h}$, corresponding to the observed log-price at the time tick just prior to the crossing of the target threshold h. Since (large) jumps tend to lead to an immediate threshold crossing, this method eliminates the

[11] Numerous tests for the presence of jumps have been also developed, e.g. Barndorff-Nielsen and Shephard (2004), Ait-Sahalia and Jacod (2006), and Lee and Mykland (2007).

effect of jumps.[12] We show in Section 6 below, that the previous tick DV estimators which we label "robust" indeed are successful in eliminating most of the effect of jumps for empirically relevant larger thresholds.

3.4 Microstructure Noise

It is well-known that high-frequency price observations are noisy due to various market microstructure features and possible data errors. This leads to a natural signal-to-noise trade-off when estimating the variance of the unobserved log-price process. An intuitive appeal of the duration-based approach in this regard is that the threshold level can be chosen large enough relative to the noise level to ensure a desired degree of robustness. In order to formally assess the level of robustness of our passage time estimators to microstructure noise we adopt the following AR(1) noise structure:

$$\begin{aligned} \widetilde{p}_i &= p_i + u_i \\ u_i &= \rho u_{i-1} + \varepsilon_i \end{aligned} \tag{14}$$

where $\widetilde{p}_i$ are the noisy log-price observations, p_i are the unobserved log-prices, and $\varepsilon_i \sim N(0, (1-\rho^2)\omega^2)$ are the innovations of the AR(1) noise process u_i so that the noise process has the unconditional moments $\mathbb{E}[u_i] = 0$, $\mathbb{E}[u_i^2] = \omega^2$.

This specification allows us to explicitly study the effect of different noise levels ω^2 and degrees of noise persistence ρ on the overall quality of our passage time estimates. The leading special cases of interest are:

(i) $\rho = 0$, in which case we obtain the ubiquitous Gaussian i.i.d. specification representative of transaction price data.

(ii) $\rho >> 0$, in which case we obtain a persistent autoregressive specification representative of quote data.[13]

Given a sample of noisy log-price observations $\widetilde{p}_i$, one can use standard projection methods to express the expectation of p_i conditional on all observables, which in this case is also equivalent to applying the Kalman filter to the state-space representation (14). For our purposes it is of primary interest to recover more generally the expected squared ratio

[12] Whenever a crossing of threshold h was due to a Brownian increment, $\tilde{h}$ will tend to be close to h while $\tilde{h}$ may be substantially smaller than h in the case of a jump crossing. In absence of jumps and for large h, the difference between the previous tick estimators and the original passage time estimators are negligible.

[13] Hasbrouck (1999), and more recently Zhang, Russell, and Tsay (2007), report estimates of ρ as high as 0.4 for the latent cost component of 15-minute quotes, which formally corresponds to $\rho > 0.99$ if brought to a 3-second frequency.

between the observed log-price difference and the underlying true log-price difference for passage times at different threshold levels. These ratios of observed versus latent transition magnitudes can be directly interpreted as relative bias measures for our duration-based estimators (and, conversely, the ratios of unobserved versus observed transition magnitudes can be interpreted as the corresponding bias correction factors).

Figures 3 and 4 plot the relative bias of the first exit time and first range time estimators respectively, obtained for three different threshold levels as a function of the noise persistence ρ. The top graph on each figure is for the case of noise-to-signal ratio $\lambda = 0.25$ (moderate noise level), while the bottom graph is for the case of noise-to-signal ratio $\lambda = 1.00$ (high noise level). The chosen threshold levels 3, 5, 7 are chosen to span the range of thresholds of greatest interest for application on real data and are expressed accordingly in units of the notional average intraday log-spread (as in sections 5 and 6 below). It is worth noting that thresholds much lower than 3 log-spreads are probably untenable in practice as we would expect the noise-to-signal ratio to be prohibitively high for small thresholds.

The main conclusions to be drawn from this analysis (Figures 3 and 4) are as follows. First, both passage time estimators are sufficiently robust to: (i) moderate noise ($\lambda = 0.25$) with arbitrary persistence, and, (ii) persistent noise ($\rho > 0.9$) regardless of the noise level. Second, the first exit time is naturally more robust to noise than the first range time. Third, the higher the chosen threshold level, the more robust to noise are the resulting passage time estimators. Fourth, the passage time estimators exhibit significant upward biases (above 2%) only in the case of non-persistent noise ($\rho \approx 0$) at high level ($\lambda = 1.00$).

These initial results provide formal evidence in support of our intuition that by setting the threshold level large enough relative to the noise level, the duration-based estimators do indeed possess an inherent degree of robustness to noise in many cases. If one is willing to be parametric about the noise structure, the outlined projection approach (or Kalman filtering) can of course be used to develop an explicit feasible noise correction of the passage time estimators in high-noise scenarios. We relegate this for future research, relying for now on demonstrating the success of the duration-based approach in moderate noise and/or persistent noise settings.

3.5 Discretely Sampled Observations

A final concern that must be addressed is time discretization, i.e. the fact that prices are observed on a discretely spaced time grid. In order to be feasible, the proposed estimators must be corrected for the discrepancy between the first passage times of the unobserved process and those measured on an observed finite sample of points. In particular, the first

passage times of a random walk overstate the Brownian first passage times. One reason for this is that the maxima of a random walk always will understate the true unobserved maxima of the underlying Brownian motion, so that it takes somewhat longer on average for the random walk to break a given threshold level. The finer is the discretization step, the smaller is the discrepancy between the random walk extrema and the Brownian extrema.

This issue is addressed by Asmussen, Glynn, and Pitman (1995). They derive exact asymptotic results for the amount by which the maximum $\widetilde{M}$ of a random walk based on k equidistant observations in a finite interval understates the Brownian maximum M in the same interval (see appendix, Lemma A.8). We adapt their results to obtain an asymptotic correction for the passage time estimators proposed above. Our main insight stemming from Asmussen, Glynn, and Pitman (1995), is that knowledge of the moments of the discrepancy due to discretization allows us to approximate the ratio between moments of the Brownian maximum/range and the random walk maximum/range as a function of the number of sample points k:

$$\begin{aligned} \mathbb{E}\left[M^2\right] &\approx f_M(k) \times \mathbb{E}\left[\widetilde{M}^2\right] \\ \mathbb{E}\left[R^2\right] &\approx f_R(k) \times \mathbb{E}\left[\widetilde{R}^2\right] \end{aligned}$$

where the scaling factors $f_M(k)$ and $f_R(k)$ approach 1 from above as k gets large (see appendix), but crucially do not depend on the parameter of interest σ^2.

From this it follows that for any given threshold h one needs to scale up the finite sample volatility estimators based on the first exit time and the first range time by a factor of $f_M(k)$ and $f_R(k)$ respectively, where k is the (varying) number of observations between the start and end point of each h-excursion[14]. By aggregating the resulting estimates at each sample point on a given grid we obtain a novel and feasible realized duration-based volatility estimator (DV) dual to RV in the sense that it is based on measuring passage times rather than price increments. The next section lays out a unified theoretical framework for DV based on first exit times and DV based on first range times.

[14]Though easy to implement, this approach cannot yield an exact small sample correction since it is not designed to account for the possibility of early crossings (i.e. Brownian excursions crossing the threshold in between random walk observations) in a passage time context. Without further small sample adjustment, this will lead to a downwards bias for the smallest thresholds while the bias quickly diminishes as threshold levels increase. An exact, albeit more computationally intensive, correction is possible by viewing the unobserved Brownian path conditional on the observed random walk as a sequence of connected Brownian bridges for which crossing probabilities and crossing time distributions can readily be calculated in the case of first hitting times and first exit times. For the first range time the situation is slightly more complex and is the subject of ongoing research.

4 Stochastic Volatility Estimators Based on Passage Times

When volatility is randomly varying throughout the trading day, we can no longer assume that observed passage times are identically distributed. This leads us to consider instead local volatility estimation as proposed by Foster and Nelson (1996) and more recently Mykland (2006). Based on consistent estimators of local volatility, an IV estimator can then be constructed as the corresponding Riemann sum.

Consider then a fixed time grid $0 \equiv t_0 < t_1 < \ldots < t_N \equiv 1$ consisting of N, not necessarily equispaced, intervals with $\Delta_i = t_{i+1} - t_i$ denoting the mesh size and where the time unit is chosen to ensure that the length of the trading day is unity. We will assume that the volatility process is "well behaved" in the sense that it can be locally approximated by a piecewise constant function as the mesh size tends to zero, e.g. due to Lipschitz continuity. We also assume independence of the volatility process and the Brownian motion driving returns (i.e. "no leverage") for our theoretical results although our Monte Carlo studies suggest no adverse effect on the DV estimators of introducing such dependence.

At a given grid point, t_i, we wish to construct an estimator of the local volatility. Given a threshold size h, we can, starting from t_i, look for the next passage time $\tau_h^+(t_i)$ and use the estimator $\frac{1}{\mu_1}\frac{h^2}{\tau_h^+(t_i)}$. However, we can in principle do better: Since the Brownian motion is time reversible, we can also, starting from t_i, look back in time for the next passage time $\tau_h^-(t_i)$ and construct the independent estimator $\frac{1}{\mu_1}\frac{h^2}{\tau_h^-(t_i)}$.

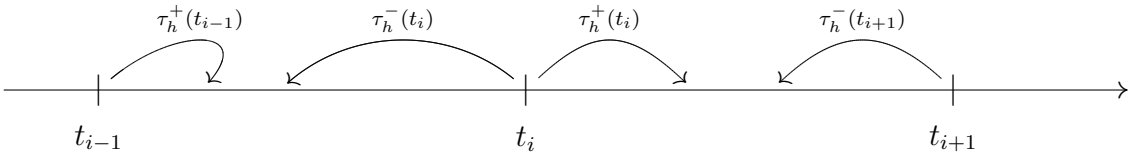

We thus have two independent estimators of local volatility at t_i which suggests using the bi-directional local volatility estimator:

$$\begin{aligned} \hat{\widehat{\sigma}}_h^2(t_i) &= \frac{1}{2\mu_1}\left[\frac{h^2}{\tau_h^+(t_i)} + \frac{h^2}{\tau_h^-(t_i)}\right] \quad \text{(bi-directional)} \\ \hat{\sigma}_h^2(t_i) &= \frac{1}{\mu_1}\frac{h^2}{\tau_h^+(t_i)} \text{ or } \frac{1}{\mu_1}\frac{h^2}{\tau_h^-(t_i)} \quad \text{(uni-directional)} \end{aligned} \tag{15}$$

By independence, we have the local variance estimates:

	$\mathbb{V}[\widehat{\hat{\sigma}}^2_h(t_i)]$	$\mathbb{V}[\hat{\sigma}^2_h(t_i)]$
(first exit time)	$0.3841\ \sigma^4_{t_i}$	$0.7681\ \sigma^4_{t_i}$
(first range time)	$0.2037\ \sigma^4_{t_i}$	$0.4073\ \sigma^4_{t_i}$
(first hitting time)	$1.0000\ \sigma^4_{t_i}$	$2.0000\ \sigma^4_{t_i}$

(16)

In practice, however, we do not use the bi-directional estimators due to the aforementioned censoring issue.[15] Instead we use the uni-directional estimator based on $\tau^+_h(t_i)$ for grid points t_i that fall in the first half of the trading day and $\tau^-_h(t_i)$ for grid points falling in the second half of the trading day. We thus have a sequence of local variance estimates $\{\hat{\sigma}^2_h(t_i)\}_{i=1,\ldots,N}$ based on passage time durations from which we can construct the estimate of integrated variance on $[0;1]$ as

$$\widehat{DV}_{N,h} = \sum_{i=0}^{N-1} \hat{\sigma}^2_h(t_i)\ \Delta_i \tag{17}$$

where $\Delta_i = \frac{1}{N}$ in the case of an equispaced time grid. Note that the distribution of (17) will depend on h although the distribution of each individual estimate $\hat{\sigma}^2_h(t_i)$ does not. This is because the covariance between neighboring volatility estimates, i.e. $Cov(\hat{\sigma}^2_h(t_i), \hat{\sigma}^2_h(t_{i-1}))$, will likely involve overlapping transitions when h is large relative to the mesh size. However, the threshold h can be chosen independently of N and we can consider letting h tend to zero at an appropriate rate so that terms in (17) have arbitrarily low correlation. In Proposition A.16, we show that the appropriate rate is $h = o(N^{-1/2})$ and the resulting estimator satisfies

$$\sqrt{N}\ \left(\widehat{DV}_{N,h} - IV\right) \sim \text{Mixed Normal}\left(0, \nu \int_0^1 \sigma^4_u\ du\right) \tag{18}$$

where ν is the constant in (16). Note that the asymptotic distribution depends on the unknown integrated quarticity. However, it is easy to show that the same localization argument can be used to consistently estimate other integrated moments of interest such as the integrated quarticity itself, thus enabling the calculation of confidence bands for IV.

In practice, the observation record is discrete and we only observe the value of the process

[15] In markets such as FX, where 24 hour trading prevails, the bidirectional approach could yield substantial efficiency gains.

at the N grid points, thus rendering the convergence rate $N^{-1/2}$ of the estimator $\widehat{DV}_{N,h}$ infeasible. Instead we can consider the construction of a set of local volatility estimates on a coarser sub-grid, consisting of K grid points $\{t_{i_1}, \ldots, t_{i_K}\}$. Here $K = o(N), K \to \infty$ so that the number of observations between adjacent grid points increases with the sample size and the discretization error tends to zero for suitably chosen threshold levels:

$$\sqrt{K}\ \left(\widehat{DV}_{K,h} - IV\right) \sim \text{Mixed Normal}\left(0, \nu \int_0^1 \sigma_u^4\ du\right) \tag{19}$$

Note that the convergence rate is now the slower $K^{-1/2}$. Part of this efficiency loss can of course be mitigated by averaging the estimator over all possible sub-grids of mesh size $\Delta = K^{-1}$. This situation is analogous to the sub-sampling strategy for the RV estimator advocated by Zhang, Mykland, and Ait Sahalia (2005).

The value of the variance factor ν is about 0.8 for the unidirectional first exit time DV and about 0.4 for the unidirectional first range time DV (see table 1) although these values will be reduced further by the subsampling scheme. This compares to 1.3 for subsampled RV and about 1.5 for subsampled BV (the values for RV and BV without subsampling are 2.0 and 2.6 respectively).[16] Thus, for suitably chosen threshold levels both the first exit time DV and the first range time DV should in practice be considerably more efficient than subsampled RV (in the absence of jumps) or subsampled BV (when jumps are present).

In what follows, we conduct extensive empirical analysis on real and simulated data with the main goal of comparing the finite sample efficiency of the DV estimators vis-a-vis subsampled BV as the benchmark jump-robust (and sufficiently noise-robust) estimator of the integrated variance.[17] In order to design realistic Monte Carlo experiments, we first analyze the full set of Dow Jones 30 stocks and document that both the first exit time DV and the first range time DV significantly outperform (optimally) subsampled BV: the DV estimators achieve the same mean estimate of the integrated variance with a lower standard deviation while remaining very highly correlated with the subsampled BV estimates.

[16] Subsampling of RV with important extensions to optimal two-scale and multi-scale RV estimators in the presence of microstructure noise has been advocated by Zhang, Mykland, and Ait Sahalia (2005) and Zhang (2006). Subsampling of BV has been empirically documented to have similar merits by Dobrev (2007), although the asymptotic distributiuonal properties have yet to be studied.

[17] We leave for future research the comparison to range-based estimators of IV developed by Christensen and Podolskij (2007b), Christensen and Podolskij (2007a) and Dobrev (2007).

5 A Realized Volatility Analysis of the Dow Jones 30

In recent years the Dow Jones 30 stocks have an increasingly dense (near second-by-second) record of intraday transaction prices and quotes. This provides an excellent laboratory for testing the empirical performance of our passage time volatility estimators on real data. For our analysis we use NYSE TAQ data for the period January 1, 2005 to May 31, 2007. Table 2 summarizes basic descriptive statistics for the Dow Jones components, including companies that have been included in or excluded from the index during this period. Ignoring short trading days around major holidays we obtain a sample of 601 regular trading days of nearly second-by-second intraday data for each stock from 9:30 am to 4:00 pm.

We apply our first exit time and first range time estimators on the series of mid-quotes after filtering out spread outliers as usual in order to avoid distortions due to bid-ask bounce and possible data errors. We also filter out consecutive duplicate mid-quotes since the measurement of first passage times is driven exclusively by the first time a given threshold level is reached. The daily sample sizes without duplicates vary from about two to eight thousand quotes, roughly corresponding to an effective highest sampling frequency of three seconds. Microstructure noise still distorts the measured returns and, hence, the measured transition times and corresponding duration-based volatility estimates. However, when considering large enough thresholds (e.g. 4-6 log-spreads) the transition time distortions will be relatively small and the quality of our first exit time and first range time DV estimates should be comparable to the quality of subsampled RV and BV estimates at modest sampling frequencies such as 2 to 5 min. As we have found in section 3.4, the impact of noise on our duration-based measurements is close to negligible for moderate noise levels and higher degree of noise persistence typical for mid-quotes. Thus, being agnostic about the exact structure of the noise process, the robustness argument for DV based on a large enough threshold is analogous to the one that justifies the use of subsampled RV or BV at a sparse enough frequency.[18]

We compare the finite sample efficiency of DV vis-a-vis subsampled BV as the benchmark jump-robust estimator of the integrated variance. The results of our analysis in the form of signature plots are presented in Appendix C (for the average across all stocks) and Appendix D (for individual stocks). We first determine a near-optimal sampling frequency for the subsampled BV estimator for the stocks in our sample. Figure 8 in Appendix C represents the cross-sectional average signature plot of BV versus RV as a function of the sampling frequency in seconds. A key feature to notice is that BV is severely downward sloping for

[18]The main advantage of DV in this regard is that the choice of threshold level directly limits the local noise import at each grid point, while the choice of sampling frequency for RV and BV controls the average noise import across all grid points.

frequencies from 3 to 120 seconds, while RV flattens much faster above the 15 or 30 second sampling frequency. It is known that the increasing gap between RV and BV at frequencies higher than 2 minutes is due to the increased number of zero returns at those frequencies. This is explicitly confirmed by the last column of Table 2 containing descriptive statistics. The median number of zero returns lasting longer than 30 seconds on each day is 161, those lasting longer than 1 minute are about 48 on each day, while the zero returns lasting longer than 2 minutes are only about 11 per day. Importantly, this pattern is observed without much variation across different stocks (reported in the table) or different trading days (not reported in the table). Therefore, the 2-minute frequency for the subsampled BV estimator appears to be a nearly optimal choice in the cross-section.

Next, treating the 2-minute subsampled BV as the benchmark estimator of the integrated variance, we analyze the cross-sectional average of our DV estimators for threshold levels expressed in units of the average log-spread. As evident from Figure 9 in Appendix C, for threshold level set to 4 log-spreads and above both our first exit time DV estimates and first range time DV estimates on average agree with the 2-min BV estimates. What is even more striking, though, is that essentially the same pattern of the signature plots emerges also for each individual stock (see appendix D). At the same time, for thresholds larger than 4 log-spreads the standard deviation of our DV estimates is markedly lower than the one of 2-min subsampled BV (see Figure 10 in Appendix C), while the average correlation between our DV estimates and the 2-min subsampled BV estimates exceeds 0.9 (see Figure 11 in Appendix C).

Overall, robustly across all stocks for threshold level 4 log-spreads and above we obtain a similar mean level of our DV estimates as 2-min subsampled BV, very high correlation with BV but markedly lower variance. This provides encouraging initial evidence that our DV estimators can significantly outperform subsampled BV as a jump-robust benchmark estimator of the integrated variance in real-world settings of interest. The next section further reinforces this conclusion by means of Monte Carlo experiments for a rich set of carefully calibrated models.

6 Monte Carlo Experiments

In this section we document the performance of the proposed duration-based DV estimators on finite samples of simulated data from a wide selection of jump-diffusion models. For each model specification, we mimic the discreteness of stock quotes observed in real data samples from frequently traded stocks. In particular, we generate random quote arrivals at an average

rate of one every three seconds over the trading hours from 9:30 am to 4:00 pm during each of 2500 trading days (roughly 10 years of data). We then analyze the performance of the first exit time DV and first range time DV estimators across a range of realistic threshold levels vis-a-vis 2-min subsampled BV (in scenarios with jumps) and 2-min subsampled RV (in scenarios without jumps).

In the Monte Carlo experiments we seek to calibrate the threshold levels for calculating the DV estimators to ensure that the environment is reminiscent of the setting in the section dealing with the Dow Jones 30 stock data in Section 5. To this end, we exploit the empirically stable relationship between the average log-spread and daily volatility (the ratio typically falls in the range $[0.02, 0.04]$ with a mean of 0.03, as shown in the second to last column of table 2). We therefore express the thresholds in units of the mean log-spread and further assume that the log-spread equals 0.03 times the daily volatility in our simulations. In this way, we maintain consistency between our plots on real and simulated data as a function of the threshold expressed in units of the mean log-spread. Furthermore, we focus on thresholds in the range from 1 to 10 times the mean log-spread, corresponding to the range from 0.03 to 0.3 times the daily volatility. This choice is reasonable as it implies a mean duration of the first exit times ranging from about 20 seconds for the smallest threshold to about 30 minutes for the largest threshold and mean duration of the first range times ranging from about 10 seconds to about 15 minutes.

The full set of data generating processes is described in detail in Appendix A.1. In order to gain more thorough understanding of the performance of our DV estimators, we first consider in detail the case of ideal sampling without microstructure noise and then repeat the analysis for two distinct AR(1) noise structures, namely non-persistent (or i.i.d.) noise representative for transaction prices and highly-persistent noise representative for mid-quotes. For each model specification, we produce signature plots of the relative bias of the integrated variance estimates as a function of the threshold level and report in table format the corresponding relative efficiency factor vis-a-vis 2-min subsampled BV (in scenarios with jumps) or 2-min subsampled RV (in scenarios without jumps).[19] The objective is to include relevant scenarios which mimic important qualitative features of the equity market results within an empirically relevant setting. As such, our extensive set of relative performance results for the simulated data serve to corroborate our interpretation of the findings for the Dow Jones 30 stock data in Section 5.

In particular, Figures 5, 6, 7 plot the relative bias of each IV estimator, while Tables 3, 4,

[19]The relative bias is calculated as the sample mean of $\widehat{IV}/IV$, while the relative efficiency factor at the 2-min sample frequency is calculated as the sample mean of $195(\widehat{IV} - IV)^2/IQ$, where IV and IQ are the true simulated integrated variance and integrated quarticity on each day, while $\widehat{IV}$ is the obtained IV estimate on each day.

and 5 show the relative mean squared error of each IV estimator (in the form of an efficiency factor at the benchmark 2-min frequency) across a broad range of considered models. The first two rows of each table correspond to the 2-min sub-sampled RV and BV estimators. The subsequent rows represent the first exit time and first range time based estimators for thresholds ranging from 3 to 8 log-spreads. The passage time estimators are the previous tick versions of the estimators that are more robust to jumps in finite samples (see Section 3.3). Below we discuss these results in greater detail first for our Monte Carlo experiments without microstructure noise and then with microstructure noise.

6.1 Simulations Without Microstructure Noise

6.1.1 Deterministic Volatility

In the constant volatility model SV0-C the annualized volatility is set to 20%, so that the daily variance is 1.59×10^{-4} (assuming 252 trading days per year). Figure 5-A shows that the first exit time DV and first range time DV estimators behave very similarly in terms of their finite sample biases as a function of the threshold level and there is virtually no bias for threshold level larger than 3 log-spreads. The first column in Table 3 displays the relative efficiency factor of the two DV estimators for thresholds in the no-bias range from 3 to 8 log-spreads vis-a-vis the 2-min subsampled BV and RV benchmark. Both DV estimators are considerably more efficient than the 2-min BV and RV benchmarks over a very wide range of thresholds from 3 to 5 log-spreads for the first exit time and from 3 to 7 log-spreads for the first range time. The efficiency of each DV estimator decreases as the threshold level goes up due to the inflated variance stemming from the increasing overlap between observed passage times starting from neighboring grid points. Importantly, for any given threshold the first range time estimator is consistently more efficient than the first exit time estimator and beats the 2 minute BV benchmark in relative MSE sense by a sufficiently large factor for all thresholds in the range 3-7 log-spreads.

The overall conclusion from Figure 5 (panel A) and Table 3 (column 1) is that there is a wide range of threshold levels, roughly 3-5 log-spreads for the first exit time and 3-7 log-spreads for the first range time, offering substantial efficiency gains over 2-min subsampled BV as a measure of the daily integrated variance.

6.1.2 Stochastic Volatility

Although the asymptotics of our DV estimators is not affected by (non-explosive) intraday variation in volatility, it is important to investigate the extent to which there still might be a detrimental impact from time-varying or stochastic volatility on the finite sample performance documented under constant volatility. To this end, we repeat the same analysis for a number of alternative data generating processes involving stochastic volatility: SV1A-C (one-factor affine), SV1L-C (one-factor log), and SV2A-C (two-factor affine). The models are described in detail in Appendix A.1 and they are all calibrated to obtain the same average annualized volatility of 20%. We present the results for models without the "leverage" effect (i.e. correlation between the process driving stochastic volatility and the Brownian motion driving returns) consistent with the theoretical results derived in the Appendix. We have, however, confirmed that simulating models with the leverage effect does not change our results or conclusions in any significant manner.

Our main finding is that there is very little difference between the observed relative performance of DV versus BV under each stochastic volatility model in comparison to the constant volatility case. For example, representative for all three models, Figure 5-B for model SV2A-C shows that both DV estimators are virtually unbiased for threshold level larger than 3 log-spreads exactly as in the constant volatility case (c.f. figure 5-A). Likewise, the first four columns of Table 3 show that the relative MSE gains of DV versus 2-min subsampled DV for each stochastic volatility model are practically about the same as those documented under constant volatility.

The finding that our results are robust to time-varying volatility should not be surprising given that (for small enough thresholds) volatility is locally constant to a good first order of approximation, which is the main requirement for our DV estimators to work well in practice. Thus, the range of thresholds for which the DV estimators achieve superior performance relative to the 2-min subsampled BV remains 3-5 log-spreads (first exit time) and 3-7 log-spreads (first range time).

6.1.3 Stochastic Volatility with U-Shaped Intraday Pattern and Jumps

It is well known that intraday stock returns exhibit a pronounced U-shaped pattern of intraday volatility along with other activity-related variables such as trading volume, number of transactions, and quoted spread. On average, the variance in the first hour of trading is often three times larger than the variance in the middle of the day and peaks again to a somewhat lower level in the last hour of trading. Therefore, we augment our baseline stochastic volatility specifications with a deterministic time-of-the-day volatility multiplier

having a U-shaped pattern. In particular, our time-of-the-day multiplier takes an additive form of exponentials popular in the market microstructure literature (see Appendix A.1 for details of the implementation).

Likewise, to accommodate naturally occurring infrequent instantaneous price revisions that can lead to path discontinuities (e.g. upon the arrival of big news), we add also a finite activity jump component to our baseline stochastic volatility specifications. This allows us to study the performance of our DV estimators on "jump" days subject also to a realistic strong U-shaped intraday volatility pattern that interferes with the jumps by generating large enough pure diffusive increments at the start and end of the day. In particular, we simulate one jump on each day with a 25% average contribution to the daily diffusive integrated variance and carry out the same relative performance analysis as above.

An important feature of the first exit time and first range time DV estimators established in the theory section is their asymptotic robustness to jumps due to the inherent truncation via the chosen threshold of arbitrary large log-price increments (the smaller the threshold, the higher the degree of jump-robustness). In particular, in section 3.3 we have motivated the "previous tick" method for calculating the passage times involved in our DV estimators that achieves nearly perfect immunity to the presence of a single large jump on each day both asymptotically and in finite samples. Therefore we focus our analysis on these asymptotically equivalent "robust" versions of our first exit time DV and first range time DV estimators.

Figure 5-C for model SV2A-UJ (representative for all four models with jumps) shows that, indeed, the combined presence of jumps and a strong U-shape volatility pattern has very little impact on the relative bias of our DV estimators. While the 2-min subsampled BV exhibits a noticeable upward bias due to finite-sample jump distortion[20], both DV estimators remain unbiased for threshold levels 3 to 6 log-spreads and less biased than BV for thresholds up to 8 log-spreads. Importantly, as revealed by the last four columns of Table 3, this leads also to further improvement of the relative MSE factors of the DV estimators vis-a-vis 2-min subsampled BV. Thus, the overall conclusion from Figure 5 and Table 3 is that as a jump-robust integrated variance estimator DV for thresholds 3-6 log-spreads outperforms the 2-min subsampled BV benchmark by an even wider margin on days with jumps compared to days without jumps.

[20]It is well known that the BV estimator does not fully eliminate the impact of jumps and in fact has an upward bias of roughly 5.4% in our simulations.

6.2 Simulations With Microstructure Noise

Next we further extend our simulation setup by producing noisy observations based on the AR(1) microstructure noise specification of equation 14 introduced in Section 3.4. Our goal is to study the effect of different noise levels (noise-to-signal ratio λ) and different noise persistence (first order autocorrelation ρ) on the relative efficiency of our DV estimators. We focus our analysis on four distinct cases:

(A) Non-persistent noise ($\rho = 0$) at moderate level ($\lambda = 0.25$)

(B) Persistent noise ($\rho = 0.99$) at moderate level ($\lambda = 0.25$)

(C) Non-persistent noise ($\rho = 0$) at high level ($\lambda = 1.00$)

(D) Persistent noise ($\rho = 0.99$) at high level ($\lambda = 1.00$)

Based on our findings in Section 3.4 with regard to the degree of distortion of individual passage time measurements, we should expect a dramatic deterioration of the relative efficiency of the first exit time DV and, even more so, the first range time DV only in case (C) of non-persistent noise at high level. This is indeed our main finding when we repeat our previous analysis under the considered noise specifications first for the four SV-C models without jumps and U-shaped volatility pattern and then for the four SV-UJ models with U-shaped pattern and jumps.

6.2.1 Noise Impact on DV Under Stochastic Volatility

Figure 6 shows that moderate noise at any persistence (first row panels A and B) or persistent noise at any level (second column panels B and D) have a negligible impact on the relative bias of our DV estimators compared to the case without noise (Figure 5, panel B). By contrast, non-persistent noise at high level (Panel C) appears to be quite detrimental. As predicted by our analysis in Section 3.4, now there is an upward bias of our DV estimators across the full range of empirically relevant thresholds. Likewise, comparing the MSE factors with noise reported in Table 4 to their corresponding values without noise (Table 3) shows that the relative efficiency of DV versus 2-min subsampled BV and RV is largely unaffected by moderate noise at any persistence (columns with $\lambda = 0.25$) or persistent noise at any level (columns with $\rho = 0$). However, non-persistent noise at high level (columns with $\lambda = 1.00$) leads to severe deterioration of the relative efficiency of DV, making it somewhat worse than 2-min subsampled BV, which unlike DV remains nearly unbiased also in this case.

The overall conclusion to be drawn from this analysis is that the presence of microstructure noise should not generally be a major concern for our duration-based approach, as long as the noise-to-signal ratio is moderate or the noise is sufficiently persistent. The special case of non-persistent noise at a detrimentally high level is easy to detect by inspecting

whether the DV signature plots as a function of the threshold level are upward sloping as the thresholds go down. Clearly, this is not the case for our sample of mid-quotes for the Dow Jones 30 stocks (see signature plots in Appendix C and D), further corroborating the interpretation of our empirical findings in Section 5.

6.2.2 Noise Impact on DV Under Stochastic Volatility with U-Shaped Intraday Pattern and Jumps

As a final check of the relative performance of our DV estimators, we repeat the above analysis with microstructure noise for our SV-UJ models featuring a pronounced U-shape intraday pattern and jumps. We arrive at exactly the same conclusion for such "jump" days after comparing Figure 7 with the corresponding signature plots without noise (Figure 5, panel B), as well as Table 5 with the corresponding efficiency factors without noise (Table 3). Leaving aside the special case of non-persistent noise at a detrimentally high level, both the first exit time DV and the first range time DV significantly outperform 2-min subsampled BV as jump-robust estimators of the integrated variance over a wide range of thresholds from 3 to 6 log-spreads.

7 Conclusion

In this paper we propose a new methodology for integrated variance estimation based on a localization argument and the theory of Brownian passage times. We exploit suitably scaled reciprocal passage times for a given threshold as the dual analog to squared/absolute returns and ranges for a given time unit and introduce novel duration-based estimators DV as natural counterparts to commonly used RV estimators. Our DV estimators are asymptotically superior to subsampled RV and BV estimators in the infeasible case with continuous observations and no jumps. Moreover, the proposed duration-based estimators perform very well in finite samples in both Monte Carlo experiments and an empirical analysis of the stocks in the Dow Jones 30 index. The rationale behind this performance is quite intuitive: as long as the threshold is chosen large enough, the market microstructure noise distortion of the observed passage times will be small. On the other hand, as long as the threshold is small enough, individual large jumps will automatically be truncated and thus will only affect the local volatility estimate at a single grid point. As we have demonstrated in the Monte Carlo experiments, this jump robustness can be further strengthened by using the previous tick versions of the DV estimators. This leaves us with an intermediate range

of thresholds ranging from roughly 3 to 6 log-spreads for which our estimators have good robustness properties with respect to both jumps and microstructure noise.[21] Importantly, the estimates are relatively stable with respect to the choice of threshold within this range and practical implementation will therefore not need to involve any delicate first step estimation of an 'optimal' threshold.

Overall, the very encouraging results for the Dow Jones 30 stocks and a broad range of Monte Carlo experiments present supportive evidence that the asymptotic efficiency of the introduced realized duration-based volatility estimators can be exploited in practice. At the same time, certain aspects of the behavior of our DV estimators on real data call for further investigation. In particular, future research is needed to shed more light on what type of assets and markets offer the most suitable high-frequency price-time data for duration-based volatility estimation.

The duration based approach outlined in this paper for robust integrated variance estimation applies more generally to the robust estimation of other power variations, of which the integrated quarticity is of particular interest in finance applications. The estimation of these quantities follows immediately from the results in Appendix A.2, which outlines the basic duality between reciprocal passage times and certain magnitude-based functionals of the Brownian motion. Another intriguing avenue of future research is multivariate extensions of duration based techniques to the estimation of covariances. We leave these and other natural extensions for future work.

[21] Although the asymptotic properties of the DV estimators have been derived assuming "no leverage", extensive Monte Carlo experiments have confirmed that leverage does not affect the performance of the DV estimators.

References

Ait-Sahalia, Y. and J. Jacod (2006). Testing for the presence of jumps in a discretely observed process.

Andersen, T. G., L. Benzoni, and J. Lund (2002). An empirical investigation of continuous-time equity return models. http://www.nber.org/papers/w8510.pdf.

Andersen, T. G. and T. Bollerslev (1998). Answering the skeptics: Yes, standard volatility models do provide accurate forecasts. *International Economic Review 39*(4), 885–905.

Andersen, T. G., T. Bollerslev, and F. X. Diebold (2007). Roughing it up: Including jump components in the measurement, modeling, and forecasting of return volatility. *Review of Economics and Statistics 89*(4), 701–720.

Andersen, T. G., T. Bollerslev, and F. X. Diebold (2008, Yacine Ait-Sahalia, Lars P. Hansen, and Jose A. Scheinkman Eds.). Parametric and nonparametric volatility measurement. *In Handbook of Financial Econometrics* (North Holland).

Andersen, T. G., T. Bollerslev, and N. Meddahi (2005). Correcting the errors: Volatility forecast evaluation using high-frequency data and realized volatilities. *Econometrica 73*(1), 279–96.

Andersen, T. G. and V. Todorov (forthcoming 2007). *Realized Volatility and Multipower Variation*. Wiley. in Encyclopedia of Quantitative Finance, Rama Cont (Eds.).

Asmussen, S., P. Glynn, and J. Pitman (1995). Discretization error in simulation of one-dimensional reflecting brownian motion. *The Annals of Applied Probability 5*(4), 875–896.

Back, K. (1991). Asset pricing for general processes. *Journal of Mathematical Economics 20*(4), 371–95.

Barndorff-Nielsen, O. E., S. E. Graversen, J. Jacod, and N. Shephard (2006). Limit theorems for bipower variation in financial econometrics. *Econometric Theory 22*(4), 677–719.

Barndorff-Nielsen, O. E., P. R. Hansen, A. Lunde, and N. Shephard (2007). Designing kernels to measure the ex-post variation of equity prices in the presence of noise. Working Paper; University of Aarhus, Stanford University and University of Oxford.

Barndorff-Nielsen, O. E. and N. Shephard (2002). Estimating quadratic variation using realized variance. *Journal of Applied Econometrics 17*(5), 457–77.

Barndorff-Nielsen, O. E. and N. Shephard (2004). Power and bipower variation with stochastic volatility and jumps. *Journal of Financial Econometrics 2*(1), 1–37.

Barndorff-Nielsen, O. E., N. Shephard, and M. Winkel (2006). Limit theorems for multipower variation in the presence of jumps. *Stochastic Processes and Their Applications 116*, 796–806.

Bauwens, L. and N. Hautsch (2008). *Modeling Financial High Frequency Data Using Point Processes*. Berlin: Springer Verlag.

Borodin, A. N. and P. Salminen (2002). *Handbook of Brownian motion : facts and formulae* (2nd ed.). Probability and its applications. Basel ; Boston: Birkhäuser.

Cho, D. C. and E. W. Frees (1988). Estimating the volatility of discrete stock prices. *Journal of Finance 43*(2), 451–66.

Christensen, K. and M. Podolskij (2007a). Range-based estimation of quadratic variation. *working paper, Ruhr-Universität Bochum.*

Christensen, K. and M. Podolskij (2007b). Realized range-based estimation of integrated variance. *Journal of Econometrics 141*(2), 323–49.

Dobrev, D. (2007). Capturing volatility from large price moves: generalized range theory and applications. *working paper Northwestern University.*

Engle, R. and J. R. Russell (2004, Yacine Ait-Sahalia, Lars P. Hansen, and Jose A. Scheinkman Eds.). Analysis of high frequency data. *In Handbook of Financial Econometrics* (North Holland).

Engle, R. F. and J. R. Russell (1998). Autoregressive conditional duration: A new model for irregularly spaced transaction data. *Econometrica 66*(5), 1127–62.

Foster, D. P. and D. B. Nelson (1996). Continuous record asymptotics for rolling sample variance estimators. *Econometrica 64*(1), 139–74.

Fung, W. K. H. and D. A. Hsieh (1991). Empirical analysis of implied volatility: Stocks, bonds and currencies. *working paper, Duke University.*

Hasbrouck, J. (1999). The dynamics of discrete bid and ask quotes. *Journal of Finance 54*(6), 2109–42.

Kamstra, M. and M. A. Milevsky (2005). Waiting for returns: Using space-time duality to calibrate financial diffusions. *Quantitative Finance 5*(3), 237–44.

Karatzas, I. and S. E. Shreve (1991). *Brownian motion and stochastic calculus* (2nd ed.). Graduate texts in mathematics ;. New York: Springer-Verlag.

Lee, S. S. and P. A. Mykland (2007, December). Jumps in financial markets: A new non-parametric test and jump dynamics. *Review of Financial Studies 20.*

Lunde, A. and A. Timmermann (2004). Duration dependence in stock prices: An analysis of bull and bear markets. *Journal of Business and Economic Statistics 22*(3), 253–73.

Mancini, C. (2006). Estimating the integrated volatility in stochastic volatility models with levy type jumps. *working paper, University of Firenze*.

Mykland, P. A. (2006). A gaussian calculus for inference from high frequency data. *Department of Statistics, University of Chicago Technical report*(563).

Pacurar, M. (2008, forthcoming). Autoregressive conditional duration (acd) models in finance: A survey of the theoretical and empirical literature. *Journal of Economic Surveys*.

Park, H. Y. (1993). Trading mechanisms and price volatility: Spot versus futures. *Review of Economics and Statistics 75*(1), 175–79.

Parkinson, M. (1980). The extreme value method for estimating the variance of the rate of return. *Journal of Business 53*(1), 61–65.

Zhang, L. (2006). Efficient estimation of stochastic volatility using noisy observations: a multi-scale approach. *Bernouilli 12*, 1019–1043.

Zhang, L., P. A. Mykland, and Y. Ait Sahalia (2005). A tale of two time scales: Determining integrated volatility with noisy high-frequency data. *Journal of the American Statistical Association 100*(472), 1394–1411.

Zhang, M. Y., J. R. Russell, and R. S. Tsay (2007). Determinants of bid and ask quotes and implications for the cost of trading.

Zumbach, G. O. (1998, March). Considering time as the random variable: the first hitting time. *Neutral Network World*, 243–253.

A Technical Appendix

A.1 Monte Carlo Experiment

The models considered in our Monte Carlo experiments are **SV0** (constant deterministic volatility)**, SV1A** (one-factor affine stochastic volatility)**, SV1L** (one-factor log stochastic volatility)**, SV2A** (two-factor affine stochastic volatility). In each model, the price process follows a driftless Brownian motion with instantaneous volatility $\sigma(t)$:

$$dp(t) = \sigma(t)\ dW_1(t)$$

We analyze separately core model specifications **SV-C** and extended specifications **SV-UJ** incorporating a U-shaped intraday volatility pattern and jumps.

A.1.1 Core Stochastic Volatility Models SV-C

The deterministic and one-factor volatility models are described by

$$\begin{array}{lcll} \textbf{SV0-C} & : & \sigma(t) & = \theta \\ \textbf{SV1A-C} & : & d\sigma^2(t) & = \eta\ \left[\theta - \sigma^2(t)\right] dt + \nu\sigma(t)\ dW_2(t) \\ \textbf{SV1L-C} & : & d\log\sigma^2(t) & = \eta\ \left[\theta - \log\sigma^2(t)\right] dt + \nu\ dW_2(t) \end{array}$$

with the leverage effect in the one-factor models captured by the instantaneous correlation

$$\rho = corr(dW_1(t), dW_2(t))$$

The parameters for the one factor models are calibrated as in Andersen, Benzoni, and Lund (2002).

The two-factor stochastic volatility model is described by

$$\begin{array}{lcll} \textbf{SV2A-C} & : & \sigma^2(t) & = \sigma_1^2(t) + \sigma_2^2(t) \\ & & d\sigma_1^2(t) & = \eta_1\ \left[\theta_1 - \sigma_1^2(t)\right] dt + \nu_1\sigma_1(t)\ dW_{21}(t) \\ & & d\sigma_2^2(t) & = \eta_2\ \left[\theta_2 - \sigma_2^2(t)\right] dt + \nu_2\sigma_2(t)\ dW_{22}(t) \end{array}$$

with W_{21}, W_{22} independent and the leverage effect captured by the instantaneous correlations

$$\begin{array}{lcl} \rho_1 & = & corr(dW_1(t), dW_{21}(t)) \\ \rho_2 & = & corr(dW_1(t), dW_{22}(t)) \end{array}$$

The two factor model parameters are calibrated as in Andersen, Bollerslev, and Meddahi (2005).

Across all model specifications, the unconditional IV of each day is calibrated to $\theta = \theta_1 + \theta_2 = 0.000159$ corresponding to an annualized volatility of 20% (assuming 252 trading days per year). This roughly matches the average level of volatility observed in our DJ 30 sample between January 2005 and May 2007.

A.1.2 Models SV-UJ with Intraday U-Shaped Volatility Pattern and Jumps

We extend each of the above four core models to incorporate both a deterministic intraday U-shaped volatility pattern and price jumps, resulting in the models **SV0-UJ, SV1A-UJ, SV1L-UJ,** and **SV2A-UJ**.

Following Hasbrouck (1999) we model the diurnal volatility U-shape as the sum of two exponentials:

$$\mathbb{E}\left[\sigma(t)\right] = C + A\ \left[e^{-at} + e^{-b(1-t)}\right]\ ,\quad t \in [0;1]$$

where the constants are calibrated to produce a strong asymmetric U-shape with variance at the open ($t = 0$) more than 3 times the midday variance ($t = 1/2$) and variance at the close about 1.5 times the midday variance.

Price jumps are introduced by extending the log-price process as

$$dp(t) = \sigma(t)\ dW_1(t) + dJ_t$$

where the Poisson jump process (J_t) is assumed independent of (W_1, W_2). In order to stress test our estimator, we calibrate the process to match "jump days" on which a single Gaussian jump accounts for an average increase of 25% in realized volatility (i.e. the jump contribution JV is 25% of IV or, equivalently, 20% of QV = IV + JV).

A.2 Duality Results

Proposition A.1 *Define the following standard Brownian functionals*

$$H_t = \sup_{\theta\in[0;t]} B_\theta,\quad M_t = \sup_{\theta\in[0;t]} |B_\theta|\,,\quad R_t = \sup_{\theta\in[0;t]} B_\theta - \inf_{\theta\in[0;t]} B_\theta$$

and let (for $h > 0$)

$$\tau_h^{HT} = \inf\{t|H_t = h\},\quad \tau_h^{ET} = \inf\{t|M_t = h\},\quad \tau_h^{RT} = \inf\{t|R_t = h\}$$

be the first range time, first exit time and first hitting time respectively, then we have the following identities in distribution

$$H_1 \overset{\mathcal{D}}{=} \frac{1}{\left(\tau_1^{HT}\right)^{1/2}},\quad M_1 \overset{\mathcal{D}}{=} \frac{1}{\left(\tau_1^{ET}\right)^{1/2}},\quad R_1 \overset{\mathcal{D}}{=} \frac{1}{\left(\tau_1^{RT}\right)^{1/2}},$$

Proof. *The scaling property of Brownian motion*

$$B_{t/h^2} \overset{\mathcal{D}}{=} \frac{1}{h} B_t$$

implies that :

$$\begin{aligned}\Pr\left\{H_t < h\right\} &= \Pr\left\{\sup_{0\le t\le 1} \frac{1}{h} B_t < 1\right\} = \Pr\left\{\sup_{0\le t\le h^{-2}} B_t < 1\right\} \\ &= \Pr\left\{\tau_1^{HT} > h^{-2}\right\} = \Pr\left\{\frac{1}{\left(\tau_1^{HT}\right)^{1/2}} < h\right\}\end{aligned}$$

The corresponding results for M_t and R_t are obtained analogously. ■

It follows that the passage time estimators of σ^p based on $[\tau_1^{HT}]^{-p/2}$, $[\tau_1^{ET}]^{-p/2}$, $[\tau_1^{RT}]^{-p/2}$ are the duals to the corresponding magnitude-based estimators using H_1^p, M_1^p, R_1^p. The powers of particular interest for finance applications are $p = 1, 2, 4$.

A.3 Passage time results

Lemma A.2 *Let τ_h be the first exit time, the first hitting time or the first range time as given in (6) for a driftless Brownian motion with constant volatility σ^2, then*

$$\tau_h \overset{\mathcal{D}}{=} \frac{h^2}{\sigma^2}\tilde{\tau}_1$$

where $\tilde{\tau}_1$ is the corresponding passage time of a standard Brownian motion with threshold $h = 1$.

Proof. This is clear from the moment generating functions given in Table 1:

$$\mathbb{E}\left[e^{-\alpha\left(\tilde{\tau}_1 \frac{h^2}{\sigma^2}\right)}\right] = \mathbb{E}\left[e^{-\left(\alpha \frac{h^2}{\sigma^2}\right)\ \tilde{\tau}_1}\right] = \mathcal{L}_{\tau_h}(\alpha)$$

■

Proposition A.3 *If $\{\tau_{i,h}\}$ is an i.i.d sample of N first passage times from the interval $[-h; h]$ of a driftless Brownian motion with $B_0 = 0$ and constant volatility σ, then the expected value of the volatility estimator based on the first exit time moment is given by*

$$\mathbb{E}\left[\frac{h^2}{\frac{1}{N}\sum_{i=1}^{N}\tau_{i,h}}\right] = \mu_1^{(N)}\ \sigma^2$$

where

$$\mu_1^{(N)} = \begin{cases} N\int_0^\infty \frac{1}{\left[\cosh(\sqrt{2\lambda})\right]^N} d\lambda & \textit{(first exit time)} \\ N\int_0^\infty \frac{1}{\left[\cosh(\sqrt{\lambda/2})\right]^{2N}} d\lambda & \textit{(first range time)} \\ \frac{1}{N} & \textit{(first hitting time)} \end{cases}$$

Moreover, asymptotically as $N \to \infty$

$$\mu_1^{(N)} = \begin{cases} 1 + \frac{2}{3N} + O(\frac{1}{N^2}) & \textit{(first exit time)} \\ 1 + \frac{1}{3N} + O(\frac{1}{N^2}) & \textit{(first range time)} \end{cases}$$

Proof. *By independence the moment generating function of the convolution $\tau_{1,h} + \cdots + \tau_{N,h}$ is given by $\left[\mathcal{L}_{\tau_h}(\alpha)\right]^N$. We therefore have*

$$\mathbb{E}\left[\frac{h^2}{\frac{1}{N}\sum_{i=1}^{N}\tau_i}\right] = h^2 N \int_0^\infty \left[\mathcal{L}_{\tau_h}(\alpha)\right]^N\ d\alpha$$

The result then follows from the change of variables $\lambda = \frac{\alpha h^2}{\sigma^2}$. The asymptotic approximation can be derived for the first exit time and the first range time via a mean value expansion:

$$\mathbb{E}\left[\frac{h^2}{\frac{1}{N}\sum_{i=1}^{N}\tau_i}\right] = \mathbb{E}\left[\frac{h^2}{\mathbb{E}\tau + \frac{1}{N}\sum_{i=1}^{N}(\tau_i - \mathbb{E}\tau)}\right] = \sigma^2 \times \mathbb{E}\left[\frac{1}{1 + \frac{\frac{1}{N}\sum_{i=1}^{N}(\tau_i - \mathbb{E}\tau)}{\mathbb{E}\tau}}\right]$$

A second order Taylor expansion of $1/(1+x)$ *around* 1 *yields:*

$$\begin{aligned} &\approx \quad \sigma^2 \times \mathbb{E}\left[1 - \frac{\frac{1}{N}\sum_{i=1}^{N}(\tau_i - \mathbb{E}\tau)}{\mathbb{E}\tau} + \left(\frac{\frac{1}{N}\sum_{i=1}^{N}(\tau_i - \mathbb{E}\tau)}{\mathbb{E}\tau}\right)^2 - \cdots\right] \\ &\approx \quad \sigma^2 \times \left[1 + \frac{\mathbb{E}\frac{1}{N^2}\sum_{i=1}^{N}(\tau_i - \mathbb{E}\tau)^2}{(\mathbb{E}\tau)^2} + O(1/N^2)\right] = \sigma^2\left[1 + \frac{1}{N}\frac{\mathbb{V}\tau}{(\mathbb{E}\tau)^2} + O(1/N^2)\right] \end{aligned}$$

from which the result follows by calculation of the first two moments of the relevant passage time using the moment generating function. ■

Corollary A.4 *The expectation of the reciprocal passage time satisfies*

$$\mathbb{E}\left[\frac{h^2}{\tau_h}\right] \equiv \mu_1\ \sigma^2 = \begin{cases} 2\mathcal{C}\ \sigma^2 & \textit{(first exit time)} \\ (4\log 2)\ \sigma^2 & \textit{(first range time)} \\ \sigma^2 & \textit{(first hitting time)} \end{cases}$$

Proof. *Apply Proposition A.3 with* $N = 1$. ■

Proposition A.5 *If* $\{\tau_{i,h}\}$ *is an i.i.d sample of* N *first exit times from the interval* $[-h; h]$ *of a driftless Brownian motion with* $B_0 = 0$ *and constant volatility* σ*, then the second moment of the volatility estimator based on the first exit time moment is given by*

$$\mathbb{E}\left[\frac{h^4}{\left(\frac{1}{N}\sum_{i=1}^{N}\tau_{i,h}\right)^2}\right] = \mu_2^{(N)}\ \sigma^4$$

where

$$\mu_2^{(N)} = \begin{cases} N^2\int_0^\infty\int_\Lambda^\infty \frac{1}{\left[\cosh(\sqrt{2\lambda})\right]^N}\ d\lambda\ d\Lambda & \textit{(first exit time)} \\ N^2\int_0^\infty\int_\Lambda^\infty \frac{1}{\left[\cosh(\sqrt{\lambda/2})\right]^{2N}}\ d\lambda\ d\Lambda & \textit{(first range time)} \\ \frac{3}{N^2} & \textit{(first hitting time)} \end{cases}$$

Proof. *By independence the moment generating function of the convolution* $\tau_{1,h} + \cdots + \tau_{N,h}$ *is given by* $\left[\mathcal{L}_{\tau_h}(\alpha)\right]^N$*. We therefore have*

$$E\left[\frac{1}{\left(\sum_{i=1}^{N}\tau_{i,h}\right)^2}\right] = \int_0^\infty\int_A^\infty \left[\mathcal{L}_{\tau_h}(\alpha)\right]^N\ d\alpha\ dA$$

■

Corollary A.6 *The second moment of the reciprocal passage time satisfies*

$$\mathbb{E}\left[\frac{h^4}{\tau_h^2}\right] \equiv \mu_2\ \sigma^4 = \begin{cases} 6\ \beta(4)\ \sigma^4 & \textit{(first exit time)} \\ 9\ \zeta(3)\ \sigma^4 & \textit{(first range time)} \\ 3\ \sigma^4 & \textit{(first hitting time)} \end{cases}$$

Proof. *Apply Proposition A.5 with* $N = 1$. ■

Corollary A.7 *Let $\hat{\sigma}_i^2 = \frac{1}{\mu_1}\frac{h^2}{\tau_h(t_i)}$ be the volatility estimate based on a single passage time observation $\tau_h(t_i)$, then $\mathbb{E}[\hat{\sigma}_i^2] = \sigma^2$ and*

$$\mathbb{V}[\hat{\sigma}_i^2] = \left(\frac{\mu_2}{\mu_1^2} - 1\right)\ \sigma^4 = \begin{cases} \left(\frac{6}{4\beta(2)^2} - 1\right)\sigma^4 & \approx & 0.7681\ \sigma^4 & \textit{(first exit time)} \\ \left(\frac{9}{(4\log 2)^2}\frac{\zeta(3)\ \sigma^4}{} - 1\right)\sigma^4 & \approx & 0.4073\ \sigma^4 & \textit{(first range time)} \\ \left(\frac{3}{2^2} - 1\right)\sigma^4 & \approx & 2.000\ \sigma^4 & \textit{(first hitting time)} \end{cases}$$

Proof. *Apply Corollary A.4 and A.6.* ■

A.4 Discretization bias correction

We state the multiplicative discretization bias corrections based on the following asymptotic results due to Asmussen, Glynn, and Pitman (1995).

Lemma A.8 *Let B_t be a driftless Brownian motion on $[0;1]$ with volatility σ^2 and let $X_t = B_{\frac{[tN]}{N}}$ be the embedded (discretely observed) random walk observed at N points. Define $M = \sup_{t\in[0;1]} |B_t|$, $R = \sup_{t\in[0;1]} B_t - \inf_{t\in[0;1]} B_t$, $M_N = \sup_{t\in[0;1]} |X_t|$, $R_N = \sup_{t\in[0;1]} X_t - \inf_{t\in[0;1]} X_t$. Then*

$$\begin{aligned} \mathbb{E}[M_N] &= \mathbb{E}[M] + \frac{\zeta(1/2)}{\sqrt{2\pi}}\frac{\sigma}{\sqrt{N}} + o(\frac{1}{\sqrt{N}}) \\ \mathbb{E}[R_N] &= \mathbb{E}[R] + 2\frac{\zeta(1/2)}{\sqrt{2\pi}}\frac{\sigma}{\sqrt{N}} + o(\frac{1}{\sqrt{N}}) \\ \mathbb{E}[M_N^2] &= \mathbb{E}[M^2] + 2\sqrt{\frac{\pi}{2}}\frac{\zeta(1/2)}{\sqrt{2\pi}}\frac{\sigma^2}{\sqrt{N}} + o(\frac{1}{\sqrt{N}}) \\ \mathbb{E}[R_N^2] &= \mathbb{E}[R^2] + 4\sqrt{\frac{8}{\pi}}\frac{\zeta(1/2)}{\sqrt{2\pi}}\frac{\sigma^2}{\sqrt{N}} + o(\frac{1}{\sqrt{N}}) \end{aligned}$$

where $\zeta(1/2)/\sqrt{2\pi} \approx -0.5826$.

Proof. Follows by specializing Proposition 3 in Asmussen, Glynn, and Pitman (1995) for M_N and R_N. ■

Corollary A.9 *The following relationships hold approximately for the absolute maximum M and the range R of a Brownian motion and the absolute maximum M_N and the range R_N of a random walk in the same interval, as defined above:*

$$\begin{aligned} \mathbb{E}\left[M^2\right] &\approx f_M(N) \times \mathbb{E}\left[M_N^2\right] \\ \mathbb{E}\left[R^2\right] &\approx f_R(N) \times \mathbb{E}\left[R_N^2\right] \end{aligned}$$

where

$$\begin{aligned} f_M(N) &= 1 - \frac{1}{2\mathcal{C}}\zeta(1/2)\frac{1}{\sqrt{N}} \\ f_R(N) &= 1 - \frac{2}{\pi\ln 2}\zeta(1/2)\frac{1}{\sqrt{N}} \end{aligned}$$

and $\mathcal{C}$ is Catalan's constant.

Proof. Obtained by rearranging the last two expressions and substituting the known values $\mathbb{E}\left[R^2\right] = 4\ln 2\ \sigma^2$ and $\mathbb{E}\left[M^2\right] = 2\mathcal{C}\ \sigma^2$. ■

A.5 Constant Volatility

For simplicity we here limit attention to the uni-directional IV estimation. The derivation for the bi-directional case follows analogously. Let $0 \equiv t_0, t_1, \ldots, t_N \equiv 1$ be a set of grid points partitioning the interval $[0;1]$ and let $\Delta_i = t_{i+1} - t_i$ be the mesh size. The passage time based IV estimators are of the form

$$\widehat{DV}_{N,h} = \sum_{i=0}^{N-1} \mu_1^{-1} \frac{h^2}{\tau_h(t_i)} \Delta_i \tag{20}$$

where μ_1 is the constant given in Table 1 for the first hitting time, first exit time and first range time based estimators respectively. It is then clear that $\mathbb{E}[\widehat{DV}_{N,h}] = \sigma^2 = IV$ so that the estimator is unbiased.

The variance of the estimator $\widehat{DV}_{N,h}$ is given by

$$Var[\widehat{DV}_{N,h}] = \sum_{i=0}^{N-1} Var[\mu_1^{-1} \frac{h^2}{\tau_h(t_i)}]\ \Delta_i^2 + \mu_1^{-2} h^4 \sum_{i \neq j} \Delta_i \Delta_j Cov\left(\frac{1}{\tau_h(t_i)}, \frac{1}{\tau_h(t_j)}\right) \tag{21}$$

We would like to show that, if h shrinks to zero at an appropriate rate, then $Var[\widehat{DV}_{N,h}] = O\left(1/N\right)$ and, moreover, that the local estimates of volatility at distinct grid points are asymptotically independent (i.e the second term in (21) is $o(1/N)$).

The first term is

$$\sum_{i=0}^{N-1} Var[\mu_1^{-1} \frac{h^2}{\tau_h(t_i)}]\ \Delta_i^2 = \left(\frac{\mu_2}{\mu_1^2} - 1\right) \sigma^4 \sum_{i=0}^{N-1} \Delta_i^2$$

A sufficient condition for this term to be $O(1/N)$ is therefore that the mesh size satisfies $\max_{0 \leq i \leq N} \Delta_i = O(1/N)$.

Next we consider the second term involving the covariance between reciprocal passage times measured from distinct grid points $t_i < t_j$ with $\Delta_{i,j} = t_j - t_i$ (to simplify notation we write $\tau_h(t_i) = \tau_i$ and $\tau_h(t_j) = \tau_j$) :

$$Cov\left(\frac{1}{\tau_i}, \frac{1}{\tau_j}\right) = \mathbb{E}\left(\frac{1}{\tau_i}\frac{1}{\tau_j}\right) - \mathbb{E}\left(\frac{1}{\tau_i}\right)\mathbb{E}\left(\frac{1}{\tau_j}\right)$$

For the cross product of reciprocal waiting times we have[22]:

$$\mathbb{E}\left(\frac{1}{\tau_i}\frac{1}{\tau_j}\right) = \mathbb{E}\left(\frac{1}{\tau_i}\frac{1}{\tau_j}\middle| \tau_i < \Delta_{i,j}\right) \Pr\left\{\tau_i < \Delta_{i,j}\right\} + \mathbb{E}\left(\frac{1}{\tau_i}\frac{1}{\tau_j}\middle| \tau_i \geq \Delta_{i,j}\right) \Pr\left\{\tau_i \geq \Delta_{i,j}\right\}$$

[22]Note that τ_j is *not* independent of τ_i. We exploit here that $\mathbb{E}\left(\frac{1}{\tau_j}\middle| \tau_i \geq \Delta_{i,j}\right) = \mathbb{E}\left(\frac{1}{\tau_j}\right)$ since the event $\{\tau_i \geq \Delta_{i,j}\}$, as of time t_j, only reveals information about the initial value at t_j of the process but nothing about the subsequent passage time τ_j.

$$\leq \mathbb{E}\left(\frac{1}{\tau_i}\middle|\, \tau_i < \Delta_{i,j}\right)\mathbb{E}\left(\frac{1}{\tau_j}\right)\Pr\left\{\tau_i < \Delta_{i,j}\right\} + \mathbb{E}\left(\frac{1}{\tau_j}\middle|\, \tau_i \geq \Delta_{i,j}\right)\frac{1}{\Delta_{i,j}}\Pr\left\{\tau_i \geq \Delta_{i,j}\right\}$$

$$\leq \mathbb{E}\left(\frac{1}{\tau_i}\right)\mathbb{E}\left(\frac{1}{\tau_j}\right) + \mathbb{E}\left(\frac{1}{\tau_j}\right)\frac{1}{\Delta_{i,j}}\Pr\left\{\tau_i \geq \Delta_{i,j}\right\}$$

This leads to the estimate

$$Cov\left(\frac{1}{\tau_i}, \frac{1}{\tau_j}\right) \leq \mathbb{E}\left(\frac{1}{\tau_j}\right)\frac{1}{\Delta_{i,j}}\Pr\left\{\tau_i \geq \Delta_{i,j}\right\} = \mu_1\frac{\sigma^2}{h^2}\frac{1}{\Delta_{i,j}}\Pr\left\{\tau_i \geq \Delta_{i,j}\right\}$$

The probability $\Pr\{\tau_i \geq \Delta_{i,j}\}$ can be bounded by the hitting time probability (Table 1) for which:

$$\begin{aligned}
\Pr\left\{\tau_i \geq \Delta_{i,j}\right\} &= \int_{\Delta_{i,j}}^{\infty}\frac{h}{\sigma\sqrt{2\pi}t^{3/2}}e^{-\frac{h^2}{2t\sigma^2}}dt = -\frac{2}{\sqrt{\pi}}\int_{\Delta_{i,j}}^{\infty}e^{-\frac{h^2}{2t\sigma^2}}d\sqrt{\frac{h^2}{2t\sigma^2}} \\
&= -\frac{2}{\sqrt{\pi}}\int_{\frac{h}{\sigma\sqrt{2\Delta_{i,j}}}}^{0}e^{-z^2}dz = \frac{2}{\sqrt{\pi}}\int_{0}^{\frac{h}{\sigma\sqrt{2\Delta_{i,j}}}}e^{-z^2}dz \\
&= \mathrm{Erf}\left[\frac{h}{\sigma\sqrt{2\Delta_{i,j}}}\right] = \sqrt{\frac{2}{\pi}}\frac{1}{\sigma\sqrt{\Delta_{i,j}}}h + O\left(\frac{h^3}{\Delta_{i,j}^{3/2}}\right) ,
\end{aligned}$$

where the last equality follows from the Taylor series expansion of the Erf function,

$$\mathrm{Erf}[x] = \frac{2}{\sqrt{\pi}}\sum_{n=0}^{\infty}\frac{(-1)^n}{(2n+1)n!}x^{2n+1} .$$

Thus, for small h,

$$Cov\left(\frac{1}{\tau_i}, \frac{1}{\tau_j}\right) \leq \sqrt{\frac{2}{\pi}}\mu_1\frac{\sigma}{h}\frac{1}{\Delta_{i,j}^{3/2}} + O\left(\frac{h}{\Delta_{i,j}^{5/2}}\right)$$

and

$$\mu_1^{-2}h^4\sum_{i\neq j}\Delta_i\Delta_j Cov\left(\frac{1}{\tau_i}, \frac{1}{\tau_j}\right) \leq \sqrt{\frac{2}{\pi}}\mu_1^{-1}\sigma h^3\sum_{i\neq j}\frac{\Delta_i\Delta_j}{\Delta_{i,j}^{3/2}} + \sum_{i\neq j}\frac{\Delta_i\Delta_j}{\Delta_{i,j}^{5/2}}O\left(h^5\right) \tag{22}$$

Under the (slightly) strengthened assumption that $\forall i : \Delta_i = O(1/N)$, we have

$$\begin{aligned}
\left|\sum_{i\neq j}\frac{\Delta_i\Delta_j}{\Delta_{i,j}^{3/2}}\right| &\approx \frac{1}{\sqrt{N}}\sum_{i\neq j}\frac{1}{|j-i|^{3/2}} = O\left(\sqrt{N}\right) \\
\left|\sum_{i\neq j}\frac{\Delta_i\Delta_j}{\Delta_{i,j}^{5/2}}\right| &\approx \sqrt{N}\sum_{i\neq j}\frac{1}{|j-i|^{5/2}} = O\left(N^{3/2}\right)
\end{aligned}$$

so that (22) will be of order $o(1/N)$ if $h = o(N^{-1/2})$. Thus the local volatility estimates corre-

sponding to distinct grid points are asymptotically uncorrelated if the squared thresholds shrink faster than the mesh size:

Proposition A.10 *Define* $\widehat{DV}_{N,h} = \sum_{i=0}^{N-1} \mu_1^{-1} \frac{h^2}{\tau_h(t_i)} \Delta_i$ *as the IV estimator based on passage time durations (either the first hitting time, the first exit time or the first range time), where* N *denotes the number of grid points and* h *denotes the threshold level. If the mesh size is* $\Delta_i = O(1/N)$ *and the threshold is chosen to be* $h = o(N^{-1/2})$*, then, as* $N \to \infty$

$$\sqrt{N}(\widehat{DV}_{N,h} - IV) \xrightarrow{D} N(0, (\mu_2/\mu_1^2 - 1)\ \sigma^4)$$

where the constants μ_1, μ_2 *are given in Table 1.*

A.6 Stochastic volatility

Assumption (SV) *Assume that the volatility process is independent of the Brownian motion and that*

$$\exists \kappa > 0 : \sup_{s,t} |\sigma_s^2 - \sigma_t^2| < \kappa |s - t| \qquad (SV_1)$$

$$\forall i : \Delta_i = O\left(\tfrac{1}{N}\right) \qquad (SV_2)$$

$$\inf_t\ \sigma_t^2 \geq \varepsilon > 0 \qquad (SV_3)$$

$$h = o(N^{-1/2}) \qquad (SV_4)$$

The IV estimation error can be decomposed as

$$IV - \widehat{DV}_{N,h} = \int_0^1 \sigma_u^2\ du - \sum_{i=0}^{N-1} \hat{\sigma}_{t_i}^2 \Delta_i = \underbrace{\int_0^1 \sigma_u^2\ du - \sum_{i=0}^{N-1} \sigma_{t_i}^2 \Delta_i}_{\text{Riemann approximation}} + \underbrace{\sum_{i=0}^{N-1} \left(\sigma_{t_i}^2 - \hat{\sigma}_{t_i}^2\right) \Delta_i}_{\text{sum of local estimation errors}} \qquad (23)$$

where the local estimator of volatility at the grid point t_i is given by $\hat{\sigma}_{t_i}^2 = \mu_1^{-1} \frac{h^2}{\tau_h(t_i)}$ and define the passage time with stochastic volatility as in (6) where $B_t = \int_0^t \sigma_u\ dW_u$

The first term in (23) is easily dealt with:

Lemma A.11 *The Riemann approximation error is* $O(N^{-1})$ *as the mesh size,* $\max_i \Delta_i \to 0$.

Proof. *This follows readily from the Lipschitz assumption* (SV_1) *and mesh size assumption* (SV_2)*,*

$$\left| \int_0^1 \sigma_u^2\ du - \sum_{i=0}^{N-1} \sigma_{t_i}^2 \Delta_i \right| = \sum_{i=0}^{N-1} \int_0^{\Delta_i} \left| (\sigma_{t_i+u}^2 - \sigma_{t_i}^2) \right|\ du \leq \sum_{i=0}^{N-1} \int_0^{\Delta_i} \kappa u\ du = \frac{1}{2}\kappa \sum_{i=0}^{N-1} \Delta_i^2 = O\left(\frac{1}{N}\right) \qquad (24)$$

■

This implies that, under Assumption SV, the Riemann approximation error will not matter asymptotically.

Next we turn to the sum of local estimation errors which we shall first consider term by term. We will need the following lemmas and definitions.

Lemma A.12 *If Assumption SV is satisfied, then, conditional on the value of* $IV = \int_0^1 \sigma_u^2 \, du$*, the terms in the sum* $\sum_{i=0}^{N-1} \left(\sigma_{t_i}^2 - \hat{\sigma}_{t_i}^2 \right) \Delta_i$ *are asymptotically uncorrelated in the sense that*

$$\sum_{i \neq j} \Delta_i \Delta_j Cov \left(\hat{\sigma}_{t_i}^2, \hat{\sigma}_{t_j}^2 \right) = o(N^{-1})$$

Proof. *From the Lipschitz assumption, it follows that* $\sup_{t \in [0;1]} \sigma_t^2 \leq \bar{\sigma}_{\max}^2 \equiv IV + \frac{1}{2}\kappa$ *must hold. Borrowing from the arguments in the constant volatility case we then have*

$$Cov \left(\frac{h^2}{\tau_h(t_i)}, \frac{h^2}{\tau_h(t_j)} \right) \leq h^4 \, \mathbb{E} \left(\frac{1}{\tau_h(t_j)} \right) \frac{1}{\Delta_{i,j}} \Pr \left\{ \tau_h(t_i) \geq \Delta_{i,j} \right\} \leq h^4 \, \mu_1 \frac{\bar{\sigma}_{\max}^2}{h^2} \frac{1}{\Delta_{i,j}} \Pr \left\{ \tau_h(t_i) \geq \Delta_{i,j} \right\}$$

and the asymptotic uncorrelatedness follows from the conditions of Assumption SV (in particular $(SV_2) - (SV_4)$*) which imply that the right hand side is* $o(1/N)$*.* ■

We are therefore justified in focusing on the asymptotic behavior of the local estimation error at each grid point. We proceed by introducing the time changed process:

Definition A.13 *For each* t_i*, let* B^* *be a Brownian motion with* $B_0^* = 0$ *and define the time change* $T_t = \int_0^t \sigma_{t_i+u}^2 du$ *and the stopping times (depending on which estimator is considered)*

$$\tau_h^*(t_i) = \begin{cases} \inf \left\{ t \mid \left| B_{T_t}^* \right| > h \right\} & \textit{(first exit time)} \\ \inf \left\{ t \mid \max_{0 \leq u \leq t} B_{T_t}^* - \min_{0 \leq u \leq t} B_{T_t}^* > h \right\} & \textit{(first range time)} \\ \inf \left\{ t \mid B_{T_t}^* > h \right\} & \textit{(first hitting time)} \end{cases}$$

$$\tilde{\tau}_h^*(t_i) = \begin{cases} \inf \left\{ t \mid \left| B_{t\sigma_{t_i}^2}^* \right| > h \right\} & \textit{(first exit time)} \\ \inf \left\{ t \mid \max_{0 \leq u \leq t} B_{t\sigma_{t_i}^2}^* - \min_{0 \leq u \leq t} B_{t\sigma_{t_i}^2}^* > h \right\} & \textit{(first range time)} \\ \inf \left\{ t \mid B_{t\sigma_{t_i}^2}^* > h \right\} & \textit{(first hitting time)} \end{cases}$$

$$\tau_h^{\max} = \inf \left\{ t \mid B_{t\varepsilon}^* > h \right\}$$

Lemma A.14 *We have the following relationships (for a given passage time estimator)*

$$\begin{aligned} &\tau_h(t_i) \stackrel{\mathcal{D}}{=} \tau_h^*(t_i) && (i) \\ &0 \leq \tau_h^*(t_i) \leq \tau_h^{\max} = O_p(h) && (ii) \\ &E \left[\tfrac{1}{\tilde{\tau}_h^*(t_i)} \right] = \mu_1 \tfrac{\sigma_{t_i}^2}{h^2} && (iii) \\ &\tfrac{1}{\tilde{\tau}_h^*(t_i)} - \tfrac{1}{\tau_h^*(t_i)} = O_p(1) && (iv) \end{aligned}$$

Proof. *(i) follows directly from a standard time change argument. (ii) is immediate from the definition and the fact that* $\tau_h^{\max}$ *can be seen as the first hitting time of a Brownian motion with constant volatility* ε*. Similarly (iii) follows from the interpretation of* $\tilde{\tau}_h^*(t_i)$ *as the first passage time of a constant volatility Brownian motion. To get (iv) we exploit the pathwise relationship* $\sigma_{t_i}^2 \tilde{\tau}_h^*(t_i) = \int_0^{\tau_h^*(t_i)} \sigma_{t_i+u}^2 du$ *and the Lipschitz assumption* (SV_1) *:*

$$\sigma_{t_i}^2 \tau_h^* - \tfrac{1}{2}\kappa\tau_h^{*2} \leq \left| \int_0^{\tau_h^*} \sigma_{t_i+u}^2 \, du \right| \leq \sigma_{t_i}^2 \tau_h^* + \tfrac{1}{2}\kappa\tau_h^{*2} \tag{25}$$

Thus we have the bounds on τ_h^* *in terms of* $\tilde{\tau}_h^*$ *:*

$$\frac{-\sigma_{t_i}^2 + \sqrt{\sigma_{t_i}^4 + 2\kappa\sigma_{t_i}^2 \tilde{\tau}_h^*}}{\kappa} \leq \tau_h^* \leq \frac{\sigma_{t_i}^2 - \sqrt{\sigma_{t_i}^4 - 2\kappa\sigma_{t_i}^2 \tilde{\tau}_h^*}}{\kappa}$$

from which it follows that

$$\liminf_{\tilde{\tau}_h^* \to 0} \frac{1}{\tilde{\tau}_h^*} - \frac{1}{\tau_h^*} = \liminf_{\tilde{\tau}_h^* \to 0} \frac{\tau_h^* - \tilde{\tau}_h^*}{\tilde{\tau}_h^* \tau_h^*} = \lim_{\tilde{\tau}_h^* \to 0} \frac{-\sigma_{t_i}^2 + \sqrt{\sigma_{t_i}^4 + 2\kappa\sigma_{t_i}^2 \tilde{\tau}_h^*} - \kappa\tilde{\tau}_h^*}{\tilde{\tau}_h^* \left(-\sigma_{t_i}^2 + \sqrt{\sigma_{t_i}^4 + 2\kappa\sigma_{t_i}^2 \tilde{\tau}_h^*}\right)} = -\frac{\kappa}{2\sigma_{t_i}^2}$$

$$\limsup_{\tilde{\tau}_h^* \to 0} \frac{1}{\tilde{\tau}_h^*} - \frac{1}{\tau_h^*} = \limsup_{\tilde{\tau}_h^* \to 0} \frac{\tau_h^* - \tilde{\tau}_h^*}{\tilde{\tau}_h^* \tau_h^*} = \lim_{\tilde{\tau}_h^* \to 0} \frac{\sigma_{t_i}^2 - \sqrt{\sigma_{t_i}^4 - 2\kappa\sigma_{t_i}^2 \tilde{\tau}_h^*} - \kappa\tilde{\tau}_h^*}{\tilde{\tau}_h^* \left(\sigma_{t_i}^2 - \sqrt{\sigma_{t_i}^4 - 2\kappa\sigma_{t_i}^2 \tilde{\tau}_h^*}\right)} = +\frac{\kappa}{2\sigma_{t_i}^2}$$

Finally, since $\tilde{\tau}_h^* = O_p(h)$*, we have that* $\frac{1}{\tilde{\tau}_h^*} - \frac{1}{\tau_h^*} = O_p(1)$ *as* $h \to 0$*.* ■

Lemma A.15 *Let* $\hat{\sigma}_{t_i}^{*2} = \mu_1^{-1} \frac{h^2}{\tau_h^*(t_i)}$ *and* $\tilde{\sigma}_{t_i}^{*2} = \mu_1^{-1} \frac{h^2}{\tilde{\tau}_h^*(t_i)}$ *then* $\hat{\sigma}_{t_i}^2 \overset{\mathcal{D}}{=} \hat{\sigma}_{t_i}^{*2}$ *and* $\hat{\sigma}_{t_i}^{*2} - \tilde{\sigma}_{t_i}^{*2} = O_p(h^2)$*.*
Proof. *Follows directly from Lemma A.14.* ■

We are now ready to present our main result for the passage time estimator under stochastic volatility.

Proposition A.16 *Let* $\widehat{DV}_{N,h}$ *denote the passage time based IV estimator (either the first hitting time, the first exit time or the first range time) where* N *denotes the number of grid points. Under the conditions of Assumption SV we have as* $N \to \infty$

$$\sqrt{N}(\widehat{DV}_N - IV) \Big| IV \xrightarrow{\mathcal{D}} N(0, (\mu_2/\mu_1^2 - 1) \int_0^1 \sigma_u^4 \, du)$$

where $\nu = (\mu_2/\mu_1^2 - 1)$ *is given in (16).*
Proof. *First note that from Lemma A.15 and Assumption SV, we have*

$$\begin{aligned} &(\sigma_{t_i}^2 - \hat{\sigma}_{t_i}^2) \, \Delta_i \overset{\mathcal{D}}{=} (\sigma_{t_i}^2 - \hat{\sigma}_{t_i}^{*2}) \, \Delta_i \\ &= \underbrace{(\sigma_{t_i}^2 - \tilde{\sigma}_{t_i}^{*2}) \, \Delta_i}_{\text{“constant” volatility term}} + \underbrace{(\tilde{\sigma}_{t_i}^{*2} - \hat{\sigma}_{t_i}^{*2}) \, \Delta_i}_{\text{stochastic volatility term}} \end{aligned} \tag{26}$$

where $E\left((\sigma_{t_i}^2 - \tilde{\sigma}_{t_i}^{*2})\ \Delta_i\right) = 0$ *and* $Var\left[(\sigma_{t_i}^2 - \tilde{\sigma}_{t_i}^{*2})\ \Delta_i\right] = (\mu_2/\mu_1^2 - 1)\sigma_{t_i}^4 \Delta_i^2$. *The "stochastic volatility" term is* $(\tilde{\sigma}_{t_i}^{*2} - \hat{\sigma}_{t_i}^{*2})\ \Delta_i = O_p(N^{-4})$ *and thus will not play a role asymptotically:*

$$\sqrt{N} \sum_{i=0}^{N-1} \left(\sigma_{t_i}^2 - \hat{\sigma}_{t_i}^2\right) \Delta_i \overset{\mathcal{D}}{=} \sqrt{N} \sum_{i=0}^{N-1} (\sigma_{t_i}^2 - \tilde{\sigma}_{t_i}^{*2})\ \Delta_i + o(N^{-2})$$

Conditional on IV, Lemma A.12 guarantees that the terms are asymptotically uncorrelated so that (taking $\Delta_i = 1/N$*) :*

$$Var\left[\sqrt{N} \sum_{i=0}^{N-1} (\sigma_{t_i}^2 - \tilde{\sigma}_{t_i}^{*2})\ \Delta_i\right] = (\mu_2/\mu_1^2 - 1) \sum_{i=0}^{N-1} \sigma_{t_i}^4 \Delta_i$$

which leads to

$$\sqrt{N} \sum_{i=0}^{N-1} (\sigma_{t_i}^2 - \tilde{\sigma}_{t_i}^{*2})\ \Delta_i \xrightarrow{\mathcal{D}} N(0, (\mu_2/\mu_1^2 - 1) \int_0^1 \sigma_u^4\ du)$$

■

B Tables and Figures

Table 1: Summary of the properties of the first hitting time, the first exit time and the first range time estimators.

	First Hitting Time for Threshold $h \neq 0$	First Exit Time for Threshold $h > 0$	First Range Time for Threshold $h > 0$
Definition	$\tau_h^+(t) = \min_{\theta>0}\{W_{t+\theta} - W_t = h\}$ $\tau_h^-(t) = \min_{\theta>0}\{W_{t-\theta} - W_t = h\}$	$\tau_h^+(t) = \min_{\theta>0}\{\lvert W_{t+\theta} - W_t\rvert = h\}$ $\tau_h^-(t) = \min_{\theta>0}\{\lvert W_{t-\theta} - W_t\rvert = h\}$	$\tau_h^+(t) = \min_{\theta>0}\{\sup_{[t,t+\theta]} W_s - \inf_{[t,t+\theta]} W_s = h\}$ $\tau_h^-(t) = \min_{\theta>0}\{\sup_{[t-\theta,t]} W_s - \inf_{[t-\theta,t]} W_s = h\}$
Laplace Transform	$\mathcal{L}_{\tau_h}(\alpha) = e^{-\frac{h}{\sigma}\sqrt{2\alpha}}$	$\mathcal{L}_{\tau_h}(\alpha) = \frac{1}{\cosh\left(\frac{h}{\sigma}\sqrt{2\alpha}\right)}$	$\mathcal{L}_{\tau_h}(\alpha) = \frac{1}{\cosh^2\left(\frac{h}{\sigma}\sqrt{\frac{\alpha}{2}}\right)}$
PDF	$p_{\tau_h}(t) = \frac{h}{\sigma\sqrt{2\pi}t^{3/2}} e^{-\frac{h^2}{2t\sigma^2}}$	$p_{\tau_h}(t) = \sum_{k=-\infty}^{\infty} \frac{2h(1+4k)}{\sigma\sqrt{2\pi}t^{3/2}} e^{-\frac{(1+4k)^2h^2}{2t\sigma^2}}$	$p_{\tau_h}(t) = \sum_{k=1}^{\infty} \frac{4h(-1)^{k-1}k^2}{\sigma\sqrt{2\pi}t^{3/2}} e^{-\frac{k^2h^2}{2t\sigma^2}}$
Reciprocal Moments	$m_1 = \mathbb{E}\left[(\tau_h)^{-1}\right] = 1 \times \frac{\sigma^2}{h^2}$ $m_2 = \mathbb{E}\left[(\tau_h)^{-2}\right] = 3 \times \frac{\sigma^4}{h^4}$	$m_1 = \mathbb{E}\left[(\tau_h)^{-1}\right] = 2\beta(2) \times \frac{\sigma^2}{h^2}$ $m_2 = \mathbb{E}\left[(\tau_h)^{-2}\right] = 6\beta(4) \times \frac{\sigma^4}{h^4}$	$m_1 = \mathbb{E}\left[(\tau_h)^{-1}\right] = 4\ln 2 \times \frac{\sigma^2}{h^2}$ $m_2 = \mathbb{E}\left[(\tau_h)^{-2}\right] = 9\zeta(3) \times \frac{\sigma^4}{h^4}$
Scaling Factors	$\mu_1 = 1$ $\mu_2 = 3$	$\mu_1 = 2\beta(2) \approx 1.83193$ $\mu_2 = 6\beta(4) \approx 5.93367$	$\mu_1 = 4\ln 2 \approx 2.77259$ $\mu_2 = 9\zeta(3) \approx 10.81851$
Unidirectional Estimators	$\frac{h^2}{\mu_1\tau_h^+(t)}$ or $\frac{h^2}{\mu_1\tau_h^-(t)}$	$\frac{h^2}{\mu_1\tau_h^+(t)}$ or $\frac{h^2}{\mu_1\tau_h^-(t)}$	$\frac{h^2}{\mu_1\tau_h^+(t)}$ or $\frac{h^2}{\mu_1\tau_h^-(t)}$
Bidirectional Estimator	$\frac{1}{2}\left[\frac{h^2}{\mu_1\tau_h^+(t)} + \frac{h^2}{\mu_1\tau_h^-(t)}\right]$	$\frac{1}{2}\left[\frac{h^2}{\mu_1\tau_h^+(t)} + \frac{h^2}{\mu_1\tau_h^-(t)}\right]$	$\frac{1}{2}\left[\frac{h^2}{\mu_1\tau_h^+(t)} + \frac{h^2}{\mu_1\tau_h^-(t)}\right]$
Unidirectional Variance	$\left(\frac{\mu_2}{\mu_1^2} - 1\right) \times \sigma^4 = 2 \times \sigma^4$	$\left(\frac{\mu_2}{\mu_1^2} - 1\right) \times \sigma^4 \approx 0.76809 \times \sigma^4$	$\left(\frac{\mu_2}{\mu_1^2} - 1\right) \times \sigma^4 \approx 0.40733 \times \sigma^4$
Bidirectional Variance	$\frac{1}{2}\left(\frac{\mu_2}{\mu_1^2} - 1\right) \times \sigma^4 = 1 \times \sigma^4$	$\frac{1}{2}\left(\frac{\mu_2}{\mu_1^2} - 1\right) \times \sigma^4 \approx 0.38405 \times \sigma^4$	$\frac{1}{2}\left(\frac{\mu_2}{\mu_1^2} - 1\right) \times \sigma^4 \approx 0.20367 \times \sigma^4$

Table 2: Descriptive statistics for the 33 stocks that were part of the Dow Jones 30 index between January 1, 2005 and May 31, 2007.

Symbol	Average Price ($)	Average 2-min RV ($\times 10^{-4}$)	Average 2-min BV ($\times 10^{-4}$)	Average Log Spread ($\times 10^{-4}$)	Average Ratio Log Spread/Sigma	Average # zero returns per day lasting above 30s / 60s / 120s
AA	30	2.22	2.10	4.80	0.03	161 / 48 / 11
AIG	64	1.00	0.95	2.73	0.03	127 / 30 / 5
AXP	55	0.81	0.76	2.84	0.03	161 / 48 / 11
BA	74	1.26	1.19	2.97	0.03	113 / 21 / 3
BAC	48	0.68	0.64	2.87	0.04	161 / 49 / 11
C	49	0.77	0.73	2.70	0.03	144 / 42 / 9
CAT	71	1.62	1.54	3.01	0.02	131 / 27 / 4
CVX	63	1.64	1.58	2.88	0.02	82 / 15 / 2
DD	45	1.19	1.12	3.48	0.03	154 / 45 / 10
DIS	29	1.08	1.01	4.46	0.04	177 / 67 / 19
EK	26	2.19	1.93	5.48	0.04	189 / 81 / 28
GE	35	0.63	0.59	3.35	0.04	182 / 70 / 20
GM	30	3.70	3.49	5.09	0.03	162 / 51 / 13
HD	39	1.35	1.28	3.69	0.03	149 / 39 / 8
HPQ	32	1.61	1.50	4.32	0.04	163 / 55 / 14
IBM	86	0.84	0.80	2.43	0.03	89 / 14 / 2
INTC	22	1.67	1.51	4.63	0.04	206 / 99 / 35
IP	34	1.36	1.25	4.28	0.04	191 / 71 / 20
JNJ	64	0.52	0.49	2.47	0.04	130 / 32 / 6
JPM	42	0.88	0.83	3.27	0.04	163 / 52 / 12
KO	44	0.59	0.55	3.15	0.04	166 / 57 / 15
MCD	36	1.22	1.13	3.90	0.04	164 / 55 / 14
MMM	78	0.91	0.87	2.74	0.03	141 / 31 / 5
MO	74	1.09	0.93	2.38	0.02	142 / 33 / 5
MRK	37	1.58	1.38	3.84	0.03	165 / 54 / 13
MSFT	27	0.94	0.84	3.80	0.04	199 / 106 / 43
PFE	26	1.12	1.06	4.63	0.05	184 / 71 / 21
PG	58	0.72	0.69	2.69	0.03	144 / 38 / 7
T	27	1.08	1.00	4.94	0.05	177 / 77 / 27
UTX	68	1.07	1.01	3.16	0.03	127 / 27 / 4
VZ	35	0.98	0.91	3.81	0.04	165 / 61 / 18
WMT	48	0.91	0.88	3.01	0.03	130 / 32 / 6
XOM	64	1.39	1.34	2.27	0.02	90 / 17 / 2
Mean ALL:	**47**	**1.23090**	**1.14720**	**0.00035**	**0.03**	**152 / 49 / 13**
Median ALL	**48**	**1.08398**	**1.00552**	**0.00033**	**0.03**	**161 / 48 / 11**
Max ALL:	**86**	**3.69647**	**3.48752**	**0.00055**	**0.05**	**206 / 106 / 43**
Min ALL:	**22**	**0.52107**	**0.49326**	**0.00023**	**0.02**	**82 / 14 / 2**

Table 3: **Relative mean squared error (MSE) factors for models without microstructure noise.** We report the MSE factors for each estimator and each model as the sample mean of $195(\widehat{IV} - IV)^2/IQ$, where IV and IQ are the true simulated integrated variance and integrated quarticity on each day. The MSE factor for 2-min subsampled RV is thus ≈ 1.33 which is the theoretical value shown by Zhang, Mykland, and Aït Sahalia (2005). Each row corresponds to a given estimator and each column to one of the models described in detail in Appendix A.1. Thus model SV0 is a model without stochastic volatility while SV1A and SV2A are one and two factor stochastic volatility models with affine structure. Model SV1L is a one-factor model written in log volatility. Entries in bold denote that the MSE factor is smaller than 2-min subsampled RV (for models without jumps) or smaller than 2-min subsampled BV (for models with jumps). In the case of the passage time estimators, the previous tick method is used for models including jumps.

		Core Models SV-C Avg Sample Freq 3sec without Noise				**Models SV-UJ with U-Shaped Volatility and 25% Mean Jump Contribution to IV Avg Sample Freq 3sec without Noise**			
		SV0-C	**SV1A-C**	**SV1L-C**	**SV2A-C**	**SV0-UJ**	**SV1A-UJ**	**SV1L-UJ**	**SV2A-UJ**
Subsampled RV_N	2-min	1.318	1.315	1.314	1.347	-	-	-	-
Subsampled BV_N	2-min	1.495	1.511	1.510	1.505	1.945	2.027	2.028	2.053
First Exit Time $DV_{N,h}$	h = 3	***0.398***	***0.413***	***0.412***	***0.407***	***0.386***	***0.393***	***0.394***	***0.389***
	h = 4	***0.582***	***0.591***	***0.590***	***0.578***	***0.513***	***0.517***	***0.517***	***0.523***
	h = 5	***0.911***	***0.889***	***0.888***	***0.898***	***0.815***	***0.817***	***0.817***	***0.816***
	h = 6	1.356	***1.289***	***1.289***	***1.343***	***1.243***	***1.239***	***1.239***	***1.260***
	h = 7	1.908	1.835	1.834	1.906	***1.820***	***1.801***	***1.802***	***1.806***
	h = 8	2.572	2.475	2.476	2.556	2.601	2.542	2.548	2.481
First Range Time $DV_{N,h}$	h = 3	***0.274***	***0.296***	***0.294***	***0.293***	***0.242***	***0.254***	***0.256***	***0.253***
	h = 4	***0.436***	***0.447***	***0.449***	***0.418***	***0.376***	***0.387***	***0.389***	***0.376***
	h = 5	***0.596***	***0.647***	***0.642***	***0.597***	***0.552***	***0.579***	***0.579***	***0.554***
	h = 6	***0.825***	***0.816***	***0.817***	***0.819***	***0.788***	***0.774***	***0.776***	***0.782***
	h = 7	***1.096***	***1.059***	***1.056***	***1.122***	***1.085***	***1.066***	***1.068***	***1.079***
	h = 8	1.437	1.406	1.402	1.449	***1.500***	***1.473***	***1.469***	***1.463***

Table 4: **Relative mean squared error (MSE) factors for models with microstructure noise without intra-day U-shape and jumps.** We report the MSE factors for each estimator and each model as the sample mean of $195(\widehat{IV} - IV)^2/IQ$, where IV and IQ are the true simulated integrated variance and integrated quarticity on each day. The MSE factor for 2-min subsampled RV is thus ≈ 1.33 which is the theoretical value shown by Zhang, Mykland, and Aït Sahalia (2005). Each row corresponds to a given estimator and each column to a given AR(1) noise structure and one of the models described in detail in Appendix A.1. Thus model SV0 is a model without stochastic volatility while SV1A and SV2A are one and two factor stochastic volatility models with affine structure. Model SV1L is a one-factor model written in log volatility. We consider two levels of noise to signal ratio: moderate ($\lambda = 0.25$) and high ($\lambda = 1.0$) and two levels of noise persistence: low ($\rho = 0.0$) and high ($\rho = 0.99$). Entries in bold denote that the MSE factor is smaller than 2-min subsampled RV.

		Core Models SV-C Avg Sample Freq 3sec with AR(1) Microstructure Noise							
		Noise Persistence ρ=0.0				**Noise Persistence ρ=0.99**			
		Noise-to-Signal Ratio λ = 0.25		**Noise-to-Signal Ratio λ = 1.00**		**Noise-to-Signal Ratio λ = 0.25**		**Noise-to-Signal Ratio λ = 1.00**	
		SV0-C	**SV2A-C**	**SV0-C**	**SV2A-C**	**SV0-C**	**SV2A-C**	**SV0-C**	**SV2A-C**
Subsampled RV_N	2-min	1.323	1.349	1.378	1.393	1.318	1.347	1.318	1.347
BV_N	2-min	1.494	1.502	1.532	1.535	1.495	1.505	1.495	1.505
First Exit Time $DV_{N,h}$	h = 3	***0.335***	***0.325***	3.472	3.447	***0.393***	***0.403***	***0.378***	***0.388***
	h = 4	***0.595***	***0.568***	1.943	1.879	***0.582***	***0.573***	***0.577***	***0.567***
	h = 5	***0.939***	***0.895***	1.650	1.555	***0.913***	***0.894***	***0.913***	***0.889***
	h = 6	1.382	***1.344***	1.806	1.720	1.358	***1.347***	1.359	***1.346***
	h = 7	1.923	1.887	2.192	2.122	1.908	1.906	1.909	1.900
	h = 8	2.592	2.521	2.757	2.661	2.576	2.553	2.577	2.545
First Range Time $DV_{N,h}$	h = 3	***0.555***	***0.539***	7.605	7.563	***0.276***	***0.292***	***0.268***	***0.282***
	h = 4	***0.548***	***0.520***	3.729	3.689	***0.432***	***0.414***	***0.424***	***0.409***
	h = 5	***0.677***	***0.652***	2.567	2.534	***0.597***	***0.602***	***0.594***	***0.600***
	h = 6	***0.878***	***0.855***	2.167	2.086	***0.829***	***0.812***	***0.826***	***0.810***
	h = 7	***1.158***	***1.131***	2.130	1.991	***1.097***	***1.126***	***1.098***	***1.118***
	h = 8	1.512	1.468	2.223	2.129	1.442	1.449	1.441	1.440

Table 5: **Relative mean squared error (MSE) factors for models with microstructure noise and including intra-day U-shape and jumps.** We report the MSE factors for each estimator and each model as the sample mean of $195(\widehat{IV} - IV)^2/IQ$, where IV and IQ are the true simulated integrated variance and integrated quarticity on each day. The MSE factor for 2-min subsampled RV is thus ≈ 1.33 which is the theoretical value shown by Zhang, Mykland, and Aït Sahalia (2005). Each row corresponds to a given estimator and each column to a given AR(1) noise structure and one of the models described in detail in Appendix A.1. Thus model SV0 is a model without stochastic volatility while SV1A and SV2A are one and two factor stochastic volatility models with affine structure. Model SV1L is a one-factor model written in log volatility. We consider two levels of noise to signal ratio: moderate ($\lambda = 0.25$) and high ($\lambda = 1.0$) and two levels of noise persistence: low ($\rho = 0.0$) and high ($\rho = 0.99$). Entries in bold denote that the MSE factor is smaller than 2-min subsampled BV. In the case of the passage time estimators, the previous tick method is used for all models.

		Models SV-UJ with U-Shaped Volatility and 25% Mean Jump Contribution to IV Avg Sample Freq 3sec with AR(1) Microstructure Noise							
		Noise Persistence ρ=0.0				**Noise Persistence ρ=0.99**			
		Noise-to-Signal Ratio λ = 0.25		**Noise-to-Signal Ratio λ = 1.00**		**Noise-to-Signal Ratio λ = 0.25**		**Noise-to-Signal Ratio λ = 1.00**	
		SV0-UJ	**SV2A-UJ**	**SV0-UJ**	**SV2A-UJ**	**SV0-UJ**	**SV2A-UJ**	**SV0-UJ**	**SV2A-UJ**
Subsampled RV_N	2-min	-	-	-	-	-	-	-	-
BV_N	2-min	1.986	2.096	2.151	2.265	1.946	2.054	1.948	2.056
First Exit Time $DV_{N,h}$	h = 3	***0.289***	***0.290***	2.873	2.811	***0.380***	***0.384***	***0.364***	***0.369***
	h = 4	***0.556***	***0.551***	***1.848***	***1.804***	***0.513***	***0.521***	***0.511***	***0.513***
	h = 5	***0.887***	***0.887***	***1.723***	***1.690***	***0.813***	***0.818***	***0.815***	***0.816***
	h = 6	***1.322***	***1.331***	***1.980***	***1.937***	***1.241***	***1.256***	***1.248***	***1.257***
	h = 7	***1.902***	***1.873***	2.456	2.385	***1.820***	***1.801***	***1.825***	***1.804***
	h = 8	2.677	2.543	3.163	2.996	2.602	2.480	2.605	2.490
First Range Time $DV_{N,h}$	h = 3	***0.564***	***0.555***	7.026	6.956	***0.245***	***0.254***	***0.242***	***0.251***
	h = 4	***0.586***	***0.565***	3.737	3.682	***0.376***	***0.377***	***0.375***	***0.375***
	h = 5	***0.722***	***0.731***	2.722	2.707	***0.547***	***0.555***	***0.551***	***0.559***
	h = 6	***0.967***	***0.937***	2.485	2.408	***0.793***	***0.784***	***0.796***	***0.785***
	h = 7	***1.256***	***1.225***	2.498	2.411	***1.092***	***1.074***	***1.099***	***1.072***
	h = 8	***1.677***	***1.620***	2.720	2.593	***1.497***	***1.466***	***1.500***	***1.471***

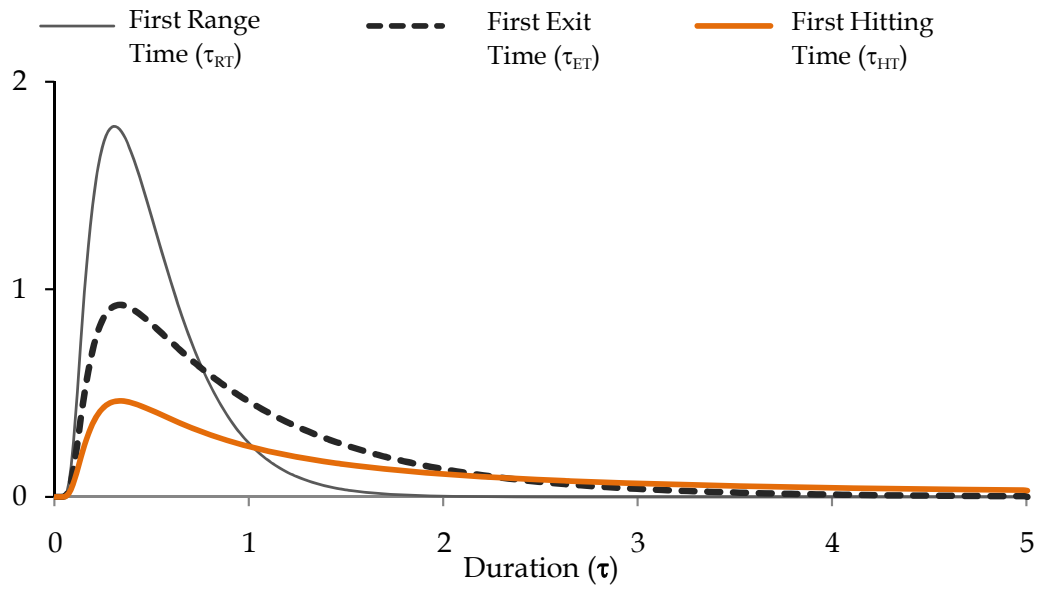

Figure 1: **The passage time densities for the baseline case ($\frac{h}{\sigma} = 1$).** The first range time (thin line), the first exit time (dashed line) and the first hitting time (thick line).

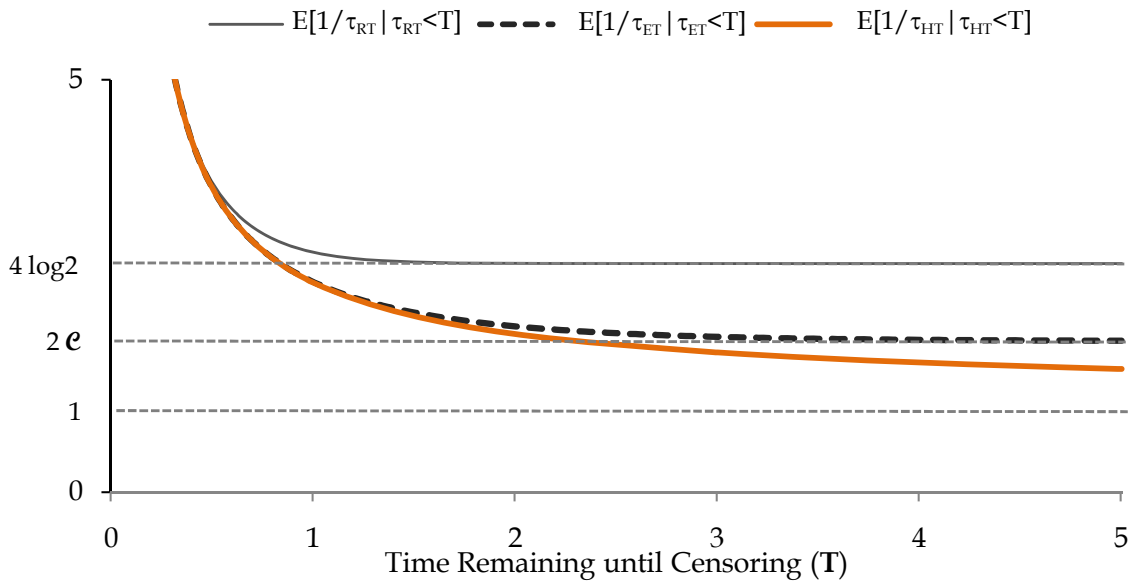

Figure 2: **Conditional expectation of reciprocal passage times for the baseline case ($\frac{h}{\sigma} = 1$).** The expected reciprocal first range time (thin line), the expected reciprocal first exit time (dashed line), and the expected reciprocal hitting time (thick line). The respective unconditional expectations are indicated by three horizontal thin dashed lines, where $\mathcal{C} \approx 0.91597$ is the Catalan constant.

Figure 3: This Figure shows the relative (upward) bias of the first exit time passage time estimator as a function of the persistence of the noise. The x-axis is the first order autocorrelation of the noise which is of the AR(1) type. Panel A shows the "moderate" noise scenario where the noise to signal ratio is $\lambda = 0.25$. Panel B shows the "high" noise scenario where the noise to signal ratio is $\lambda = 1.0$

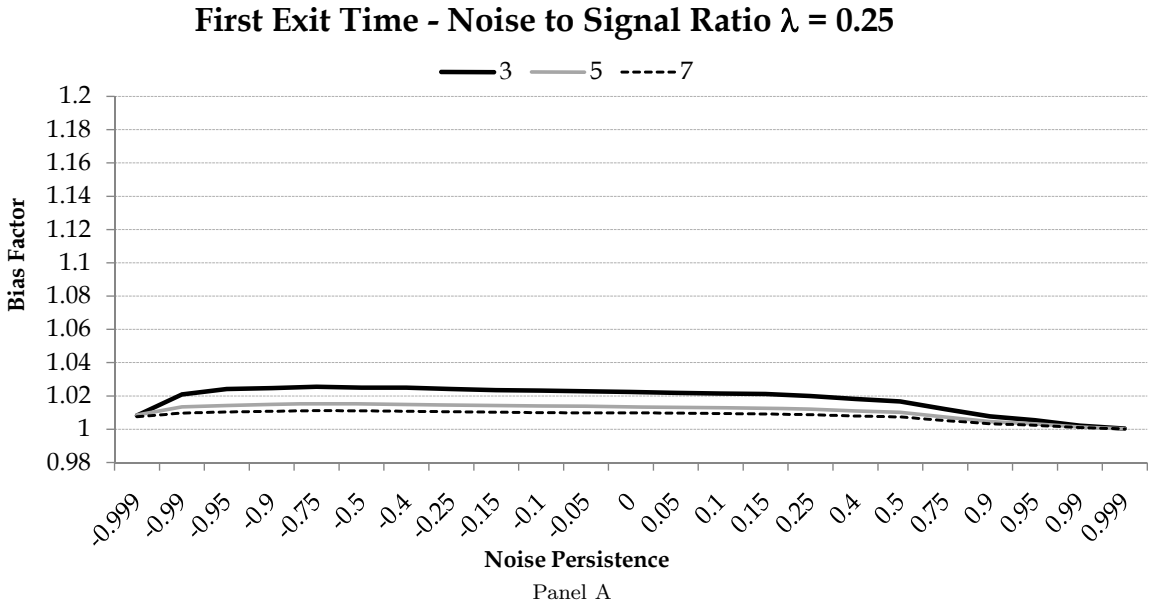

Panel A

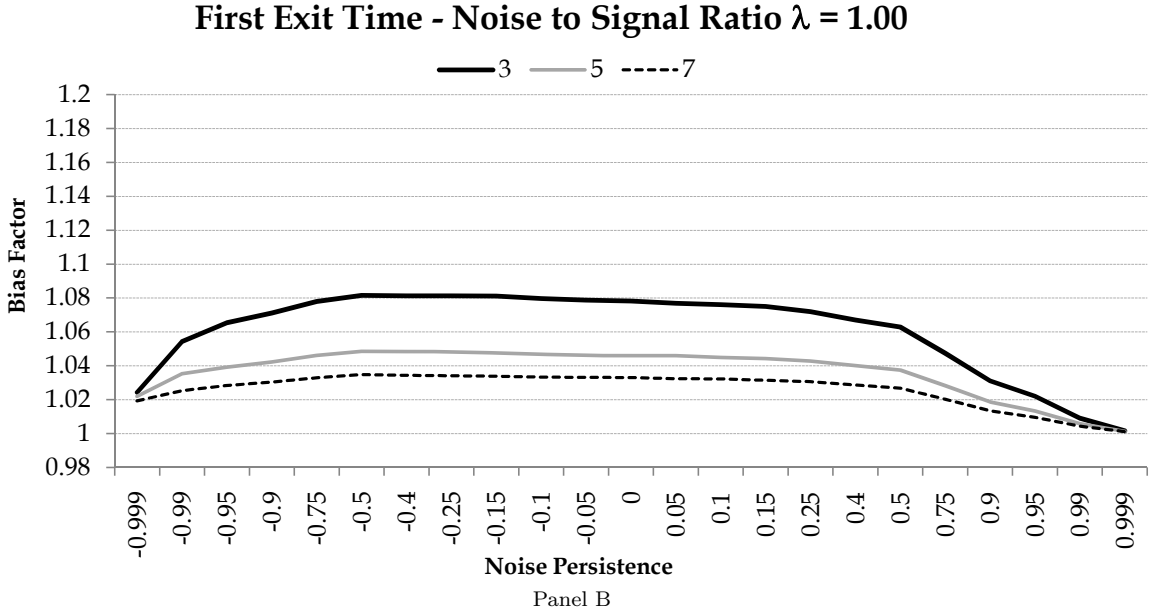

Panel B

Figure 4: This Figure shows the relative (upward) bias of the first range time passage time estimator as a function of the persistence of the noise. The x-axis is the first order autocorrelation of the noise which is of the AR(1) type. Panel A shows the "moderate" noise scenario where the noise to signal is $\lambda = 0.25$. Panel B shows the "high" noise scenario where the noise to signal ratio is $\lambda = 1.0$.

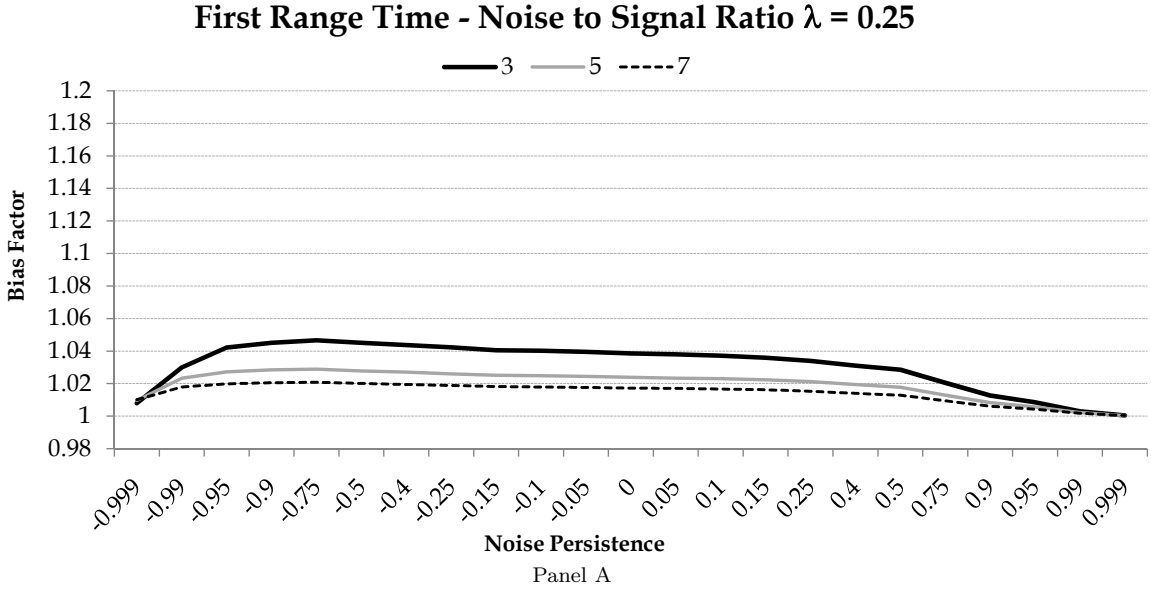

Panel A

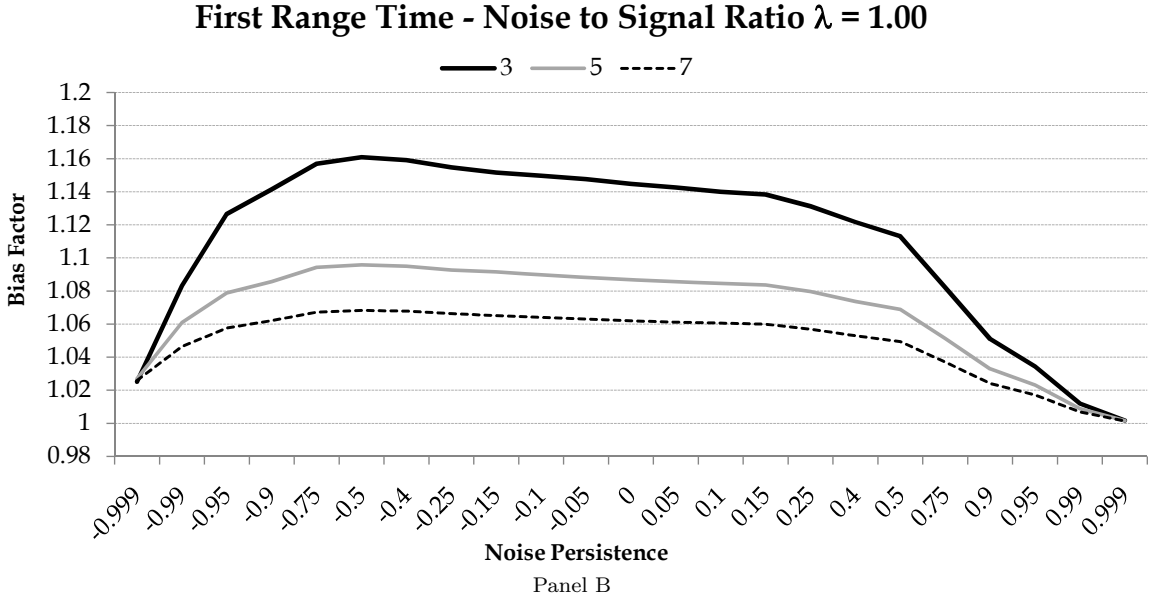

Panel B

Figure 5: Signature plots based on Monte Carlo experiments described in Section 5. The figure shows the mean relative bias $\widehat{IV}/IV$ of the first exit time DV and first range time DV as a function of the threshold.

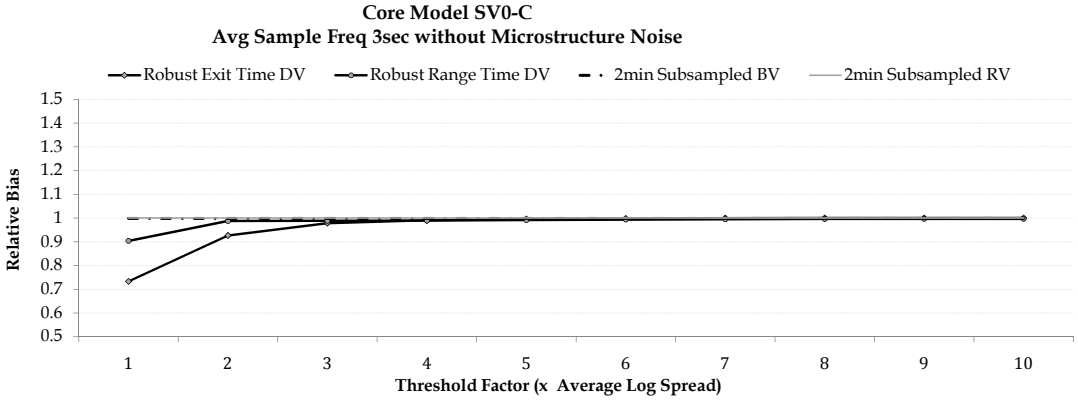

Panel A: Deterministic Volatility Model SV0-C

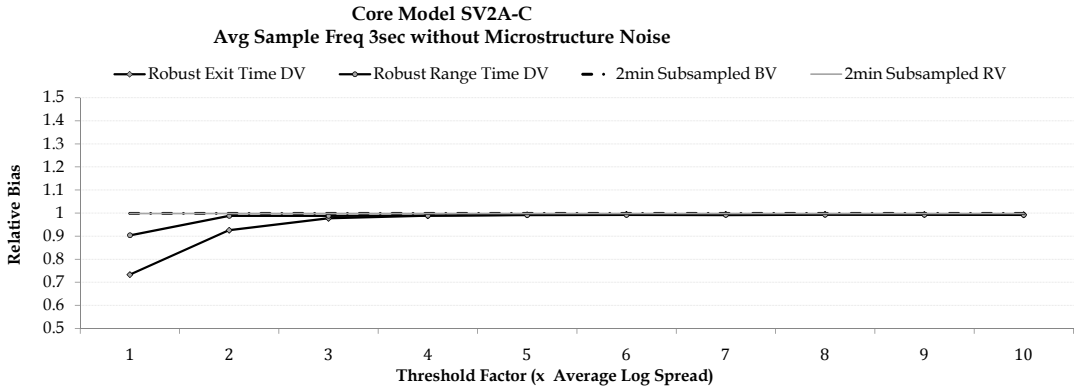

Panel B: Stochastic Volatility Model SV2A-C

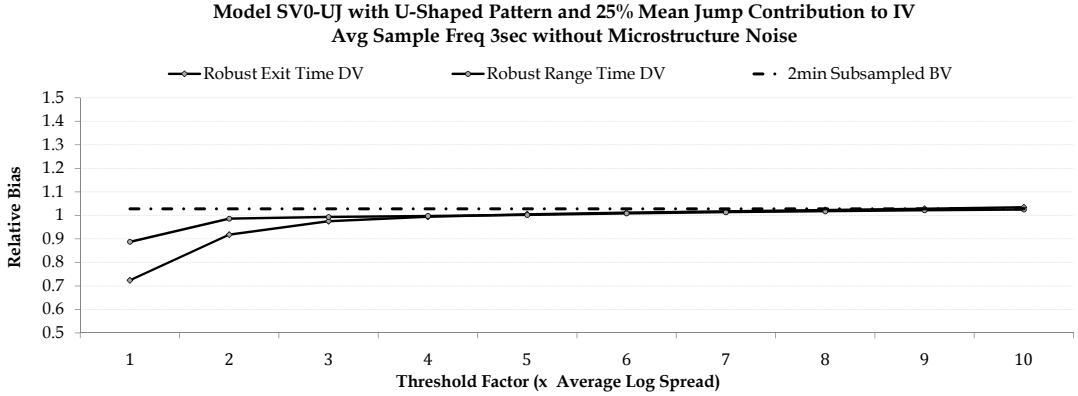

Panel C: Stochastic Volatility Model SV2A-UJ with U-Shaped Pattern and Jumps

Figure 6: The impact of microstructure noise on the first exit time DV and first range time DV estimators for the two factor stochastic volatility model without intra-day U-shape and jumps (SV2A-C). The observation frequency is 3 seconds and the noise structure is assumed to be AR(1) as described in Section 3.4.

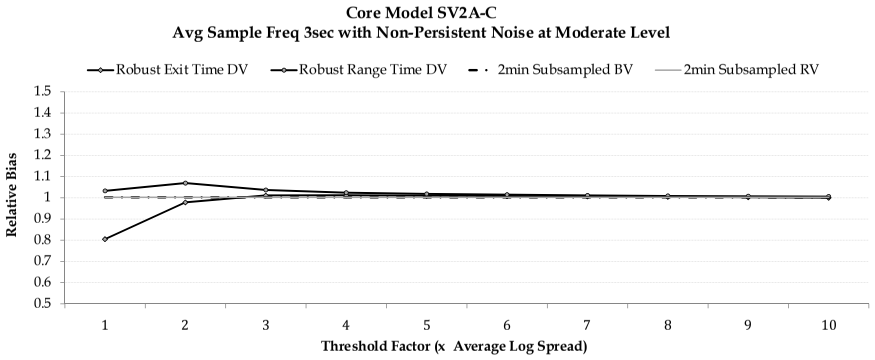

Panel A: Noise-to-signal ratio $\lambda = 0.25$, persistence $\rho = 0.0$

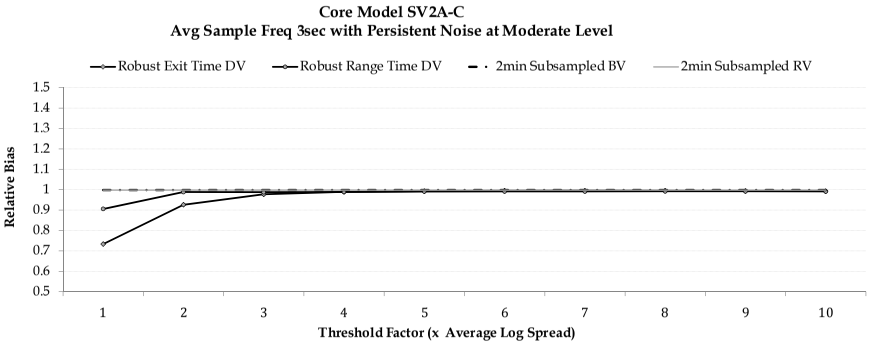

Panel B: Noise-to-signal ratio $\lambda = 0.25$, persistence $\rho = 0.99$

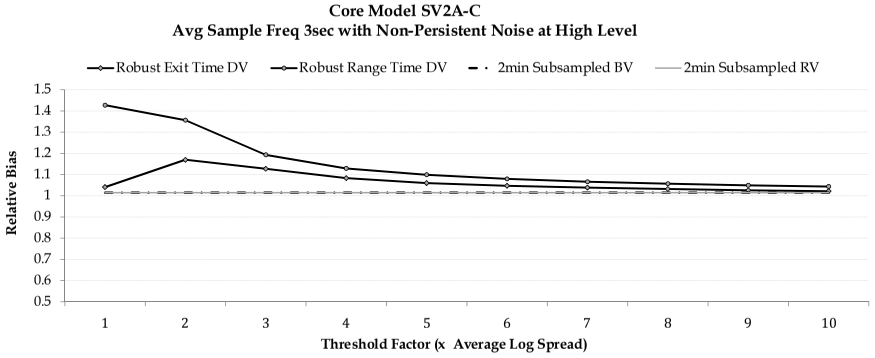

Panel C: Noise-to-signal ratio $\lambda = 1.0$, persistence $\rho = 0.0$

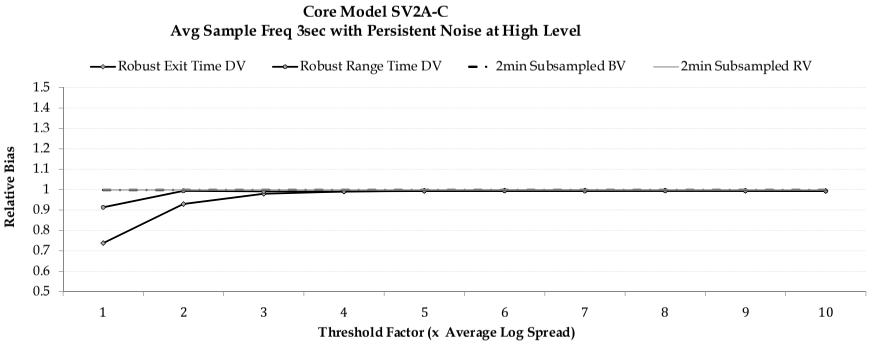

Panel D: Noise-to-signal ratio $\lambda = 1.0$, persistence $\rho = 0.99$

Figure 7: The impact of microstructure noise on the first exit time DV and first range time DV estimators for the two factor stochastic volatility model witt intra-day U-shape pattern and jumps (SV2A-UJ). The observation frequency is 3 seconds and the noise structure is assumed to be AR(1) as described in Section 3.4

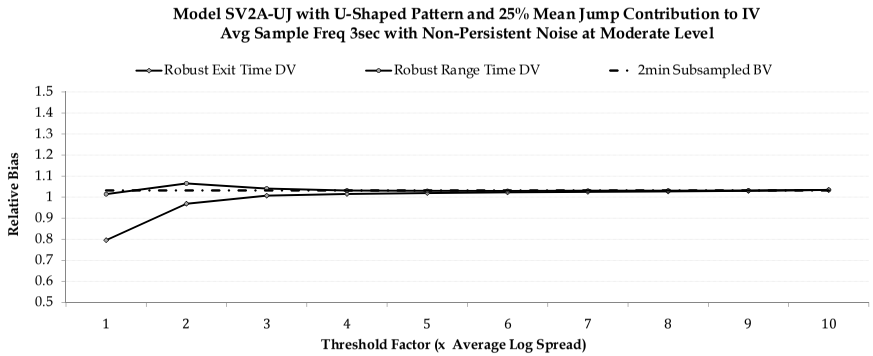

Panel A: Noise-to-signal ratio $\lambda = 0.25$, persistence $\rho = 0.0$

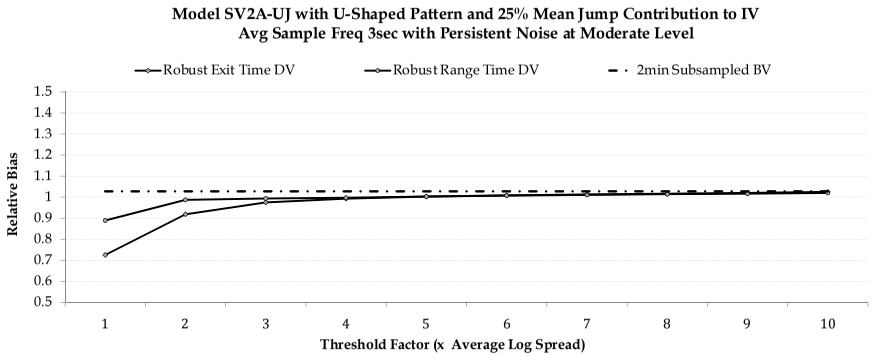

Panel B: Noise-to-signal ratio $\lambda = 0.25$, persistence $\rho = 0.99$

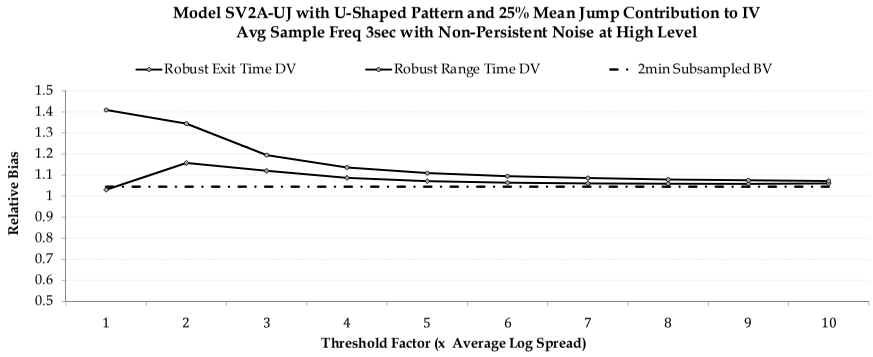

Panel C: Noise-to-signal ratio $\lambda = 1.0$, persistence $\rho = 0.0$

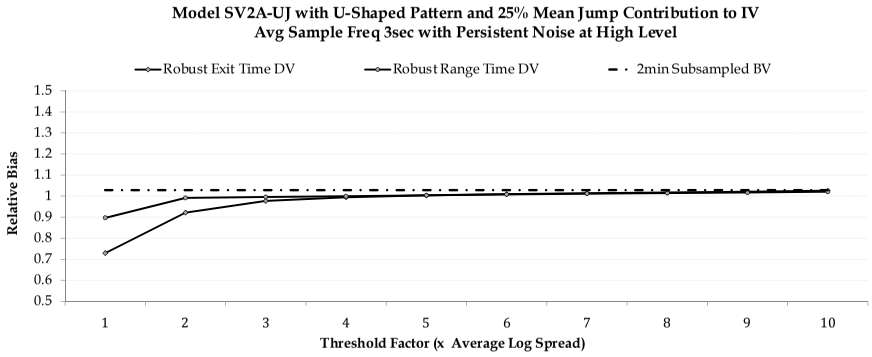

Panel D: Noise-to-signal ratio $\lambda = 1.0$, persistence $\rho = 0.99$

C Cross-Sectional Average DJ30 Signature Plots

This section displays the average performance of the duration-based integrated variance estimators (first exit time DV and first range time DV) across the 33 stocks which were part of the Dow Jones 30 index at any point during the period January 2005 through May 2007. The performance is compared to the 2-minute subsampled bi-power estimator (BV or BV1) and the 2 minute subsampled realized volatility estimator (RV). The distinction between the two BV estimators is whether adjacent absolute returns are multiplied (BV) or whether one return is skipped (BV1) as suggested by Andersen, Bollerslev, and Diebold (2007).

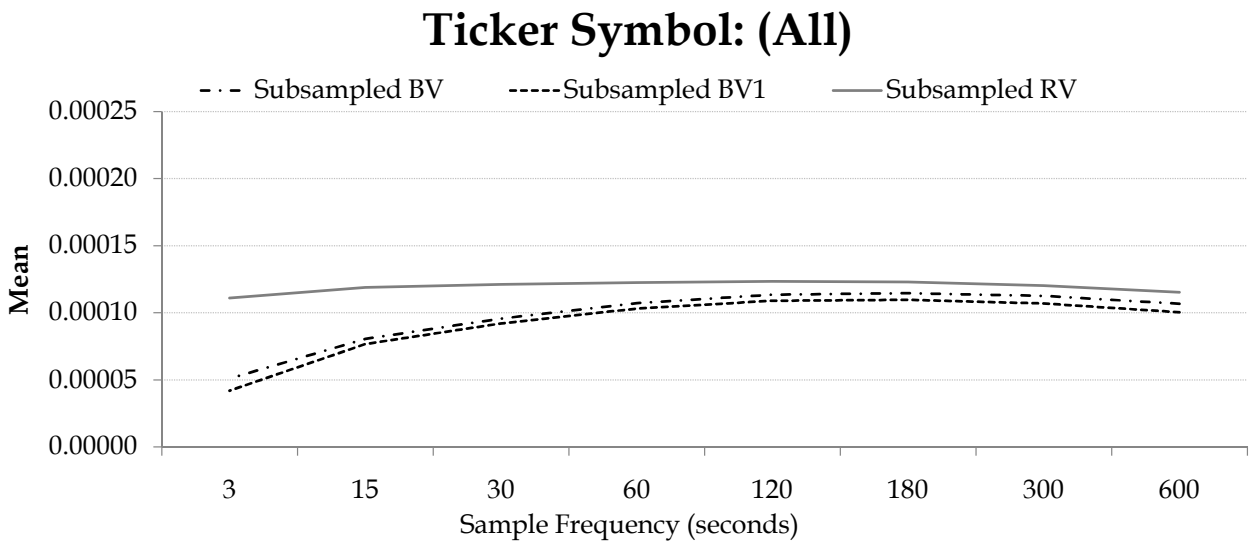

Figure 8: The cross-sectional average signature plot for the sub-sampled BV and RV estimators as a function of the sample frequency in seconds. The average is taken across the 33 DJ30 stocks in our sample.

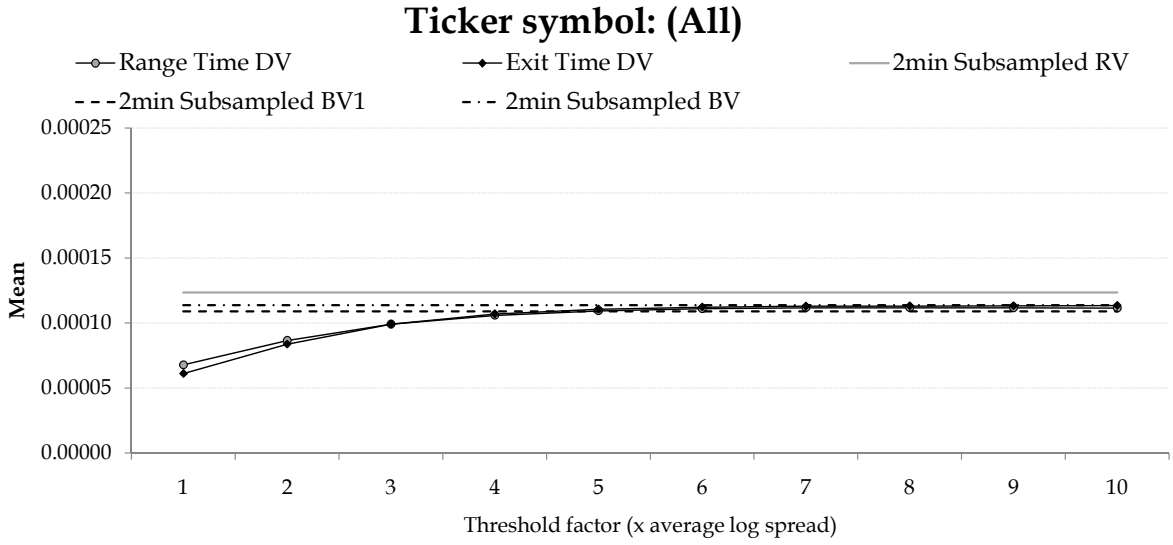

Figure 9: The cross-sectional average signature plot for duration-based integrated variance estimators (DV) as a function of the threshold level (measured in units of the average intraday log-spread).

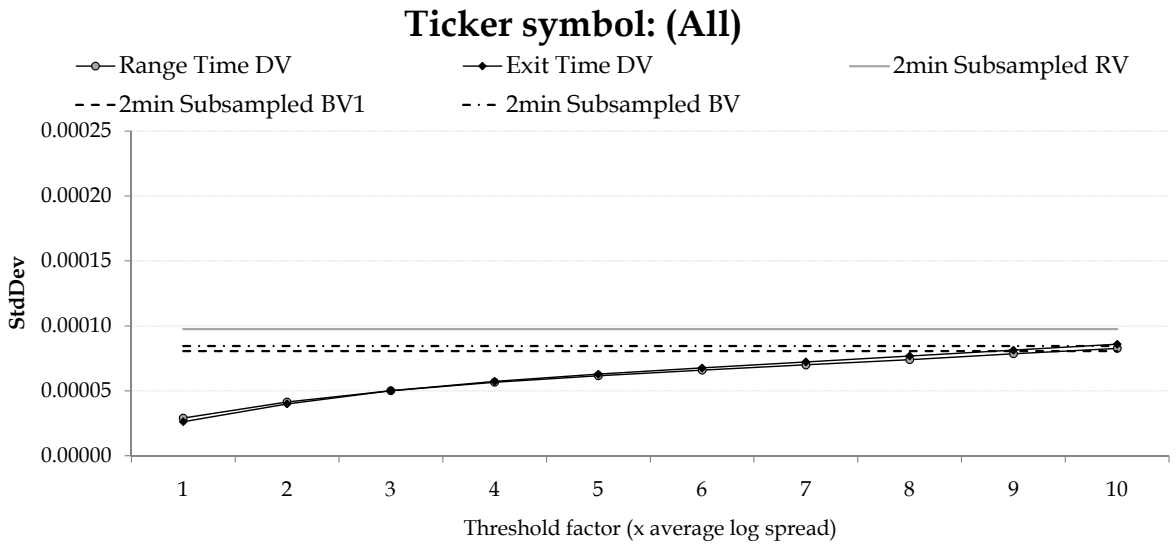

Figure 10: The cross-sectional average standard deviation of duration-based integrated variance estimators (DV) as a function of the threshold level (measured in units of the average intraday log-spread).

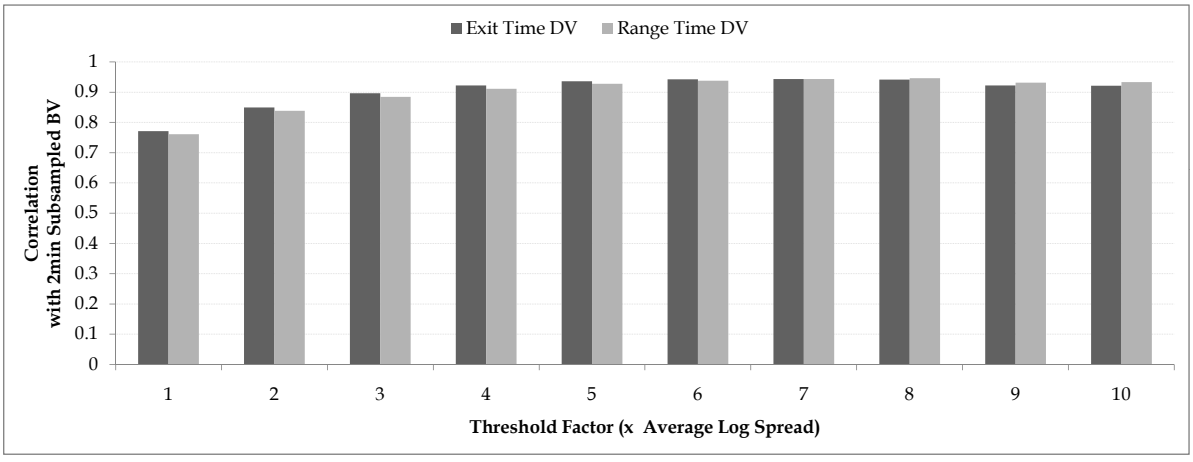

Figure 11: The cross-sectional average correlation of the 2-minute subsampled BV estimator with duration-based integrated variance estimators (DV) as a function of the threshold level (measured in units of the average intraday log-spread).

D Individual DJ30 Signature Plots

Signature plots for the duration-based integrated variance estimators for the 33 Dow Jones 30 index from January 2005 through May 2007. The benchmark estimators are the 2-min subsampled realized volatility (RV) and bi-power (BV) estimators.

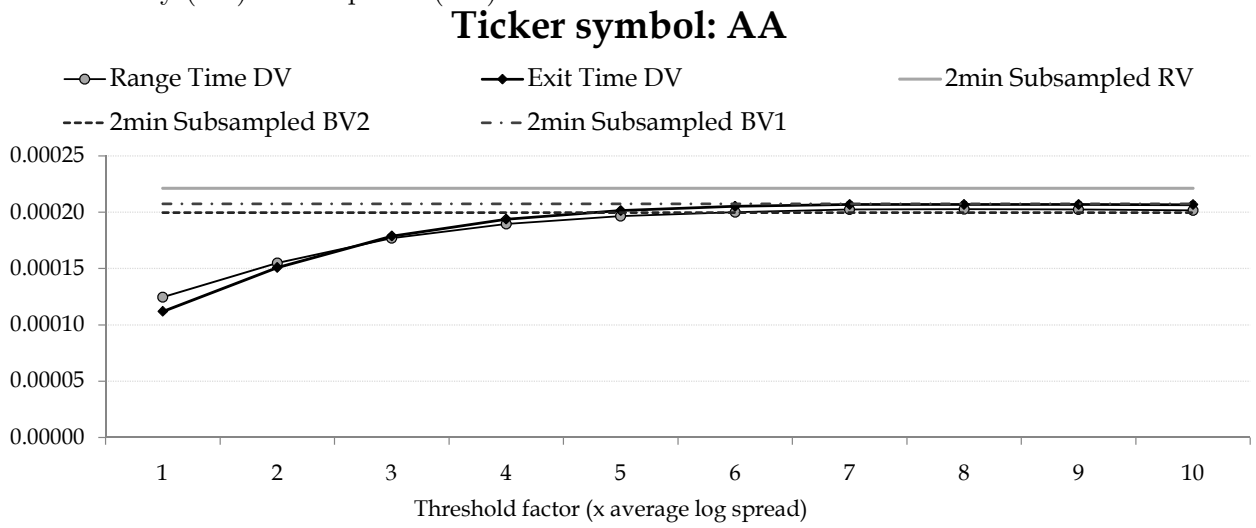

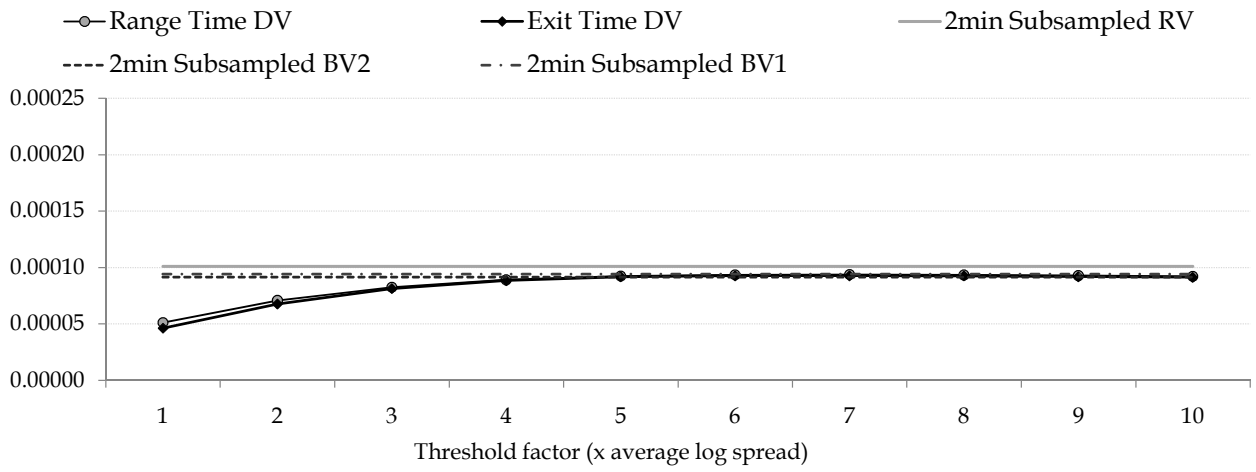

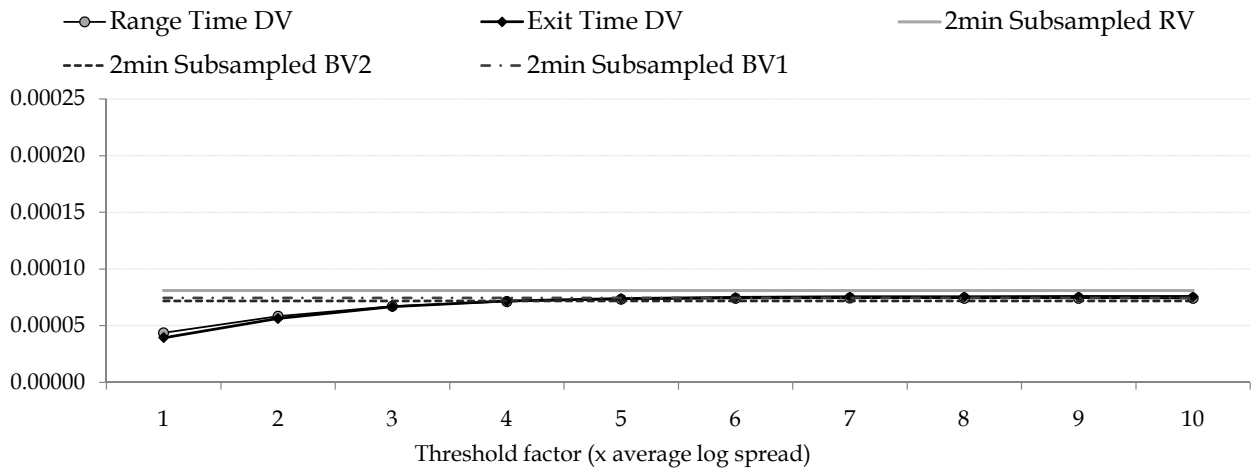

Ticker symbol: BA

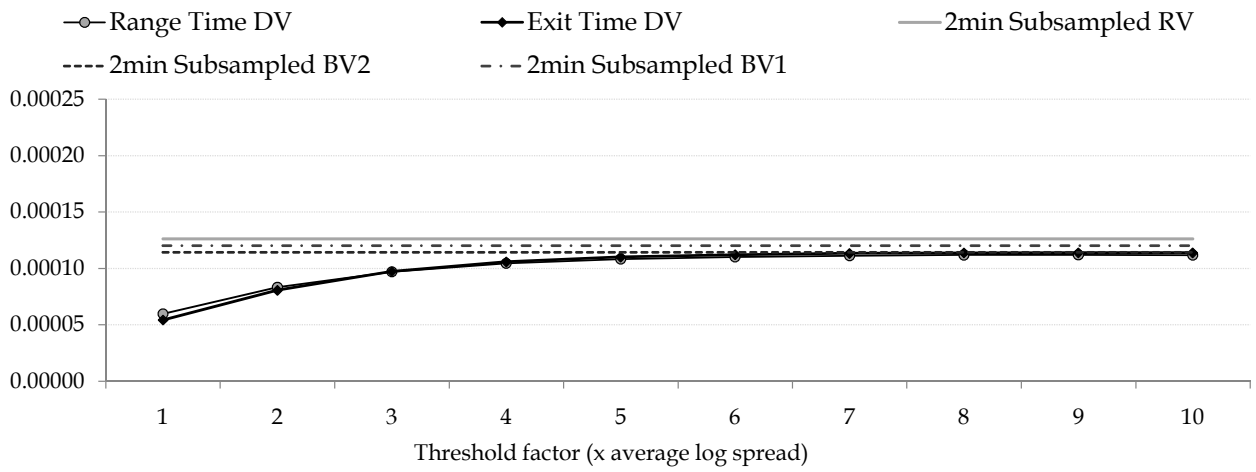

Ticker symbol: BAC

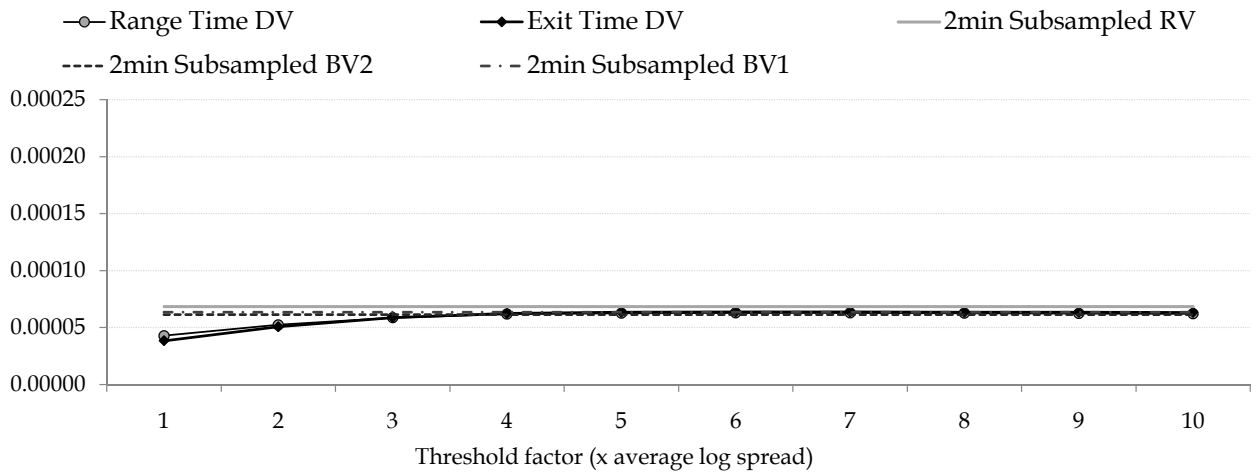

Ticker symbol: C

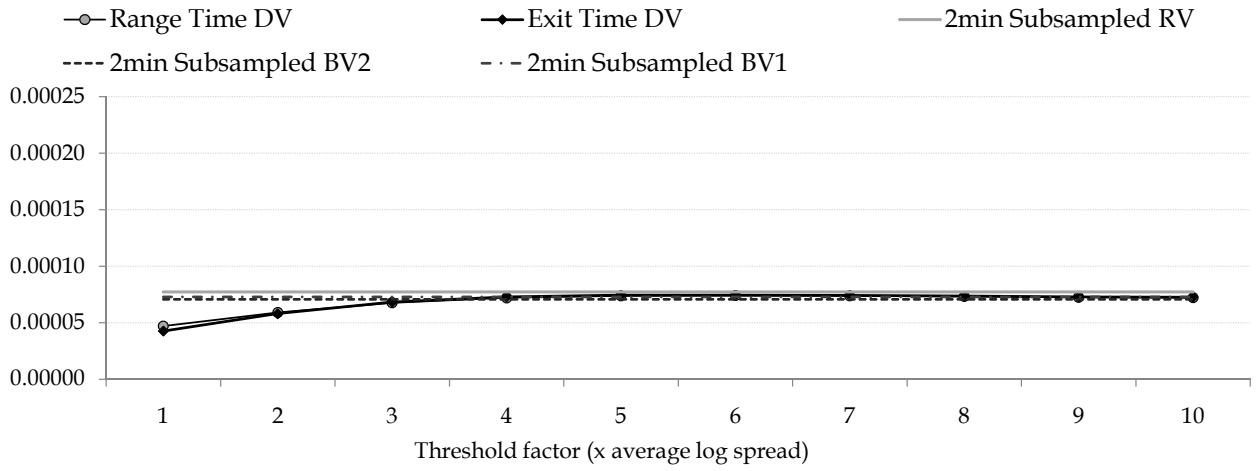

Ticker symbol: CAT

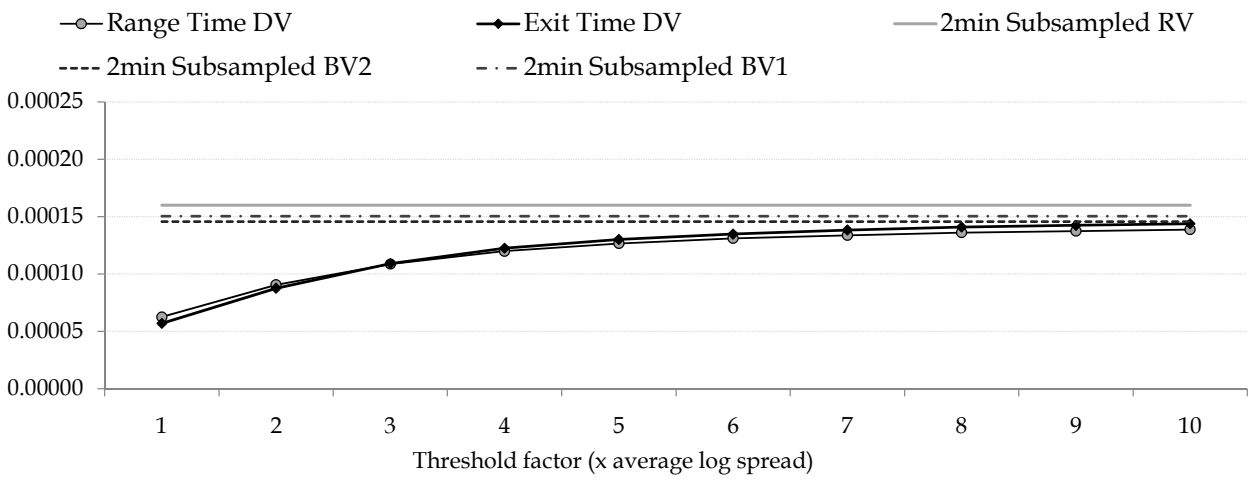

Ticker symbol: CVX

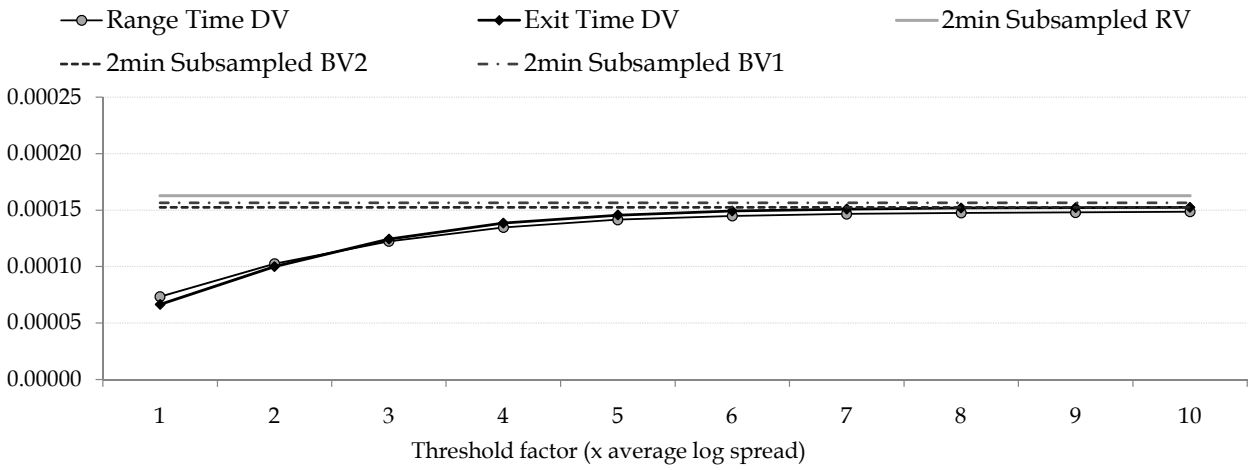

Ticker symbol: DD

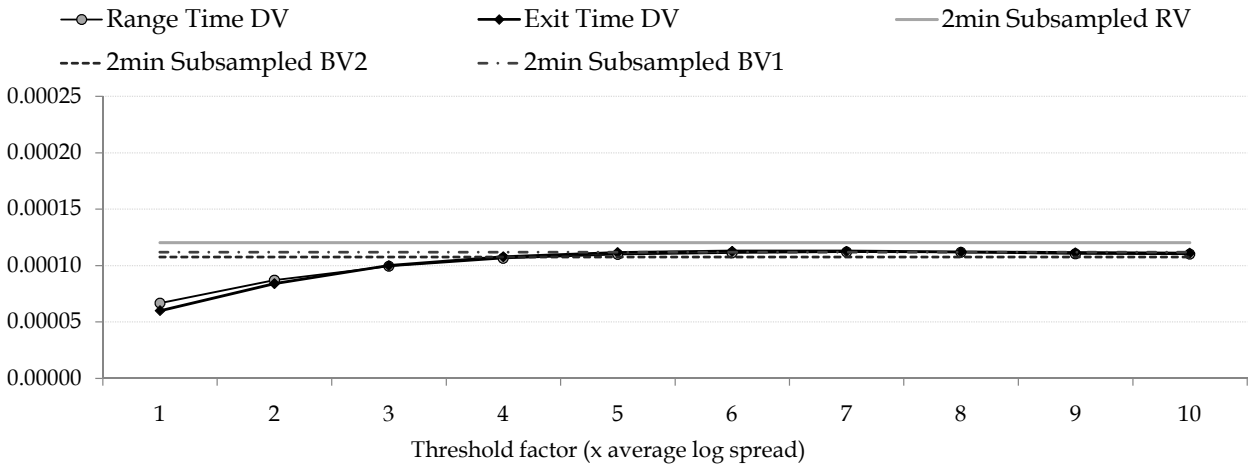

Ticker symbol: DIS

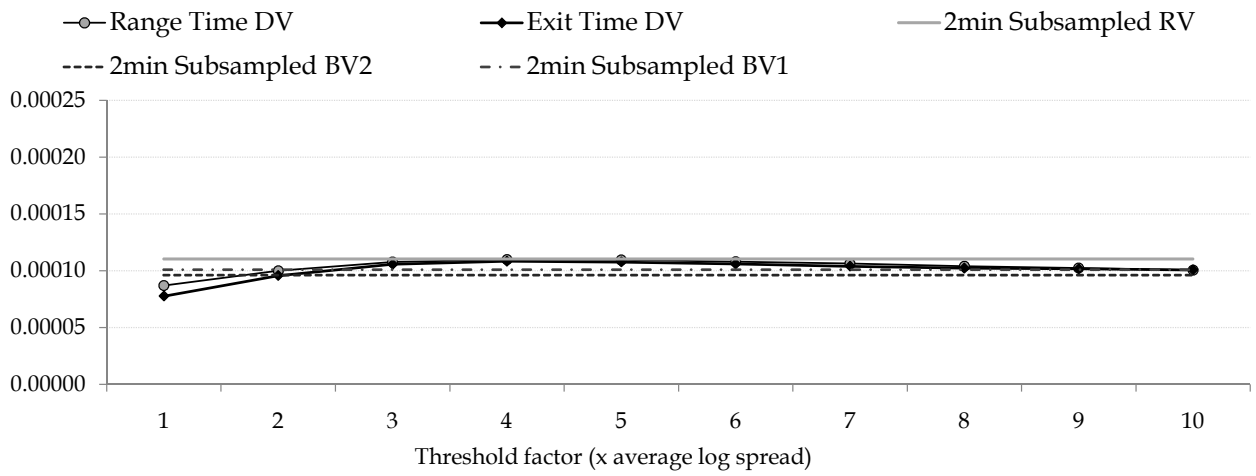

Ticker symbol: EK

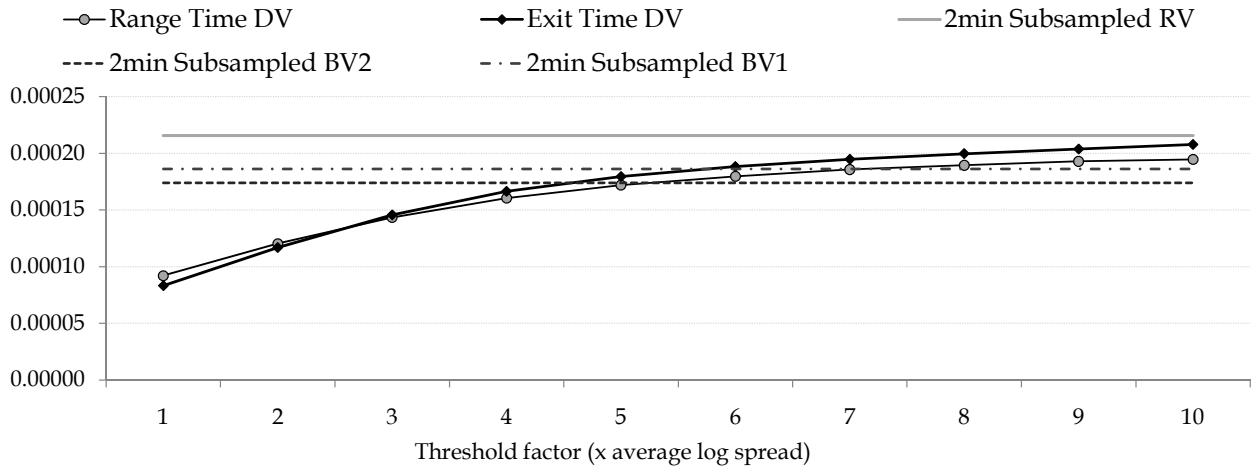

Ticker symbol: GE

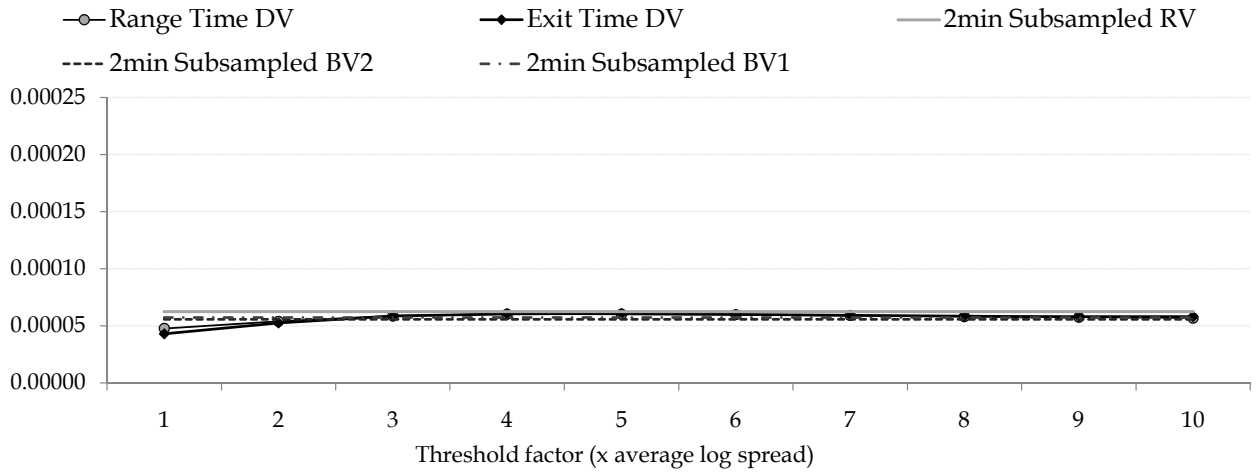

Ticker symbol: GM

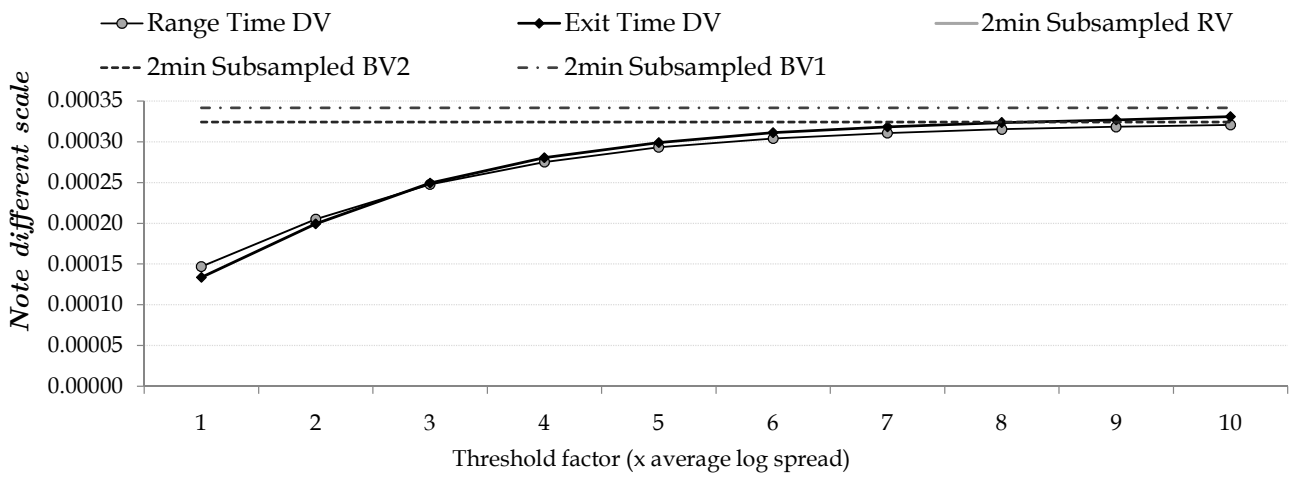

Ticker symbol: HD

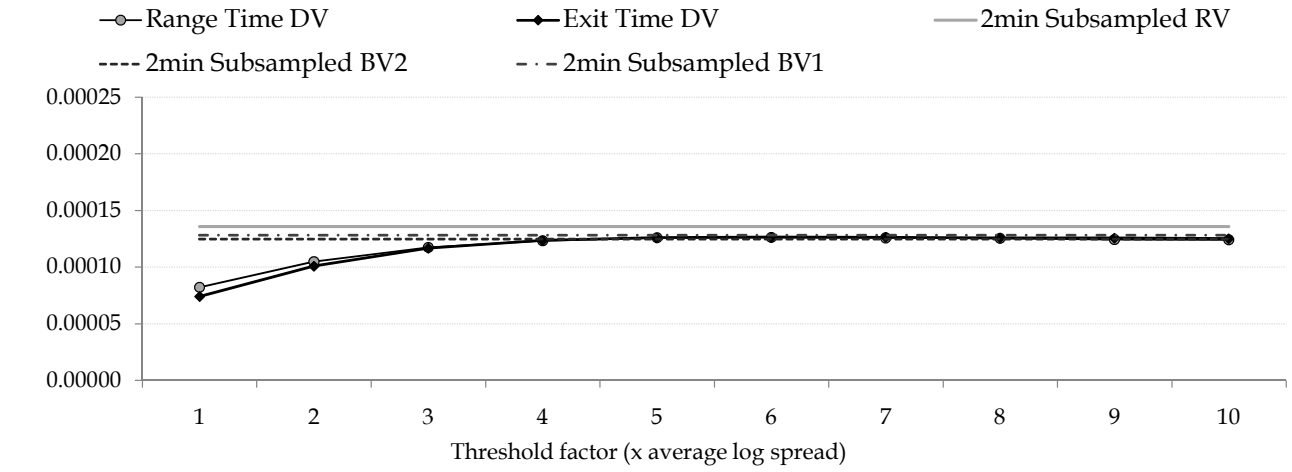

Ticker symbol: HPQ

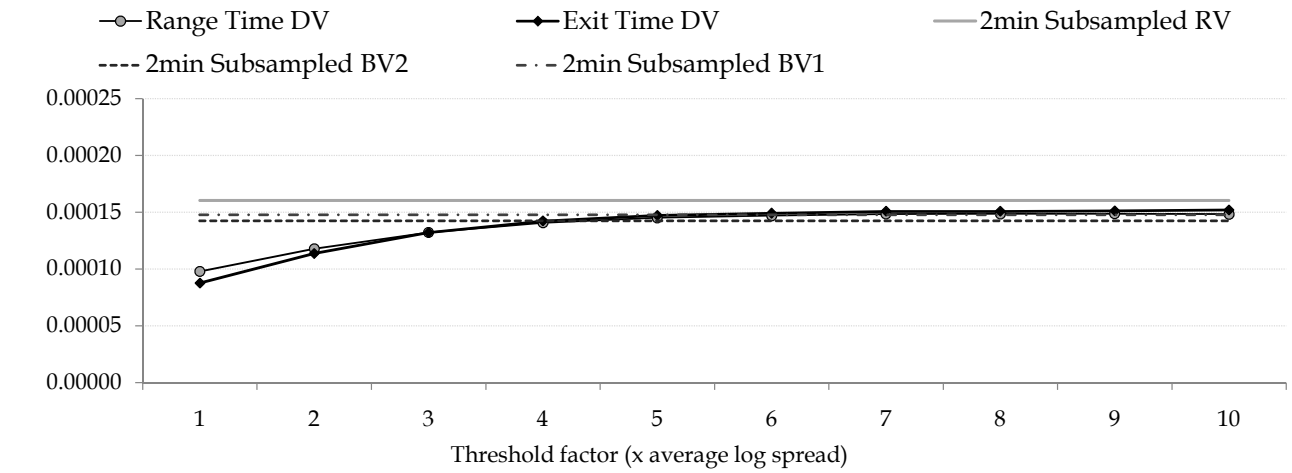

Ticker symbol: IBM

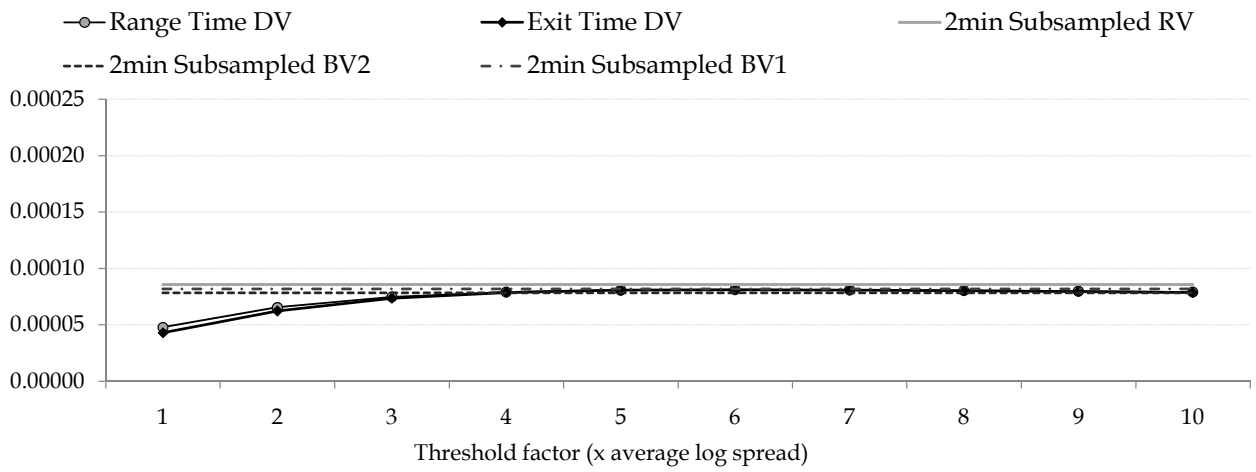

Ticker symbol: INTC

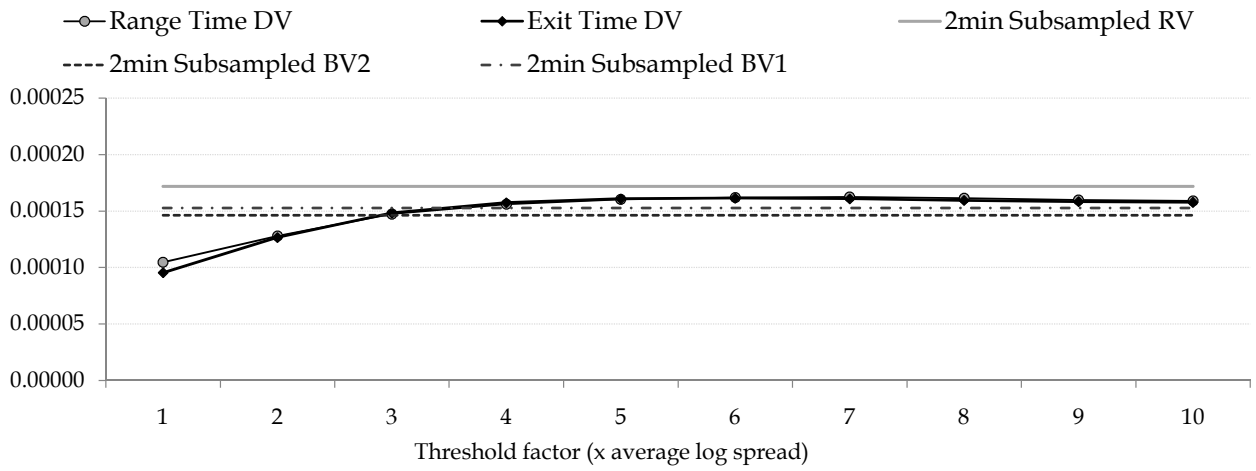

Ticker symbol: IP

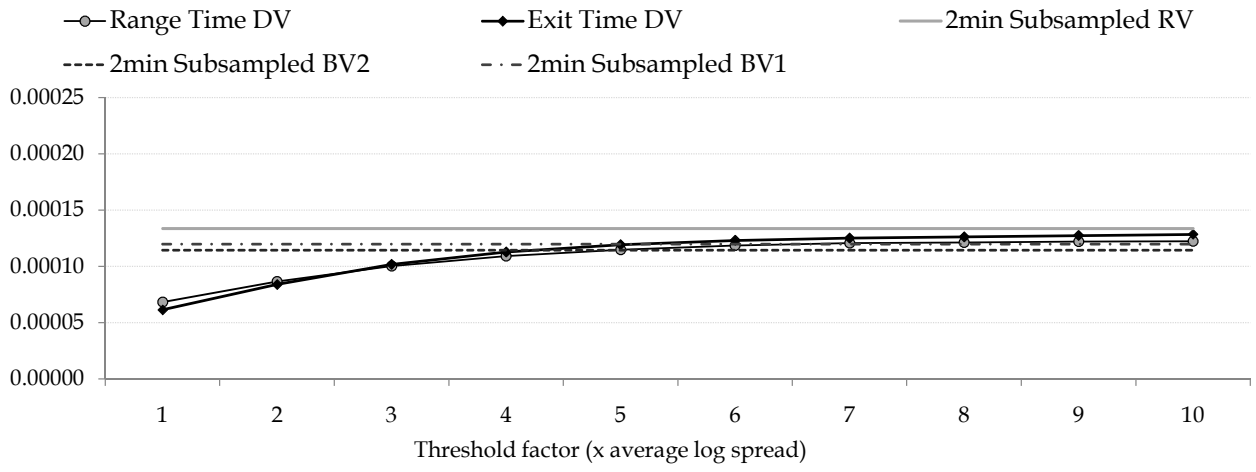

Ticker symbol: JNJ

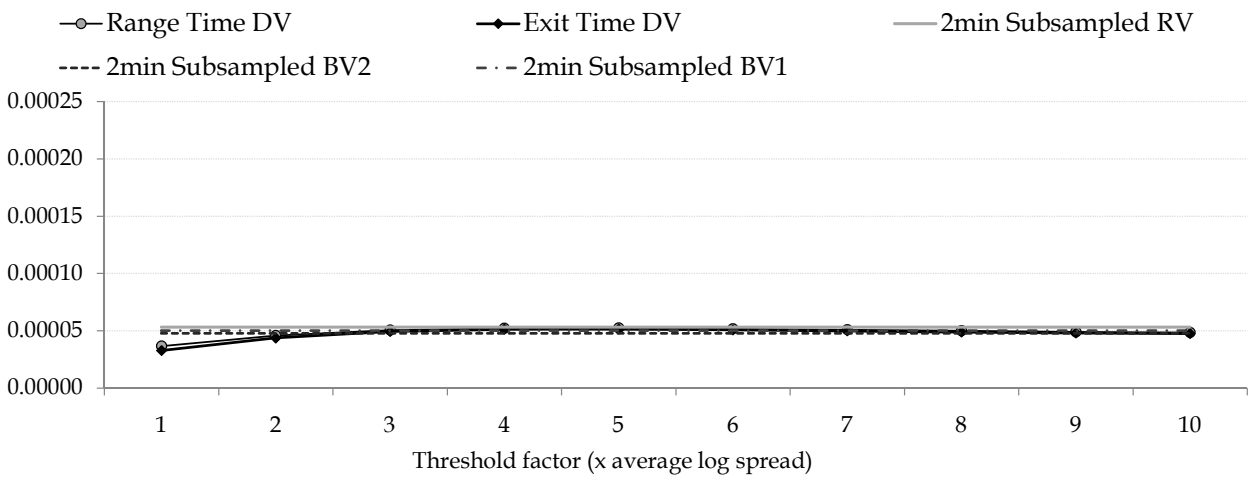

Ticker symbol: JPM

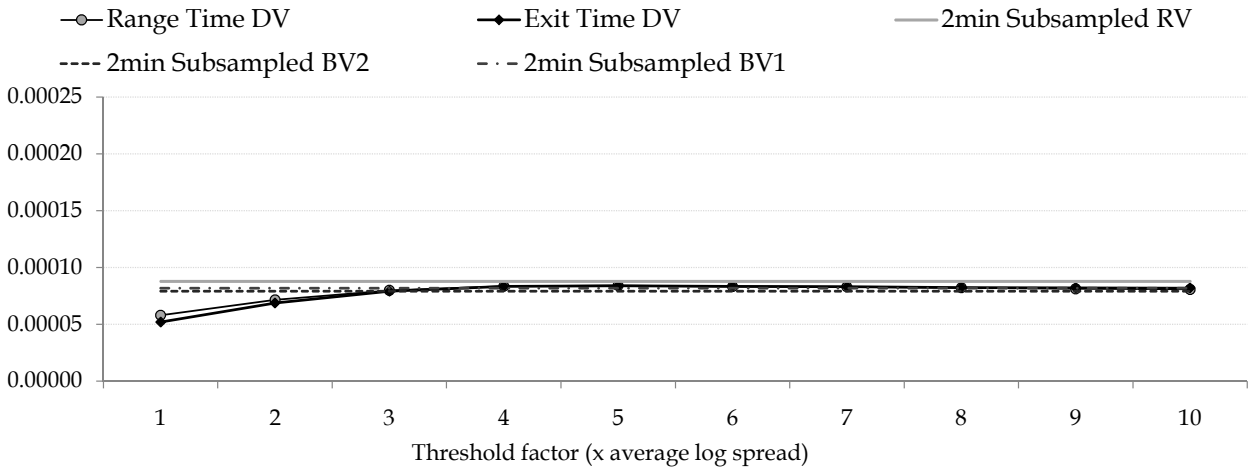

Ticker symbol: KO

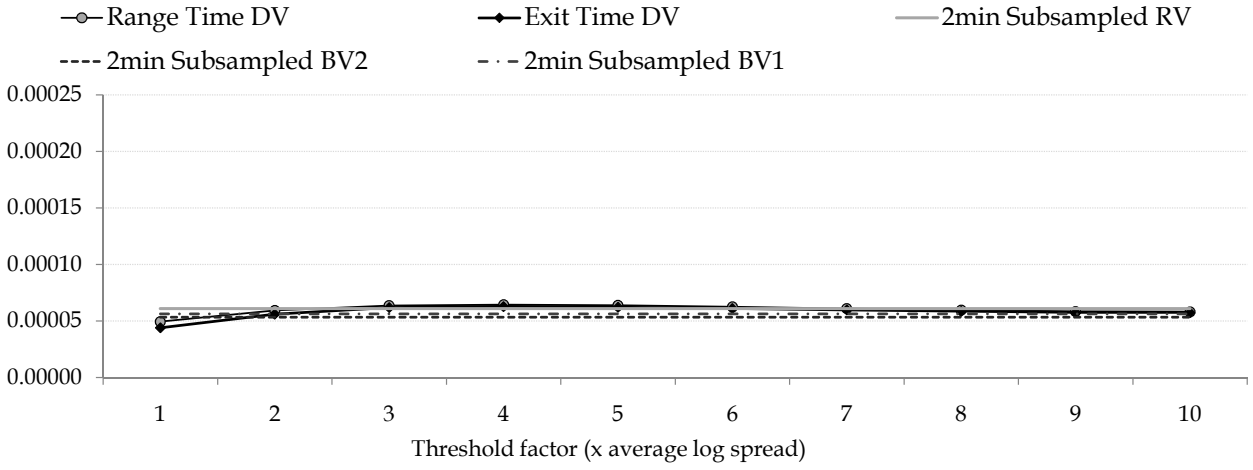

Ticker symbol: MCD

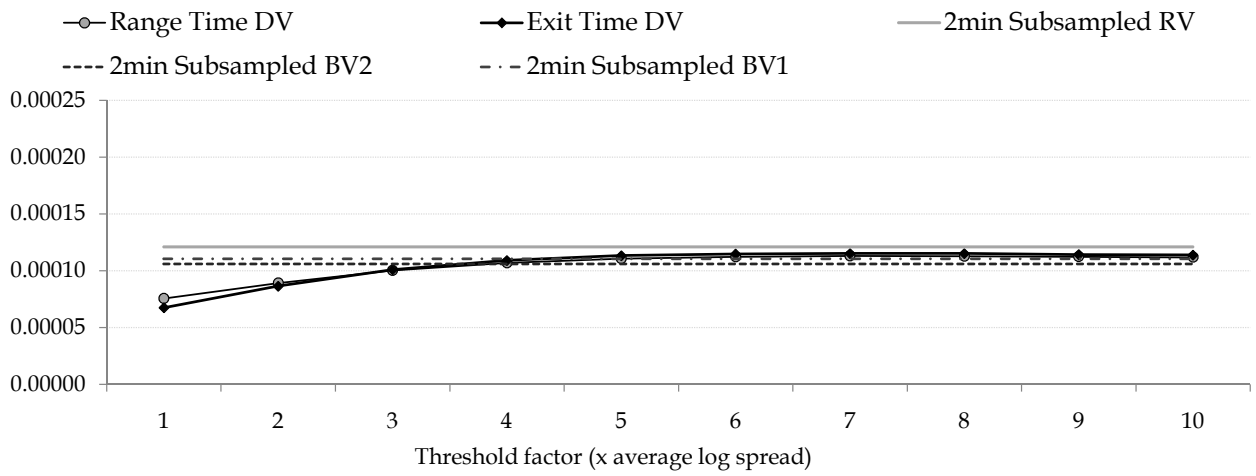

Ticker symbol: MMM

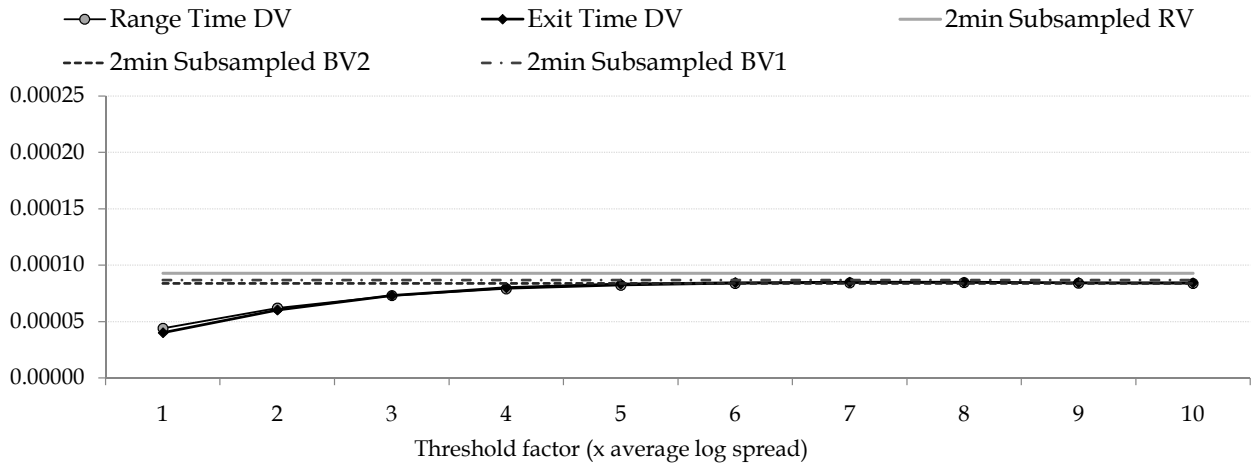

Ticker symbol: MO

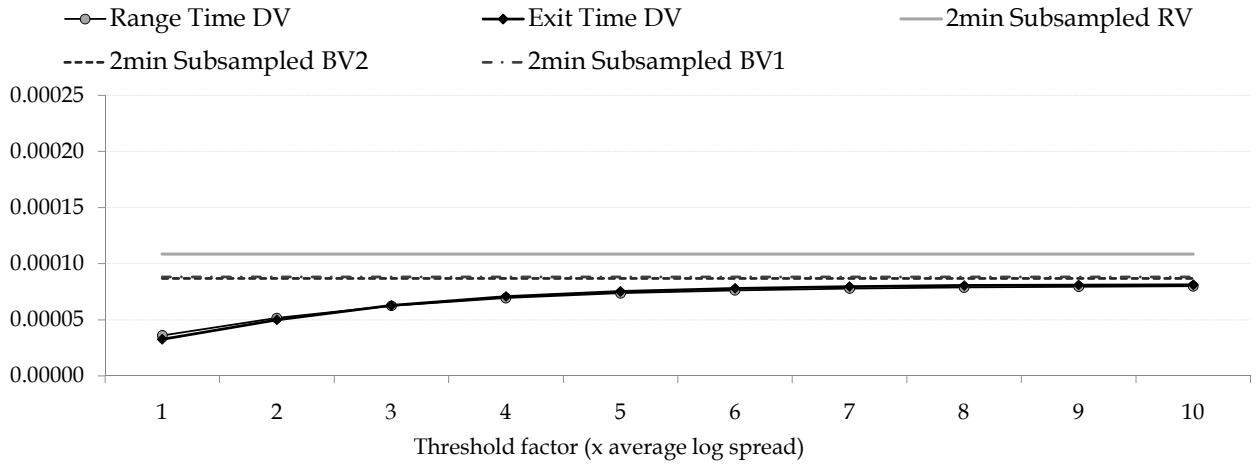

Ticker symbol: MRK

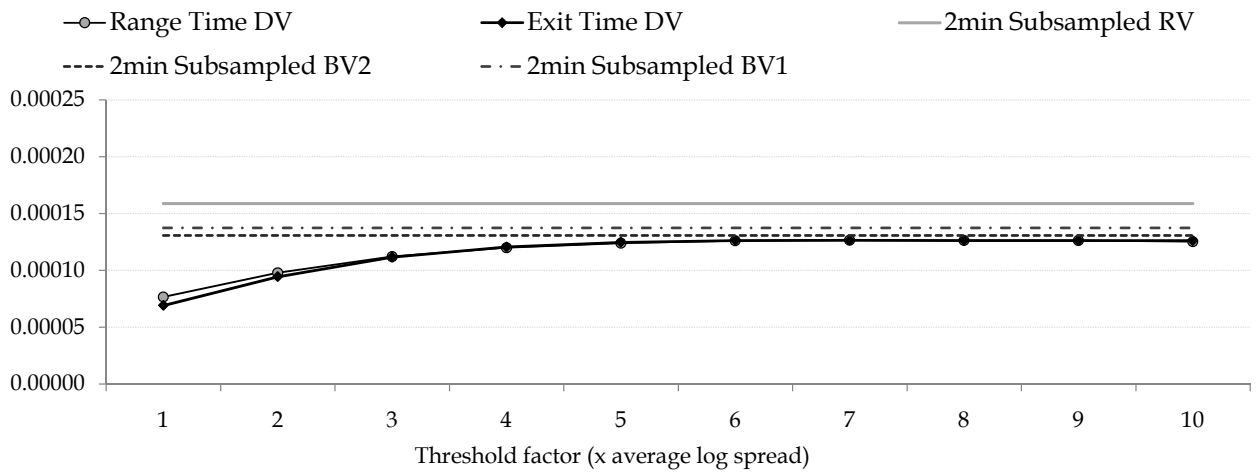

Ticker symbol: MSFT

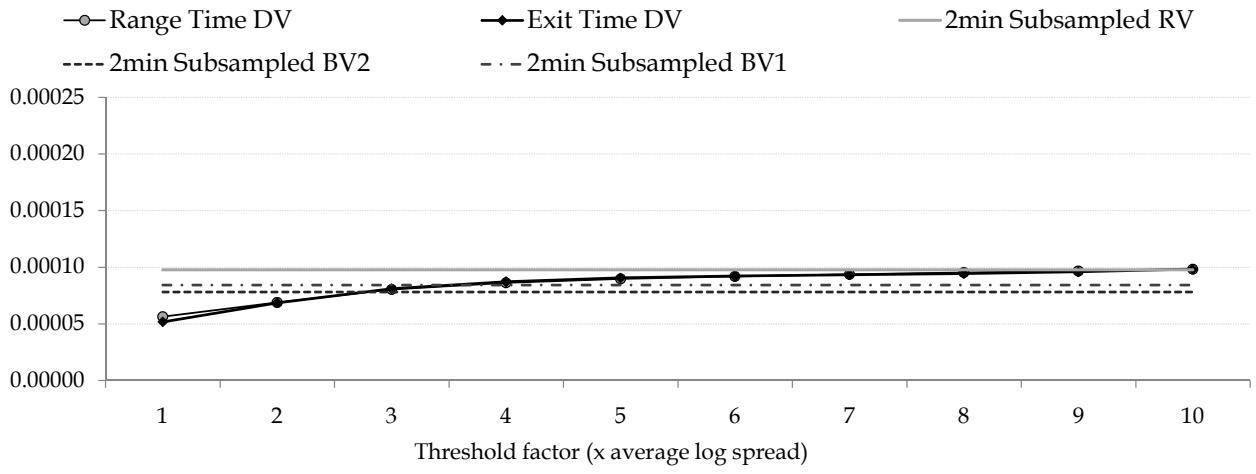

Ticker symbol: PFE

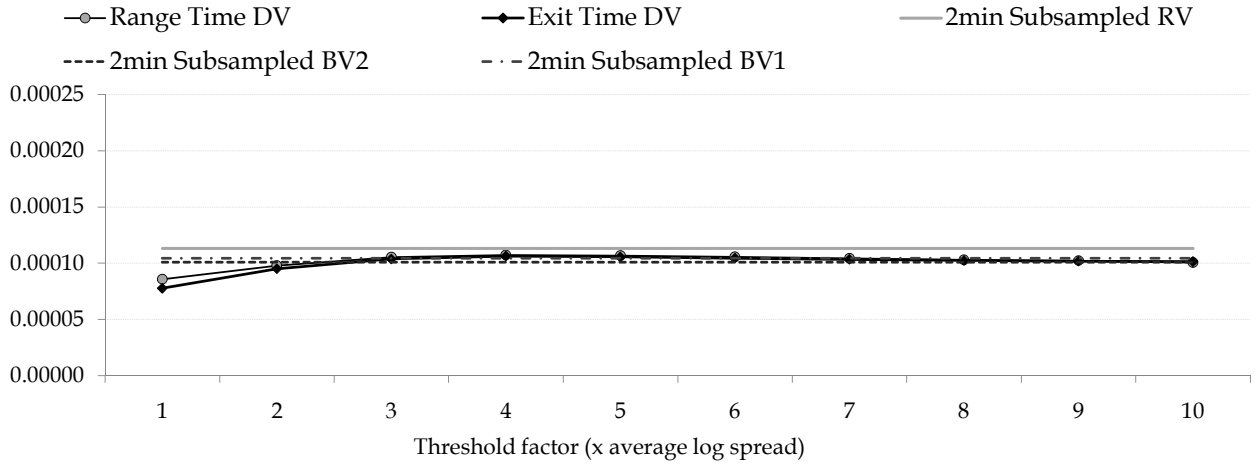

Ticker symbol: PG

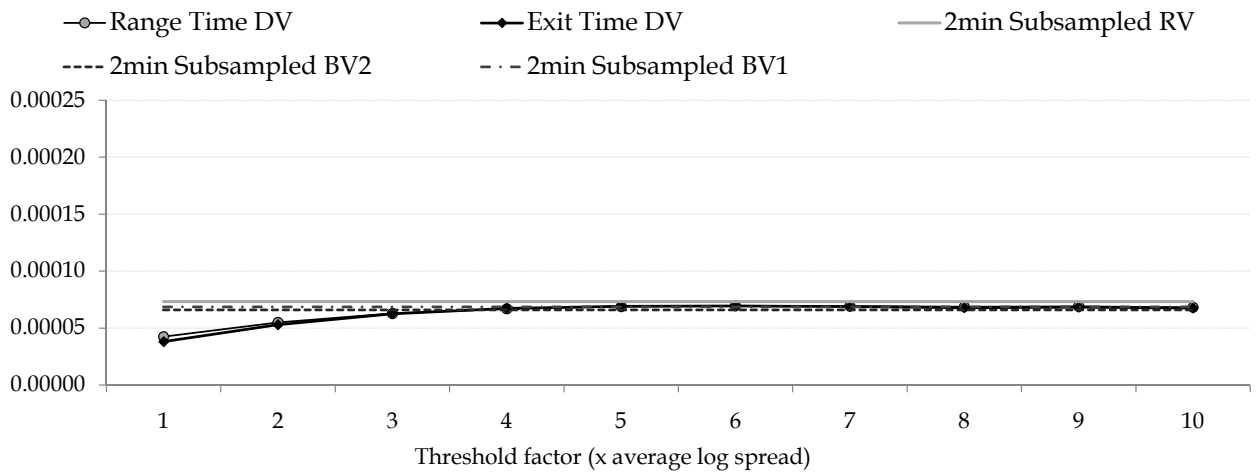

Ticker symbol: T

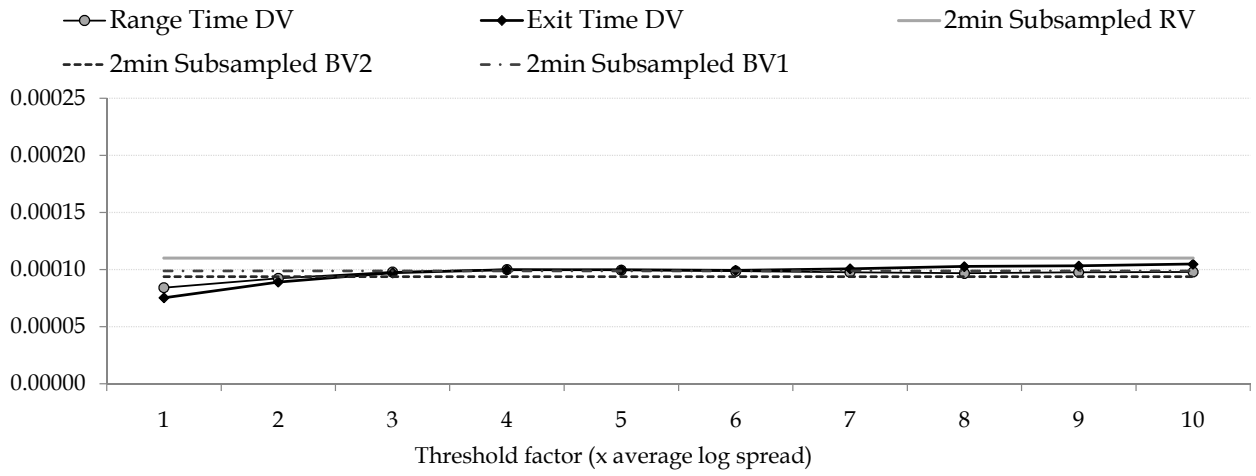

Ticker symbol: UTX

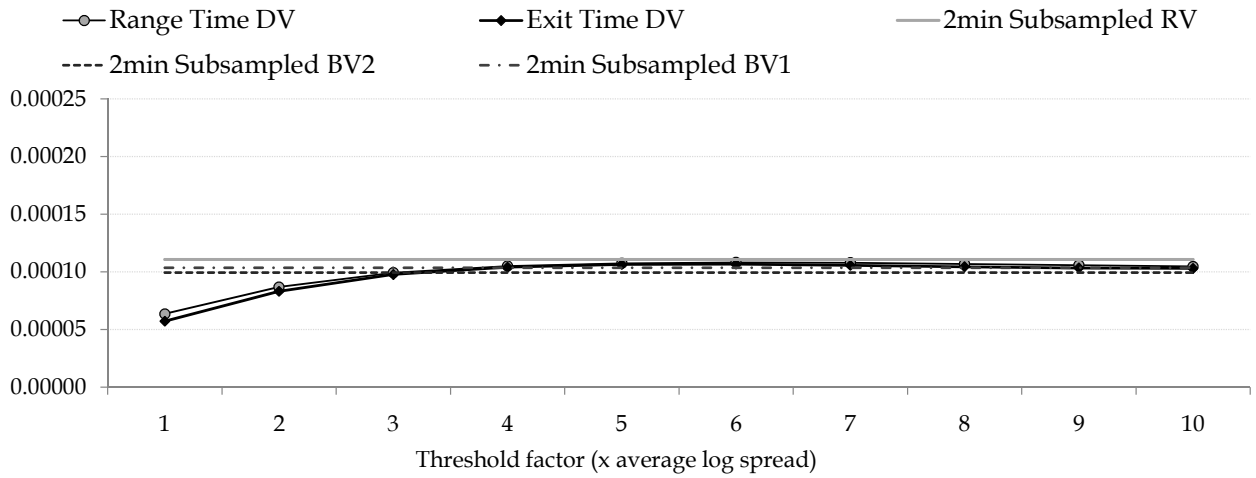

Ticker symbol: VZ

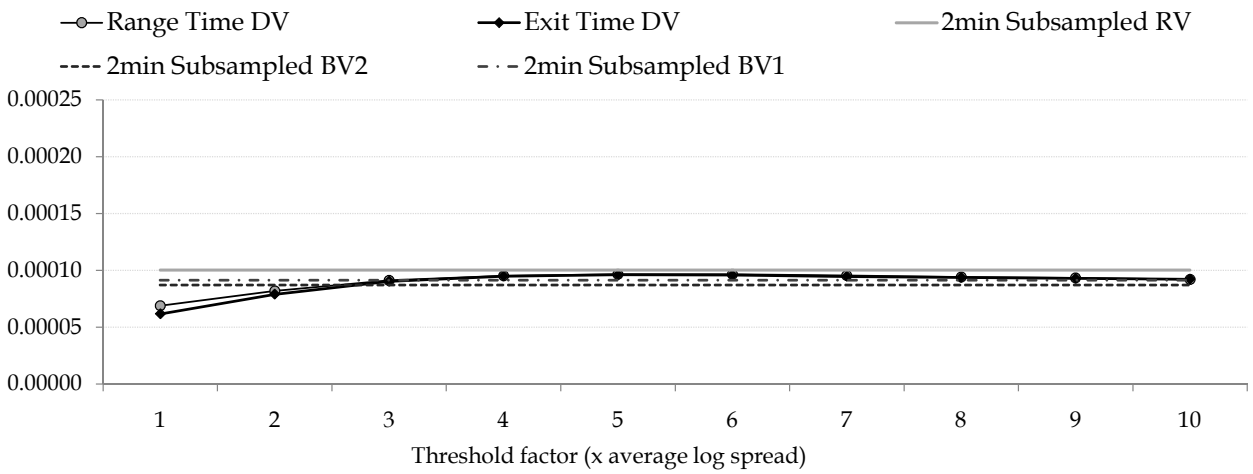

Ticker symbol: WMT

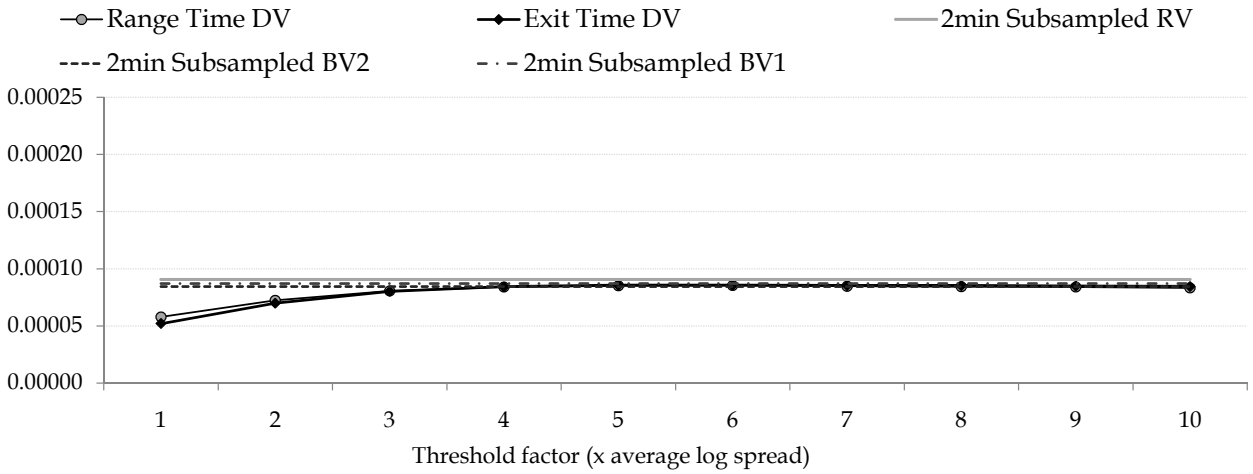

Ticker symbol: XOM